1989

Binding and Transport Properties of Lithium in Red Cells from Hypertensive Patients and Normotensive Controls

Ravichandran Ramasamy
Loyola University Chicago

BINDING AND TRANSPORT PROPERTIES OF LITHIUM IN RED CELLS FROM HYPERTENSIVE PATIENTS AND NORMOTENSIVE CONTROLS

by

RAVICHANDRAN RAMASAMY

A Dissertation Submitted to the Faculty of the Graduate School of

Loyola University of Chicago in Partial Fulfillment

of the Requirements of the Degree of

Doctor of Philosophy

September 1989

ACKNOWLEDGMENTS

I am grateful to my mentor Dr. Duarte Mota de Freitas for the excellent supervision during the entire course of this project. I am also very thankful to Dr. Duarte Mota de Freitas for the intellectual stimulation, encouragement, moral and financial support that he gracefully provided during this study. Special thanks to him for helping me to think and postulate innovative research problems of biological interest, and thereby broaden my horizons in chemistry.

My grateful appreciation to Dr. David Crumrine, Dr. A. J. Rotermund, Dr. Kenneth Olsen and Dr. K. S. Rajan for their excellent suggestions during the course of this work. I am very thankful to Dr C. Narasimhan for helping me to join the graduate program at Loyola.

I sincerely thank my labmates Mary Espanol, Lisa Wittenkeller, Aida Abraha and Sandip Vyas for their encouragements, constructive criticisms and above all coping up with my mercurial mood during the course of this project. I am very thankful to my friends S.Ramakrishnan and Glenn Noronha for helping me to maintain serenity during the course of this study.

I like to gratefully acknowledge the support of faculty, staff and all the graduate students in the Chemistry Department. I like to thank the Graduate School for the Dissertation Fellowship.

My sincere thanks and appreciation to my sister, aunt, uncle, cousins and their family for their encouragement and help during the entire duration of this project.

Special thanks go to my parents for giving me confidence and inspiration during my student days.

Finally, I am very thankful to the omniscient Lord for all of these blessings.

VITA

The author, Ravichandran Ramasamy, is the son of Rajalakshmi Ramasamy and Krishnaswamy Ramasamy. He was born March 21, 1965, in Cuddalore, India.

His elementary and high school education were obtained from Seventh Day Adventist Academy, Madras, India.

In June 1982 he entered Loyola College, Madras, India and received Bachelor of Science degree with a major in Chemistry in 1985.

In August 1985, he joined Loyola University of Chicago to pursue graduate studies in Chemistry. He was awarded a graduate research assistantship from August 1985 to December 1987. From January 1988 to August 1988, he was supported by a research assistanship as a part of a research grant awarded to Dr. Duarte Mota de Freitas by the American Heart Association of Metropolitan Chicago. In September 1989, he was awarded a Loyola University Dissertation fellowship, enabling him to complete the Doctor of Philosophy Degree in 1989, under the suprevision of Dr. Duarte Mota de Freitas.

Publications

Measurement of Lithium Transport Across Human Erythrocyte Membranes by ^{7}Li NMR Spectroscopy (1989). Mary C. Espanol, Ravichandran Ramasamy, and Duarte Mota de Freitas. In Butterfield D.A. (ed): "Biological and Synthetic Membranes", Alan R. Liss Inc., New York, pp 33-43 (1989)

Competition Between Li^{+} and Mg^{2+} for ATP in Human Erythrocytes. A ^{31}P NMR and Optical Spectroscopy Study. Ravichandran Ramasamy and Duarte Mota de Freitas. FEBS Letters 244 : 223-226 (1989).

Aqueous Shift Reagents for $^{7}Li^{+}$ NMR Transport Studies in Cell Systems. Ravichandran Ramasamy, Mary C. Espanol, Kim M. Long, Carlos C. F. G. C. Geraldes and Duarte Mota de Freitas. Inorg Chim Acta 163 : 41-52 (1989).

Influence of Li^{+} on Free Intracellular Mg^{2+} Concentration In Human Red Blood Cells. Ravichandran Ramasamy and Duarte Mota de Freitas. Biophys. J. 55 : 449a (1989).

^{7}Li NMR relaxation studies of Li^{+} storage and transport in RBC.
Duarte Mota de Freitas, Mary C. Espanol, Ravichandran Ramasamy, Aida Abraha, and Lisa Wittenkeller. J Inorg Biochem 36 : 187 (1989).

^{7}Li NMR Studies of Li^{+} Transport in Red Cells of Manic-Depressive patients and Normal Controls. Mary C Espanol, Ravichandran Ramasamy, Duarte Mota de Freitas. In Birch N. J. (ed) : " Lithium : Inorganic Pharmacology and

Psychiatric Use". IRL Press, Oxford, pp 281-284 (1988).

Investigation of the Biological Action of Lithium by ^{7}Li NMR Spectroscopy Duarte Mota de Freitas, Mary C. Espanol, Ravichandran Ramasamy , Recueil Trav. Chim. Pays-Bas. 106,389 (1987).

Nuclear Magnetic Resonance Studies of Lithium Transport in Blood of Hypertensives. Ravichandran Ramasamy, Duarte Mota de Freitas, Vinod Bansal, and Richard Labotka (submitted to Clinica Chimica Acta for publication)

Measurement of the Rates of Na^{+}-Li^{+} Countertransport and Li^{+} ratios in Human Erythrocytes by $^{7}Li^{+}$ NMR Spectroscopy. Duarte Mota de Freitas, Mary C. Espanol, Ravichandran Ramasamy, Joel Silberberg, Walter Dorus, Vinod Bansal and Richard Labotka. (submitted to Biophysical Journal for publication)

Effect of Lanthanide Shift Reagents on Red Blood Cell Shape, Size, and Lithium Transport. Ravichandran Ramasamy, Duarte Mota de Freitas, Joseph Schleup, Warren Jones, Frederick Wezeman and Richard Labotka (Submitted to Biophysical Journal for publication).

TABLE OF CONTENTS

	Page
ACKNOWLEDGEMENTS	ii
VITA	iv
LIST OF PUBLICATIONS	v
LIST OF TABLES	xi
LIST OF FIGURES	xii
LIST OF ABBREVIATIONS	xiv
CHAPTER	
I. INTRODUCTION	1
1. Lithium in Hypertension and Manic-depression	1
2. Role of Magnesium in Hypertension	7
3. Conventional Methods Used in The Study of Lithium Transport in RBCs	8
4. Chemistry of Shift Reagents	11
4.1 Selection of Shift Reagents	11
4.1.1 Selection of Lanthanide Ion	14
4.1.2 Selection of Ligands	16
4.2 Mechanism of Shifts Induced by Lanthanide Complexes	16
II. STATEMENT OF THE PROBLEM	22
III. EXPERIMENTAL METHODS	26
1 Materials	26
1.1 Reagents	26

1.2 Subjects 27

2 Instrumentation 27

2.1 NMR 27

2.2 Atomic Absorption 32

2.3 Osmometer 32

2.4 Centrifuge 32

2.5 Cell Volume Measurements 32

2.6 Scanning Electron Microscopy 32

2.7 Potentiometric Titrations 32

3 Sample Preparation **33**

3.1 Preparation of Shift Reagents 33

3.2 Preparation of Li^+-loaded RBCs 34

3.3 Preparation of Resealed RBC Ghosts 35

3.4 Determination of Na^+-Li^+ Countertransport Rates 35

3.5 SEM and Coulter Counter measurements 36

4 Data Analysis 36

4.1 Determination of Li^+ Concentrations by ^7Li NMR 37

4.2 Determinations of Li^+ Concentrations by AAS 38

4.3 Determinations of Rate Constants of Na^+-Li^+ Countertransport 39

4.4 Statistical Analysis of Data 39

IV RESULTS **40**

1 Characterization and Comparison of Aminocarboxylate Shift reagents With Triphosphate Shift Reagent 40

1.1 $^{7}Li^{+}$ NMR Paramagnetic Shifts Induced By Aminocarboxylate Complexes of Dysprosium and Thulium 40

1.2 pH Dependence of $^{7}Li^{+}$ NMR Isotropic Shifts 43

1.3 Potentiometric Titration Studies of $Dy(PPP)_2^{7-}$ 51

1.4 ^{31}P NMR Titration Studies of $Dy(PPP)_2^{7-}$ 53

1.5 Competition Between Li^{+} And Other Cations for Aminocarboxylate Shift Reagents 58

2 Characterization And Comparison of Phosphonate Shift Reagents With Triphosphate Shift Reagent 66

2.1 $^{7}Li^{+}$ and $^{23}Na^{+}$ Paramagnetic Shifts Induced By Phosphonate Complexes of Dysprosium 66

2.2 pH Dependence of $^{7}Li^{+}$ NMR Shifts Induced By Phosphonate Shift Reagents 69

2.3 Competition Between Li^{+} and other Cations for Phosphonate Shift Reagents 69

2.4 Hydrolytic Stability of Phosphonate Shift Reagents in Biological Systems Containing Phosphatases 74

2.5 Application of Shift Reagents to the Study of Li^{+} Transport in RBC 79

3 Effects of Lanthanide Shift Reagents 82

3.1 Effect of Lanthanide Shift Reagents on Shape and

Size of RBC 82

3.2 Effect of Li^+ on Shape and Size of RBC 86

3.3 Effect of Lanthanide Shift Reagents on Na^+-Li^+ Exchange by ^7Li NMR Spectroscopy 90

3.4 Effect of Lanthanide Shift Reagents on RBC Membrane Potential 92

4 Na^+-Li^+ Countertransport Measurements In RBCs From Hypertensive Patients And Normal Controls by MIR Pulse Sequence 97

5 Competition Between Li^+ And Mg^{2+} In Human RBCs 107

V DISCUSSION 117

VI BIBLIOGRAPHY 127

LIST OF TABLES

		Page
I.	^{7}Li MIR parameters	31
II.	Protonation constants obtained by potentiometric titration of tetramethylammoniun salts of PPP^{5-} and $Dy(PPP)_2^{7-}$	52
III.	^{31}P NMR chemical shifts and linewidths of α,γ- and β-phosphate resonances of $Dy(PPP)_2^{7-}$	56
IV.	Comparison of average RBC diameter obtained for Li^+-free RBCs treated with various lanthanide shift reagents	85
V.	Comparison of average diameter of Li^+ and Dy^{3+} treated RBC obtained by SEM and CC	89
VI.	Comparison of Na^+-Li^+ exchange rates in mmoles of Li^+ / (L RBCs x hour) of Li^+-loaded RBCs obtained in the presence and absence of shift reagents by AA and NMR	91
VII.	Effect of various shift reagents on the membrane potential of RBCs obtained by ^{31}P NMR	95
VIII.	Effect of various shift reagents on the membrane potential of RBCs by ^{19}F NMR.	98
IX.	Comparison of Na^+-Li^+ countertransport rates in mmoles of Li^+ / (L RBCs x hour) and rate constant in h^{-1} obtained by AA and ^{7}Li NMR (MIR) methods on normotensives and hypertensives	105
X.	Effect of Li^+ on free Mg^{2+} concentration in model systems and in RBCs obtained by ^{31}P NMR and optical absorbance techniques	114
XI.	^{7}Li NMR relaxation time measurements of Mg^{2+}-depleted and Mg^{2+}-saturated Li^+-loaded RBCs	116

LIST OF FIGURES

		Page
1.	Sodium transport pathways in RBCs	4
2.	Structure of some shift reagents	13
3.	^{7}Li NMR pulse sequence	30
4.	$^{7}Li^{+}$ NMR paramagnetic shifts induced by aminocarboxylate complexes of dysprosium and thulium	42
5.	pH dependence of $^{7}Li^{+}$ NMR isotropic shifts	45
6.	$^{7}Li^{+}$ and $^{23}Na^{+}$ NMR paramagnetic shifts of $Dy(PPP)_2^{7-}$ at various Li^{+} and Na^{+} concentration	47
7.	Hypothetical solution structures for $Dy(PPP)_2^{7-}$	50
8.	^{31}P NMR pH titration Studies of $Dy(PPP)_2^{7-}$	55
9.	Competition between Li^{+} and divalent cations for aminocarboxylate shift reagents	60
10.	Competition between Li^{+} and monovalent cations for aminocarboxylate shift reagents	62
11.	^{31}P NMR spectra of $Dy(PPP)_2^{7-}$ in the presence of calcium	65
12.	$^{7}Li^{+}$ and $^{23}Na^{+}$ paramagnetic shifts induced by phosphonate complexes of dysprosium	68
13.	pH dependence of $^{7}Li^{+}$ NMR shifts induced by phosphonate shift reagents	71
14.	Competition between Li^{+} and divalent cations for phosphonate shift reagents	73
15.	Competition between Li^{+} and monovalent cations for phosphonate shift reagents	76
16.	Hydrolytic stability of phosphonate shift reagents in biological	

systems containing phosphatases 78

17. Discrimination of intra- and extracellular Li^+ in Li^+-loaded RBCs in the presence of various shift reagents 81

18. SEM pictures on the effects of variuos shift reagents on RBCs 84

19. SEM pictures on the effect of Li^+ on RBCs 88

20. ^{31}P NMR spectra of hypophosphite in an RBC suspension 94

21. ^{7}Li MIR spectra of Li^+-loaded RBCs 100

22. Time dependence of intracellular Li^+ concentration in Li^+-loaded RBCs from a hypertensive patient and a normal control 104

23. ^{31}P NMR spectra of ATP under various conditions in RBC 109

24. ^{31}P NMR spectra of Li^+-free and Li^+-loaded RBCs 112

LIST OF ABBREVIATIONS

AA	atomic absorption
ATP	adenosine triphosphate
ADP	adenosine diphosphate
CC	coulter counter
CA	chelidamate
CPMG	Carl-Purcell-Meiboom-Gill
δ	NMR chemical shift
$\Delta\nu_{1/2}$	NMR resonance linewidth at half-height
DOTA	1,4,7,10-tetraazacyclododecane-N,N^{1},N^{11},N^{111}-tetraacetate
DOTP	1,4,7,10-tetraazacyclododecane-N,N^{1},N^{11},N^{111}-tetramethylenephosphonate
DPA	dipicolinate
DTPA	diethylenetriaminepentaacetate
DTPP	diethylenetriaminepentamethylene phosphonate
EDTA	ethylenediaminetetracetate
FE	flame emision
f_{in}	fractional intracellular NMR window
f_{out}	fractional extracellular NMR window
HEPES	[4-(2 hydroxyethyl)-1-piperazine-ethanesulfonic acid]
H_t	hematocrit
MIR	modified inversion recovery
NMR	nuclear magnetic resonance
NOTA	1,4,7-tricyclo-N,N^{1},N^{11}-tris(methylene) triacetate
NOTP	1,4,7-tricyclo-N,N^{1},N^{11}-tris(methylene) triphosphonate.

NTA	nitrilotricaetate
NTP	nitrilotris(methylene) triphosphonate
PcPcP	bis(dihydroxyphosphinylmethyl) phosphinic acid
PPP	triphosphate
RBCs	red blood cells
SEM	scanning electron microscopy
T_1	spin-lattice relaxation time
T_2	spin-spin relaxation time
TTHA	triethylenetetraminehexaacetate
TRIS	tris(hydroxymethyl)aminomethane

Chapter I

Introduction

I.1 Lithium in Hypertension and Manic-Depression

High blood pressure is an important risk factor for cardiovascular disease. The central nervous system, the kidney, and the vascular smooth muscle are among the many organ systems which contribute to the regulation of this complex quantitative trait (1). Interindividual variability of blood pressure in the population at large is characterized by a continuous unimodal frequency distribution. Persons in the upper tail of this distribution with diastolic blood pressure greater than 98 mm Hg and without any known primary lesion are considered to have essential hypertension. Hypertension has been identified as the single most common factor for cardiovascular disease in the U.S.

Factors that are considered to be responsible for interindividual variation in blood pressure include genetic differences, differences in an individual's environment, and measurement error. Several studies demonstrate that genetic differences determine blood pressure variability, but they provide no information on the number of genes involved, their allele frequencies, or the structure and function of these genes (2,3). Hypertension, unlike other cardiovascular risk factors such as cholesterol levels, is not related, at present, to any known inherited molecular factors. Identification of such factors is likely to yield crucial information on the role of specific genes in determining interindividual blood pressure variation.

The search for biochemical markers of hypertension spans many years (4). Weinshilboum (5) used a biochemical genetic approach to investigate the role of catecholamine metabolites in determining blood pressure variations. Although genetic polymorphism was identified, this was not significantly associated with blood pressure variation. The variations in red blood cell (RBC) sodium transport have been hypothesized by several investigators to be markers for hypertension.

The four major transport pathways of sodium in RBCs are shown in figure 1. The activities of these four pathways have been assayed and then compared in selective groups of hypertensives versus normotensive controls (6). Sodium transport by the ouabain sensitive, ATP dependent sodium pump is one of the major transport pathways for sodium (7). This pathway utilizes chemical energy in the form of ATP to extrude sodium from the cell while simultaneously accumulating potassium. The maximal rate of the sodium pump can be determined by measuring the ouabain-sensitive sodium efflux into a medium containing 5-10 mM potassium from cells loaded to contain 40-50 mM of sodium and potassium. It was observed that the sodium pump activity was low in black hypertensive women accompanied by marked elevations in cellular sodium (8). The sodium pump does display large interindividual differences in RBCs of human subjects but its role in hypertension is still conflicting (9). The ouabain-sensitive sodium pump generates a sodium and potassium gradient, while the ouabain-insensitive sodium transport systems are gradient dissipators. They utilize sodium, or potassium, to move with an ion partner in the same direction (cotransport) or in the opposite directions (countertransport).

The sodium-potassium cotransport system present in RBCs is an ouabain-insensitive pathway which is inhibited by furosemide and by chloride removal (10). Reported assays for this transport system have large coefficients of variation and are difficult to use clinically (11-13). Moreover the variations in the results obtained for

Figure 1. Major transport pathways of sodium ion in human RBCs (adapted from reference 5).

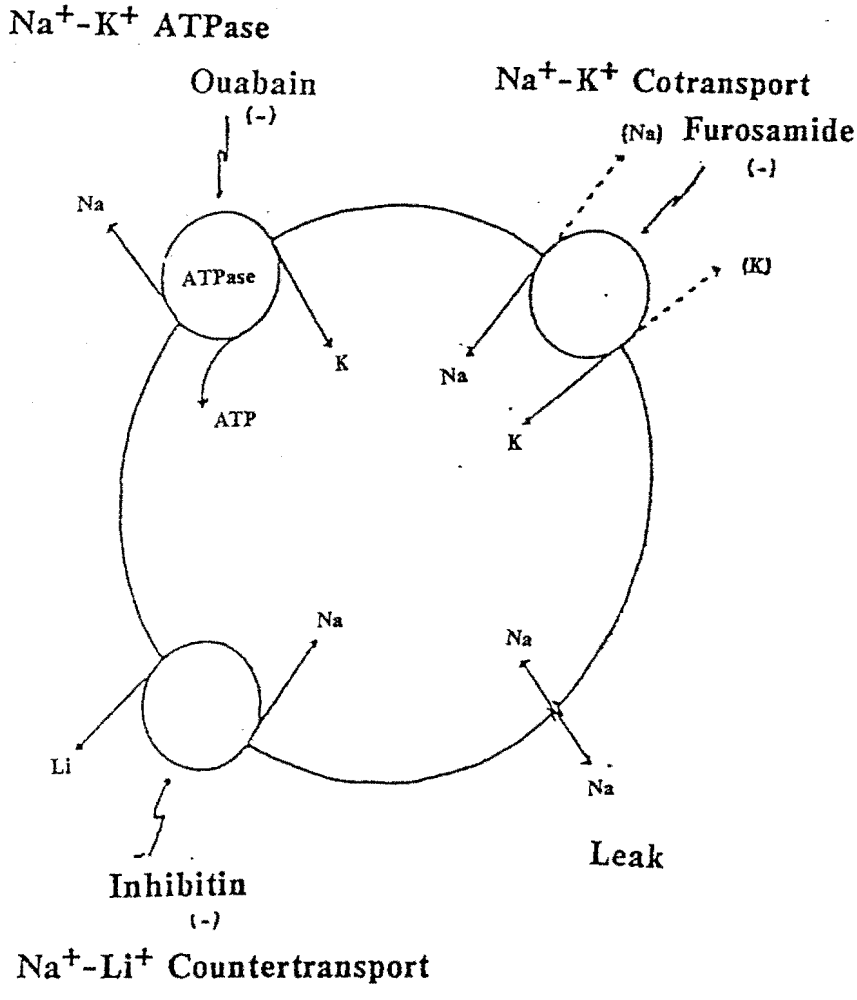
Na+-K+ ATPase
Ouabain
(-)
Na+-K+ Cotransport
(Na) Furosamide
(-)
Na
ATPase
K
ATP
(K)
Na
K
Na
Na
Li
Na
Inhibitin
(-)
Leak
Na+-Li+ Countertransport

the sodium-potassium cotransport pathway for hypertensive and normotensive RBCs are not consistent. Hence their role as a marker for hypertension is still debatable. The passive sodium leak across RBC membrane has not been found to be different between hypertensives and normotensives (9).

The sodium countertransport system promotes the exchange of sodium for sodium, lithium for sodium, or lithium for lithium (14). Haas et al. (15) described a Na^+-Li^+ countertransport system that exchanged Li^+, against its electrochemical gradient, for Na^+ and reported that this system was inhibited by phloretin (14). This system accepts only sodium or lithium and has 20 times more affinity for lithium than for sodium (16). The high affinity for lithium makes it a good marker of the sodium countertransport pathway. Canessa et al. (17) have developed an assay for the Li^+-Na^+ countertransport system based on its kinetic properties. They have taken into account the following considerations for the development of the assay: (1) only one transport system is measured, (2) a well defined mode of operation is involved, (3) kinetic variables are determined, and (4) good inter-assay and intra-assay reproducibility must be obtained. The assay developed by Canessa et al. (17) is very reproducible and has been useful in investigating the genetic, pathophysiological, and epidemiological aspects of essential hypertension. Based on kinetic studies it has been speculated that Li^+ is transported by the same mechanism that mediates Na^+-Na^+ exchange (14,16,18). Recently, it has been confirmed that indeed the Na^+-Li^+ countertransport and Na^+-Na^+ exchange are conducted through the same pathway (19,20). Moreover, these studies (19,20) reveal that inhibitin is a better inhibitor of Na^+-Li^+ countertransport than phloretin. It has been shown that inhibitin inhibits 75% of Na^+ efflux by Na^+-Na^+ exchange while phloretin inhibits 40% of Na^+ efflux (19,20).

Rates of Li^+-Na^+ exchange were reported to be higher in RBCs from hypertensive patients than normal controls (17). Increased RBC Li^+-Na^+ exchange rates in first

degree relatives of individuals with essential hypertension, but not in relatives of normotensive controls without a family history of essential hypertension, suggests that Li^+-Na^+ exchange rates may be inherited (17). Genetic studies on extended families suggest that genetic factors are the main determinants of the V_{max} of this transport system. Canessa et al. (17) have established that V_{max} of Li^+-Na^+ exchange system is determined by heritability. Cusi et al. (21) and Canessa et al. (17) have reported studies on family aggregation of Li^+-Na^+ exchange. Extensive genetic studies were carried out in hypertension prone Mormon families of Salt Lake City by Williams et al. (22) All of these studies reinforce the role of genetic factors in the observed abnormality in Li^+-Na^+ exchange rates observed for hypertensive RBCs. Studies are in progress in several groups to understand the Li^+-Na^+ exchange system in greater detail.

Other than as a marker for hypertension, lithium salts are mainly used as drugs in the treatment and maintenance of both manic and depressive episodes of bipolar patients (23). It has been established that bipolar disorder is a genetically inherited disorder (24-26). Several studies have been conducted to determine whether the abnormal Li^+-Na^+ exchange rates observed in RBCs from bipolar patients can be used as genetic markers. Several groups have reported a decrease in Li^+-Na^+ exchange rates in a subgroup of bipolar patients (27), while other investigators (28-30) obtained no significant difference between bipolar patients and normal controls.

Recent studies have suggested that, in cells other than erythrocytes, the sodium exchange system may exchange sodium for protons (31-33). It was proposed by Aronson et al. (32) that the elevation of Li^+-Na^+ exchange reflected a similar elevation of the Na^+-H^+ exchange in kidney and higher tubular sodium reabsorption. Despite the fact that the Na^+-H^+ exchanger is widely present as a pH regulatory system in most types of cells, its modes of operation and equilibrium properties are not yet understood. It has been established that Na^+-H^+ exchange is an important mechanism by which pH is

regulated in various types of cells. In human RBCs, pH is regulated by the activity of the anion exchanger. The physiological role of Na^+-H^+ exchange in RBC is still nebulous. It has been observed that the Na^+-H^+ exchanger is silent in human RBCs at pH 7.4 (34,35). However, Na^+-H^+ exchanger can be activated by: (a) increasing the cytosolic calcium concentration using the ionophore A23187 (34) and (b) decreasing cell pH (pH_i less than 7) by increasing the impermeant anions ATP and 2,3-DPG followed by treatment with DIDS and acetazolamide (to inhibit anion exchange and carbonic anhydrase) and incubation in alkaline medium to impose an outward proton gradient (35). The Na^+-H^+ exchanger in RBC has a V_{max} in the range of 20 to 50 mmol/L cells x hour at pH_i 6, pH_o 8 while the corresponding intra- and extracellular sodium concentrations are 0 and 140 mM respectively (36).

The Na^+-H^+ exchange and Li^+-Na^+ exchange have strikingly similar properties. The Li^+-Na^+ exchange is inhibited by external protons, but stimulated by cytosolic protons ($pH_i < 7.2$) (36). In fact an hypothesis has been made suggesting that under conditions of pH equilibrium higher than 7, the Na^+-H^+ exchanger may exist in a different conformational state promoting amiloride-insensitive Li^+-Na^+ exchange (37). Studies are in progress mainly by Canessa and her coworkers to investigate the above hypothesis (38).

I.2 Role of Magnesium in Hypertension and Manic-Depression

One of the possible modes of action of lithium is that Li^+ could be competing with Mg^{2+} for biomolecules, which is based on the existence of a diagonal relationship between Li^+ and Mg^{2+}. It has been shown that Li^+ competes with Mg^{2+} for biological ligands with a set of 3 oxygens and 1 nitrogen (39). Previous studies have shown that Li^+ affects serum Mg^{2+} levels of patients receiving lithium therapy (40-42) and that intracellular free Mg^{2+} concentrations are lower in RBCs from hypertensive patients than normal controls (43). Vascular tone and its response to pressor agents are

strongly influenced by Mg^{2+} levels (43,44). It has been hypothesized that low concentrations of Mg^{2+} leads to an increase in free Ca^{2+} concentrations, which in turn affects smooth muscle tension leading to high blood pressures (44). Studies have related abnormality in Na^+ transport in smooth-muscle cells to contraction and increased vascular resistance (43,44). It is interesting to investigate the possible effect of lithium on intracellular free Mg^{2+} concentrations in RBCs, along with Li^+-Na^+ exchange rate measurements.

Studies on Li^+-Na^+ exchange rates in RBCs have been monitored using invasive techniques. In the last few years, new non-invasive methods have been developed for monitoring alkali metal cation transport in RBCs. We are studying lithium transport rates using newly developed non-invasive techniques in order to establish the transport abnormality in hypertensive and bipolar patients (45,46). A comparison of conventional methods with newly developed methods for monitoring Li^+ transport in RBCs is made in the following subsection.

I.3 Conventional Methods Used in The Study of Lithium Transport in RBCs

Traditionally lithium transport has been monitored using atomic absorption (AA) and flame emission spectrometry (FE) (47,48). For most conventional methods, blood samples are subject to centrifugation followed by cell lysis before measuring Li^+ present in RBC and plasma. The intracellular and extracellular Li^+ concentrations are determined by comparison to standard Li^+ solutions with a composition similar to the blood samples being analyzed. The invasive nature of the conventional methods may lead to errors due to non-specific ion binding to membranes and cell metabolites and additional ion transport during blood processing. Crucial information on ion binding to the intact RBC membrane, its role in the etiology of a disease, and changes in membrane potential are lost by conventional methods. Sample processing in conventional methods also require time consuming procedures.

In AA and FE spectrometry, a flame is the atomization source. Li^+ containing lysed RBC and plasma samples, when exposed to the flames, are vaporized into atoms. Exposure to the flame excites atoms to a higher energy state. On return to the ground state, atoms emit light at specific wavelengths characteristic of each element. Since the atomic spectra of alkali metals are well resolved and these elements are excited at much lower temperatures than most elements, the Li emission is suitable for lithium determinations in blood samples. In the case of AA measurements, a light beam characteristic of the lithium spectrum is passed through the vaporized sample containing lithium. The intensity of the absorbed or emitted radiation measured in AA and FE determinations, respectively, are proportional to Li^+ concentration in the sample. Since a Li lamp is used in AA spectrometry, Li determinations by AA are more specific than those obtained using FE.

Li^+ concentrations in biological fluids have also been determined using optical and fluorescent dyes (49). The major drawback with the above mentioned techniques is the lack of high selectivity of dye for Li^+ ion and its possible effect on Li^+ distribution across the membrane. In blood plasma, sodium is present in one hundred-fold excess and it competes with lithium for the optical and fluorescent dyes. In addition, Na^+ and Li^+ have similar affinities for the dye. Recently some success has been achieved in the development of highly selective Li^+ optical and fluorescent dyes, such as crownazophenol-5 and 1,8-dihydroxyanthraquinone (50-52). The Li^+ levels in blood serum from bipolar patients have also been monitored using the newly developed lithium ion selective electrodes (53-56).

Li^+ distribution in tissues have also been investigated using neutron activation analysis (57). In this method, the ^6Li isotope (natural abundance of 7.4%) is subject to neutron bombardment resulting in the formation of tritium and α particles. Tritium, being a β-emitter and having a long half-life (12.3 years), can be used to probe Li^+

distributions in tissues, including brain (58).

The availability of multinuclear NMR spectrometers has made it possible to obtain spectra of biologically important cations like Na^+, K^+, Ca^{2+}, Mg^{2+}, etc (59). Recently, it was demonstrated by us and others that ^7Li NMR can be used non-invasively to discriminate between the intra- and extracellular Li^+ in Li^+-loaded RBC suspensions (45,46,60). The signals corresponding to intra- and extracellular pools of Li^+ were resolved using lanthanide shift reagents, in particular dysprosium triphosphate $Dy(PPP)_2^{7-}$ (45,60). The chemical shifts of intra- and extracellular Li^+ are not resolved in the absence of shift reagents since Li^+ ions primarily exist as hydrated ions in both pools. Moreover, the chemical shift range for the ^7Li nucleus in ionic environments is very narrow and is not sensitive to changes in ligation or solvation (59). The high negative charge on $Dy(PPP)_2^{7-}$ causes the shift reagent to be repelled by the RBC membrane phospholipids and renders it membrane impermeable. The signal due to extracellular Li^+ in contact with the shift reagent is shifted upfield while the intracellular Li^+ signal remains unshifted. Thus it is possible to discriminate and identify the two pools of Li^+ by ^7Li NMR.

^{23}Na and ^{39}K NMR studies of sodium and potassium distribution in RBC suspensions have also shown that the intra- and extracellular Na^+ and K^+ NMR signals are not resolved and yet with incorporation of shift reagents in the suspension medium, it is possible to discriminate between the two pools of cations (61,62). Among the alkali metals, cesium is the only cation that exhibits two well separated resonances for intra- and extracellular Cs^+ in RBC when probed by ^{133}Cs NMR without incorporation of shift reagent in the suspension medium (63). The mechanism by which one is able to observe the pools of Cs^+ without the addition of shift reagent is still not known (63).

Besides obtaining information on cation transport, it has been shown that information on sodium binding to RBC membranes from hypertensive patients can also be

obtained by ^{23}Na NMR (64). The extreme ease and efficiency in obtaining ion transport information has led to widespread use of the shift reagent NMR method in biomedical research.

I.4 Chemistry of Shift Reagents

Lanthanide complexes were first introduced by Hinckley in 1969 to shift proton resonances in ^{1}H NMR spectra (65). These complexes were powerful tools for structural elucidation of organic and biological compounds in the 1970s. The situation has changed in the last decade with high field magnets and 2-D NMR techniques. Examples of systems that have been studied with aqueous lanthanide shift reagents include proteins, nucleotides and nucleic acids, carbohydrates, and membranes. Recently, aqueous lanthanide shift reagents have been developed for the study of biologically important metal cations (45,60-62,67-68) and as contrast reagents for medical imaging (70).

Several studies have evaluated the effectiveness of the water soluble shift reagents shown in figure 2 for metal cations (45,60-62,66-70). $Ln(EDTA)^{-}$, $Ln(TTHA)^{3-}$, Ln(NOTA), $Ln(DOTA)^{-}$, $Ln(NTA)_2^{3-}$, $Ln(CA)_3^{6-}$, $Ln(DPA)_3^{3-}$, $Ln(PPP)_2^{7-}$, and $Ln(DTPA)^{2-}$ are the most popular shift reagents for metal cation studies. Since all these shift reagents are negatively charged (with the exception of Ln(NOTA)) and thus membrane impermeable, incorporation of LSR in the suspension medium enables one to distinguish between extra- and intracellular cations.

I.4.1 Selection of Shift Reagents

There are two variables that enter into the selection of a lanthanide shift reagent, choice of a metal and choice of ligand. It would appear that one would have an endless variety of shift reagents to choose from the combination of lanthanides and ligands available. However, the choices are not as great as they seem as shown below (71).

Figure 2. Structure of shift reagents used in this study. PPP^{5-}, $TTHA^{6-}$, NTA^{3-}, DPA^{2-}, HCA^{2-}, $DOTA^{4-}$, $NOTA^{3-}$, $EDTA^{4-}$ and $DTPA^{5-}$ represent the ligands triphosphate, triethylenetetraminehexacetate, nitrilotriacetate, dipicolinate (pyridine-2,6-dicarboxylate), chelidamate (4-oxypyridine-2,6-dicarboxylate), 1,4,7,10-tetraazacyclododecane-N,N^{1},N^{11},N^{111}-tetraacetate, 1,4,7-tricyclo-N,N^{1},N^{11}-tris(methylene) triacetate, ethylenediaminetetraacetate, and diethylenetriaminepentaacetate respectively. Water coordination in all of these shift reagents is not represented.

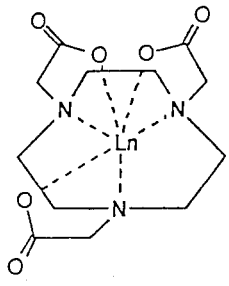

Ln (NOTA)

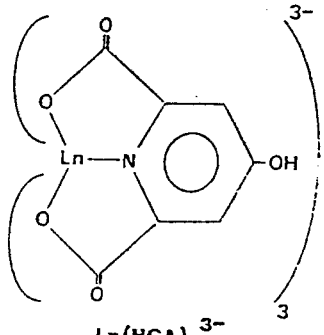

$Ln(HCA)_3^{3-}$

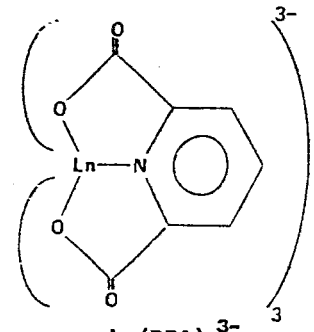

$Ln(DPA)_3^{3-}$

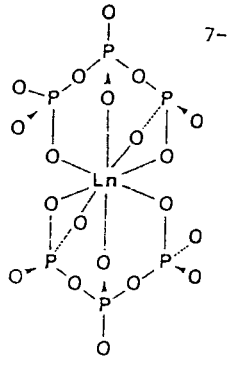

$Ln(PPP)_2^{7-}$

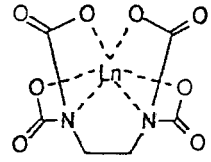

Ln (EDTA)$^-$

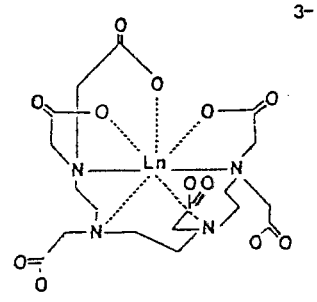

$Ln(TTHA)^{3-}$

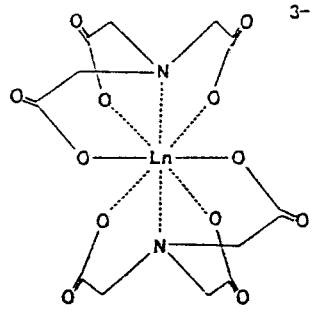

$Ln(NTA)_2^{3-}$

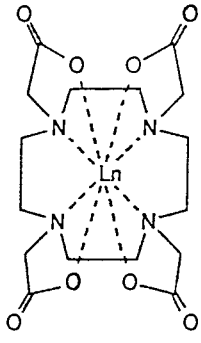

Ln (DOTA)$^-$

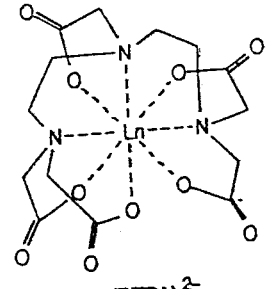

Ln (DTPA)$^{2-}$

I.4.1.1 Selection of Lanthanide Ion

The lanthanide ion is a Lewis acid and forms donor-acceptor complexes with Lewis bases. The exchange of donor between its complexed and uncomplexed form is usually rapid on the NMR time scale. Any Lewis base, containing an NMR active nucleus, will interact with lanthanide cations enabling the NMR active nuclei to feel the presence of unpaired f electrons. This interaction leads to a paramagnetic broadening or a shift in resonances of the NMR active nuclei. The magnetic properties of lanthanide ions can be used to predict the shifts observed in the presence of shift reagents (70-72).

The lanthanide metal ions that can be employed in shift reagents are the trivalent cations of praseodymium, neodymium, samarium, europium, dysprosium, terbium, holmium, erbium, thulium, and ytterbium. Lanthanum (III) and lutetium (III) are diamagnetic and hence are not suitable (71). Cerium (III) is unstable and tends to oxidize to the diamagnetic Ce (IV) in complexes (71). Promethium is a radioactive lanthanide. Gadolinium (III) with an f^7 configuration has its seven unpaired electrons distributed isotropically in the 4f shell and therefore cannot produce pseudocontact shifts in the NMR spectrum of a substrate (71). Europium (III) has a $^7F_0$ ground state that is nondegenerate and has no Zeeman splitting (73). The Eu (III) ion in the ground state cannot cause contact or pseudocontact shifts. The first excited state of Eu (III) is a $^7F_1$ state and is significantly populated at room temperature. This energy state accounts for the shift reagent properties of Eu (III) (73). The broadening caused by the paramagnetic lanthanide ions is not that severe due to short electron spin relaxation times (74). At lower temperatures, the electron spin relaxation is slower and broadening is more pronounced (75).

It has been established that complexes of Pr, Nd, Sm, Tb, Dy, and Ho are upfield shift reagents with the relative ordering of shifts being Dy > Tb > Ho > Pr > Nd > Sm

(76). Complexes of Eu, Er, Yb, and Tm are downfield shift reagents with a relative ordering Tm > Er > Yb > Eu (76). The simplified form of the dipolar shift equation is given below:

$$\Delta H/H = K\,[\chi_Z - 1/2(\chi_X + \chi_Y)][(3\cos^2\Theta - 1)/r^3] \qquad [1]$$

where χ_X, χ_Y, and χ_Z are the magnetic susceptibilities along the principal axes of the complex. The constant K in the simplified form of the dipolar shift equation contains terms that reflect the magnetic susceptibility anisotropy of the particular lanthanide ion (76). The constant K in the equation is obtained by subtracting one half of the x and one half of the y components of the magnetic susceptibility values from the z component. Since the unpaired electrons in the lanthanide series are in 4f orbitals, these terms tend to be constant for a particular metal ion in different complexes. Therefore, in general, if χ_Z is less than $1/2\ (\chi_X + \chi_Y)$ for a metal ion, complexes with that metal will shift resonances in the NMR spectrum of the substrate upfield. The resonances will be shifted downfield if χ_Z is greater than $1/2\ (\chi_X + \chi_Y)$. The magnitude of the absolute value of this term determines whether a particular metal ion produces relatively large or small shifts in the NMR spectrum of a substrate.

The downfield shifts have been observed for shift reagents containing Tm, Eu, Er, and Yb (76). Downfield shifts are observed for certain nuclei of a substrate rather than for all of the nuclei of a substrate. Changes in sign of the geometric term of the simplified dipolar shift equation or the presence of a large contact shift are considered to be the factors contributing to the observation of downfield shifts (77,78). The geometric term of the dipolar shift equation changes its sign at 54.736^o and 125.264^o. Angles between the values of 54.736^o and 125.264^o are not common in studies with LSRs. However, exceptions were observed in a few cases involving large and rigid substrates (79). Dysprosium and thulium are the most powerful shift reagent metal ions. However, complexes of these metals may broaden the spectrum of substrates resulting

in the loss of fine structure from coupling. For the study of biologically important cations, strong shift reagents must be used to distinguish intra- from extracellular cations in cells since the induced shifts in metal NMR must be large in the presence of other competing ions. Hence for the study of cations in biological systems dysprosium and thulium are the metal ions of choice for shift reagents (45,60-62,66-70).

I.4.1.2 Selection of Ligands

The choice of ligands for biological shift reagents were primarily based on the ability of the complexes to exist in aqueous medium at physiological pH and induce shifts in the NMR spectrum of a substrate. Specifically, shift reagents for alkali metal NMR studies must be membrane impermeable, water soluble, and induce shifts of a desired cation in the presence of competing physiological cations. Investigations by Gupta et al. (61) and Springer et al. (66-68) have revealed that the higher the negative charge on shift reagent the better are the induced shifts in the metal NMR spectrum. $Dy(PPP)_2^{7-}$ induces by far the largest shifts in metal NMR resonances. A lot of activity has been generated recently in several laboratories to understand the mechanism of shifts induced by lanthanide complexes on metal NMR resonances with the aim of developing better shift reagents.

I.4.2 Mechanism of Shifts Induced By Lanthanide Complexes

Paramagnetic lanthanide complexes cause shifts in the NMR spectrum of the substrate by two possible mechanisms. The two mechanisms are the pseudocontact (through-space or dipolar) shift and contact (scalar) shift. A contact shift occurs if there is a finite probability of finding the unpaired electrons of the lanthanide ion at the nucleus whose NMR spectrum is being recorded. The pseudocontact shift is a result of a dipole-dipole interaction between the magnetic moment of the electrons of the lanthanide ion and the nuclear spin of the nucleus of interest.

Quantification and/or prediction of contact shifts is difficult since it requires a

detailed evaluation of the molecular orbitals involved (71). The pseudocontact shifts are readily described for a particular nucleus and depend on the location of the nucleus relative to the lanthanide ion. Since the unpaired electrons of the lanthanide ions reside in 4f orbitals, which are shielded by filled 5s and 5p orbitals, the shift mechanism with LSR is principally pseudocontact in origin (71).

An equation that describes the pseudocontact shift in the NMR spectrum of a nucleus in the presence of a paramagnetic transition metal ion with partially filled 3d orbitals was first derived by McConnell and Robertson in 1958 (80). This equation related the dipolar shift to anisotropy in the g-tensor. This treatment predicted a temperature dependence of relaxation rate (1/T). Bleany et al. (81,82) used anisotropy in the susceptibility, rather than the g-tensor, to account for dipolar shifts with LSR and predicted a T^{-2} dependence of lanthanide ions. Bleaney's derivation assumed incorrectly that the crystal field splittings for the lowest J state were small compared to kT. Horrocks (83) employed ligand field splittings to derive an equation with a more complicated temperature dependence. This approach requires a thorough knowledge of the crystal field parameters of the lanthanide complex and is not practical for many applications (84). Other derivations of the dipolar shift equation have also been reported in the literature (84,85). While most investigators seem to favor Bleaney's theorem or a modification of Bleaney's theorem (85), there is still no clear agreement on the exact form of the temperature dependence and theoretical basis of the shifts with LSR.

The general form of the equation that describes the dipolar shifts with LSR is shown in the equation below (76,86):

$$\Delta H/H = K[\chi_Z - 1/2(\chi_X + \chi_Y)]((3\cos^2\Theta - 1)/r^3) - K[\chi_X - \chi_Y](\sin^2\Theta\cos 2A/r^3) \qquad [2]$$

The angles Θ and Λ are defined by the relations $\cos\Theta = z/r$, $\sin\Theta \cos\Lambda = x/r$, and $\sin\Theta \sin\Lambda = y/r$, where (x,y,z) are the coordinates of the NMR nucleus in the complex.

The above equation is known as the extended form of the dipolar shift equation. The magnetic terms in the second part of the equation vanish when axial (C_3 or greater) symmetry is present. Six assumptions (86) are necessary to satisfy the requirements for applications of the simplified equation 1 above. These assumptions are:

I. The observed shifts used in the analysis are purely dipolar in origin;

II. Only a single stoichiometric complex species exists in equilibrium with the uncomplexed substrate;

III. Only a single geometric isomer of the complex is present;

IV. The isomer is magnetically axially symmetric so that the shifts are proportional to the geometric factor, $[(3\cos^2\Theta - 1)/r^3]$;

V. The principal magnetic axis has a particular, known orientation with respect to the substrate ligands;

VI. The substrate ligand exists in a single conformation, or at least an appropriate averaging over internal motions can be assumed.

It is difficult to fit the data to a unique solution using the extended dipolar equation 2. For this reason, most researchers have attempted to fit lanthanide shift data using the simplified equation 1.

The presence of contact shifts can be evaluated using the methods available in the literature (87-89). The advantages and disadvantages of the available methods have been discussed in detail (90,91). The most commonly used method is the ratio method (87,92). In this procedure, a reference nucleus is selected, and the ratio of the induced shift of each nucleus to that of the reference nucleus is calculated. In the absence of a contact shift, the ratio for a particular nucleus should remain constant for different lanthanide ions. Deviations in the ratios for different lanthanide ions imply the

presence of a contact shift. In certain cases the measured lanthanide induced shifts could contain a contact component and yet the ratios may not change. For example, the lanthanide induced pseudocontact and contact values are often large for protons close to the lanthanide. The measured lanthanide induced shift ratio remains equal to the lanthanide induced pseudocontact ratio which one is interested in obtaining, despite the fact that the measured lanthanide induced shift values contained a significant contact component. This method requires that the shift reagent-substrate complexes be isostructural for the entire lanthanide series.

The second most commonly used method assumes that a particular nucleus or set of nuclei exhibit shifts that are purely pseudocontact in origin. These nuclei are then used to fit the pseudocontact equation. The resulting geometry is used to calculate dipolar shifts for those nuclei suspected of exhibiting a contact shift. Any discrepancy between the calculated and observed shifts for these suspect nuclei are considered to result from a contact mechanism (93,94).

A third method that enables the direct determination of contact shifts is to measure the shifts in the spectrum of the substrate in the presence of Gd(III) complex (95). Gd(III), with an f^7 configuration, has an isotropic magnetic field. The shifts in the spectrum of a substrate in the presence of Gd(III) result from complexation and contact effects. The complexation shifts can be measured with the diamagnetic La(III) or Lu(III) complexes. Subtraction of these values from the shifts with Gd(III) yields the magnitude of the contact shifts. The magnitude of the contact shift with other lanthanide ions can be calculated. The major drawback in using this approach is the fact that it is difficult to measure the shifts induced by the Gd^{3+} reagent due to severe line broadening.

Reilley et al. (91) have described a method to separate contact and pseudocontact shifts that involves the use of calculated values of the relative theoretical dipolar and

contact shifts for the various lanthanide ions. By recording the data for at least three lanthanide ions and using nonlinear regression analysis, it is possible to solve for the contact and pseudocontact contributions. This method requires effective axial symmetry of the shift reagent-substrate complex and assumes that the crystal field is constant for all the lanthanide ions. Most of the studies have revealed that the contact contributions are minimal with LSR for cationic resonances (87-91).

Shifts in the NMR spectrum of a substrate that are due to complexation with LSR are referred to as complex formation shifts. These shifts are usually very small in magnitude when compared to the shifts that result from the anisotropic magnetic properties of the lanthanide ion. Complexation shifts are measured by recording the spectrum of the substrate in the presence of a diamagnetic LSR, either La(III) or Lu(III). The complex formation shift is assumed to be the same for all the lanthanide complexes with a particular ligand. The shifts recorded with a paramagnetic metal are corrected by subtracting the complexation shifts. The ligand : lanthanide stoichiometry of a lanthanide complex influences the magnitude of lanthanide induced shifts. If there are two species of the lanthanide complex present in solution during the NMR measurement, an average of the lanthanide induced shift will be recorded and this could be yielding incorrect information on the structure of the substrate-lanthanide complex. In order to obtain limiting shifts given the uncertainity of the nature of species present in solution, the lanthanide induced shifts for the substrate resonance is obtained at various concentrations of the lanthanide shift reagent while maintaining a constant substrate concentration. This procedure helps to obtain the limiting lanthanide induced shifts independent of the stoichiometry of the shift reagent. The ionization state of lanthanide complexes further complicates the equilibria in aqueous solutions. In order to avoid this problem, lanthanide induced shifts are obtained at low enough pH so that the proton competition with the lanthanide complex will decrease the possibility of forming

more than one species in solution. Ionic strength changes during titration in aqueous solution do affect the lanthanide induced shifts. To alleviate this problem, an inert salt is usually added to the solution to maintain ionic strength at a constant value. Thus all the contributing factors to lanthanide induced shifts can be determined after minimizing the potential hinderances as mentioned above. For lanthanide induced shifts in cationic resonances, the major contribution is generally a pseudocontact shift.

Chapter II

STATEMENT OF THE PROBLEM

The primary goal of this project is to study the binding and transport of lithium and magnesium in human erythrocytes using novel non-invasive nuclear magnetic resonance techniques and to advance the molecular understanding of abnormal lithium and magnesium distribution in erythrocytes from hypertensive patients.

Several studies have shown that an abnormality in Na^+ transport by Na^+ countertransport exists in RBCs from hypertensive patients (11,13,17-22). The high affinity of lithium for the Na^+ countertransport system was taken advantage of in designing an assay for measuring the rates of Na^+ exchange in RBCs (17). The abnormality in the rates of Li^+-Na^+ countertransport in RBCs from hypertensive patients was used to establish the abnormality in Na^+ countertransport pathway for hypertensive patients (17-22). Assays on Li^+-Na^+ countertransport were performed using atomic absorption spectrometry (17,18) and flame emission photometry techniques (14). These conventional techniques are invasive in nature in that separation of intra- and extracellular and lysis of intracellular compartment is required prior to chemical analysis. Besides being invasive in nature, these techniques are also time consuming. Vital information on ion binding to membrane, nature of ion binding sites, and changes in membrane potential are lost by these techniques.

^7Li NMR spectroscopy provides a non-invasive approach to study Li^+ transport in

biological tissues. It has been demonstrated that ^7Li NMR could be used to monitor Li^+ transport in RBCs (45,46,60,96) and in vesicles (97-100). These studies involved incorporation of membrane impermeable shift reagents in the suspension medium to distinguish the intra- and extracellular pools of Li^+. Most investigators have concentrated their efforts on the application of the shift reagent NMR method to study ion transport in RBCs and other biological systems. It is crucial however to evaluate the effects of shift reagents on the morphology, size, membrane potential and ion transport rates before this method can be applied to biomedical and clinical research.

A NMR method based on the different relaxation properties of intra- and extracellular K^+ was recently developed to distinguish intra- from extracellular K^+ (97). A similar method was developed by us to study Li^+ transport in RBCs (46). A comparison of the rates of Li^+ transport obtained by the two NMR methods was made and the best NMR method used to study the abnormality in Li^+ transport in hypertensive RBCs.

Since both Na^+ and Mg^{2+} appear to affect vascular resistance, it is important to investigate, using Li^+ as a marker of Na^+-Na^+ exchange and as a competing ion for Mg^{2+} binding sites, whether any relationship exists between hypertension, Na^+-Li^+ countertransport rates and intracellular free Mg^{2+} concentrations in RBCs.

Specific experiments were designed in an attempt to answer the following questions:

II.1 Characterization of Lanthanide Shift Reagents For Monitoring Li^+ Transport in Human RBCs by ^7Li NMR Spectroscopy

Of the complexes of Dy^{3+} or Tm^{3+} with TTHA, DPA, CA, NTA, TTHA, NOTP, DOTP, TETP, DTPP, PPP, and PcPcP, which are the shift reagents that induce the largest shifts on the $^7Li^+$ NMR resonances under constant ionic strength conditions?

Are the shifts induced by shift reagents pH dependent? Do physiological cations Na^+, K^+, Ca^{2+}, and Mg^{2+} compete with Li^+ for the shift reagent and lower the induced shifts? What effect do these shift reagents have on RBC shape, size, membrane potential and transport rates? Are the phosphonate shift reagents inert to hydrolysis by phosphatases present in biological systems?

II.2 Li^+-Na^+ Countertransport Measurements In RBCs From Hypertensive Patients And Normal Controls By Modified Inversion Recovery Pulse Sequence (MIR) And Atomic Absorption (AA)

Can MIR pulse sequence be used to determine intracellular Li^+ concentrations and Li^+-Na^+ countertransport rates in hypertensive and normotensive RBCs? How do the rates of Li^+-Na^+ countertransport obtained by the MIR method compare with those obtained by atomic absorption spectrometry?

II.3 Competition Between Li^+ And Mg^{2+} In Human RBCs

Does Li^+ cause any changes in the ^{31}P NMR spectra of ATP in Mg^{2+}-saturated and Mg^{2+}-depleted RBCs? What effect does Li^+ have on intracellular free Mg^{2+} concentration in normal RBCs? Does Li^+ have any effect on free Mg^{2+} concentration in model systems and in resealed RBC ghost systems? Do the ^7Li NMR relaxation rates and membrane ^{31}P NMR spectra convey any information on the mechanism of competition between Li^+ and Mg^{2+} in RBCs?

The use of a biochemical marker for hypertension based on abnormal Na^+ countertransport is still ambiguous. Conventional techniques have failed to enhance our understanding of the molecular aspects of cation transport in hypertension. With the advent of non-invasive NMR spectroscopy, it is possible to obtain information on ion

binding to the cell membrane and monitor membrane potential changes in intact RBCs. The salient feature of this project is that a reliable non-invasive NMR method can be used as a tool in clinical diagnosis of hypertension. Information on shift reagent effects obtained in this dissertation is likely to change the design and usage of new shift reagents in physiological NMR applications. This is especially useful for biological systems where the MIR approach is not feasible. The MIR approach is not feasible if the difference between intra- and extracellular T_1's for the system are not sufficiently different. The data on competition between Li^+ and Mg^{2+} in RBCs is likely to serve as a database for studying a similar mechanism in other human tissues.

CHAPTER III

EXPERIMENTAL METHODS

III.1 Materials

III.1.1 Reagents

Lithium chloride (LiCl), dysprosium chloride ($DyCl_3$), triethylenetetraamine hexaacetic acid (H_6TTHA), chelidamic acid (H_3CA), nitrilotriacetic acid (H_3NTA), dipicolinic acid (H_2DPA), nitrilotris(methylene) triphosphonate (NTP), sodium triphosphate (Na_5PPP), glucose, tetramethylammonium chloride, tetramethylammonium hydroxide, choline chloride, sucrose, deuterium oxide (D_2O), sodium chloride (NaCl), potassium chloride (KCl), magnesium chloride ($MgCl_2$), calcium chloride ($CaCl_2$), thulium chloride ($TmCl_3$), ouabain, hypophosphorous acid, paraformaldehyde, trifluoroacetate and trifluoroacetamide were supplied by Aldrich Chemical Company (Milwaukee, WI). HEPES [4-(2,hydroxyethyl)-1-piperazineethanesulfonic acid], and cacodylate were obtained from Sigma chemical company (St Louis, Missouri). Glutaraldehyde and osmium tetroxide were from Ladd Research Industries. Alkaline phosphatase and ionophore A23187 were supplied by Boehringer Mannheim. Bis(dihydroxyphosphinylmethyl) phosphinic acid (H_5PcPcP) was synthesized by Medichem Research Inc. (Chicago, IL). 1,4,7-tricyclononane-N,N',N''-tris(methylene) triphosphonate (NOTP) and 1,4,7,10-tetraazacyclododecane-N, N',N'',N'''-tetramethylenephosphonate (DOTP) were gifts from Professor Carlos F. G. C. Geraldes (University of Coimbra, Portugal). Diethylenetriaminepentamethylene phosphonate (DTPP) was obtained from Monsanto

Chemical Company (St Louis, Missouri). All chemicals were used as received except sodium triphosphate which was recrystallized three times from 40% ethanol.

III.1.2 Subjects

Packed red blood cells (RBCs) were supplied by the Chicago Chapter of Life Source. Whole blood samples from hypertensive patients and normotensive controls were obtained through the Renal section, Department of Medicine, Loyola University Stritch School of Medicine. The protocols for experiments involving human blood were approved by the Institutional Review Board for the Protection of Human Subjects (Loyola University Medical Center).

We studied 10 patients with clinically established essential hypertension without evidence of renal or heart failure or severe retinopathy. The duration of hypertension ranged from two months to 20 years. Some of the patients were on antihypertensive medication and had no dietary restriction. The antihypertensive medication being taken by the patients in Table IX of this study are verapamil for patient 1, atenolol for patients 3, 6 and 7, enalapril for patients 4, 5, 6 and 8, clonidine for patient 9, and HCTZ for patient 10. None of the patients or controls suffered from family hypertension except for patients 1, 2 and 4. Their blood pressure was well controlled with antihypertensive medication at the time 15 mL of blood was drawn for this study. Sex and race matched normal controls were also studied. Normotensive subjects had no personal or family history of hypertension and were free of any disease. The ages, weights, and smoking habits of both patients and controls are also stated in Table IX. The ages of hypertensive and normotensive subjects were not matched due to the practical difficulty in obtaining RBCs from normotensive patients free of any illness in the same age group as hypertensives.

III.2 Instrumentation

III.2.1 NMR Studies

^{6}Li, ^{7}Li, ^{19}F, ^{23}Na, and ^{31}P measurements were made at 44.2, 116.5, 282.2, 79.4, and 121.4 MHz respectively on a Varian VXR-300 NMR spectrometer. The instrument was equipped with a 10 mm multinuclear probe and a variable temperature unit. The probe temperature was 37° C. Spin-lattice relaxation time (T_1) measurements were performed using the inversion recovery method while spin-spin relaxation time (T_2) measurements were done by the Carl-Purcell-Meiboom-Gill method (102).

The T_1 of intra- and extracellular $^{7}Li^{+}$ resonances of Li^{+}-loaded normal RBCs were measured to be 5 and 16.5 s, respectively (45,46,60). The T_1 of extracellular $^{7}Li^{+}$ resonance in the presence of a shift reagent was 0.1 s (45). The knowledge of a difference in T_1 values was taken into consideration in choosing the flip angle and the repetition time. In samples containing shift reagents, ^{7}Li NMR spectra were obtained using a 45° flip angle with a repetition rate of 7.5 s (1.5 T_1). Most RBC samples were run unlocked, while other samples had 17% D_2O for field frequency lock.

A standard single pulse sequence was employed to obtain the NMR spectra of samples containing shift reagents. The other ^{7}Li NMR method employs a modified inversion recovery (MIR) pulse sequence (D_1-180°-D_2-60°-Acquire) and does not involve the incorporation of a shift reagent in the suspension medium. The pulse sequences for both NMR methods are shown in Figure 3 and the acquisition parameters for the ^{7}Li MIR method in Table 1. NMR experiments were run under identical gain settings and absolute intensity conditions. Pulse-width and delay times D_1 and D_2 in the MIR sequence were checked regularly and found to be reproducible.

The ^{6}Li NMR experiments were performed using a spectral width of 8000 Hz at a probe temperature of 25° C. All ^{6}Li experiments involved measuring the T_1 of $^{6}Li^{+}$ in the presence of $Dy(PPP)_2^{7-}$. In ^{23}Na NMR experiments a 45° pulse was used to observe a spectral width of 8000 Hz with an acquisition time of 1 s.

In obtaining ^{31}P NMR spectra of $Dy(PPP)_2^{7-}$ complex, 45° pulses were used with

Figure3. (A) Standard single pulse sequence, and (B) Modified inversion recovery pulse sequence.

A

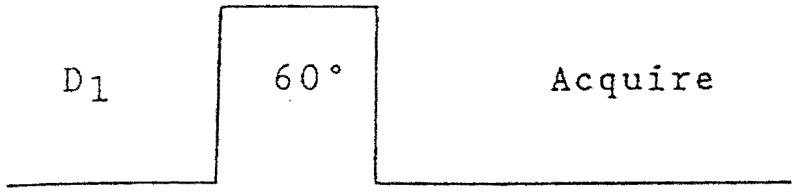

B

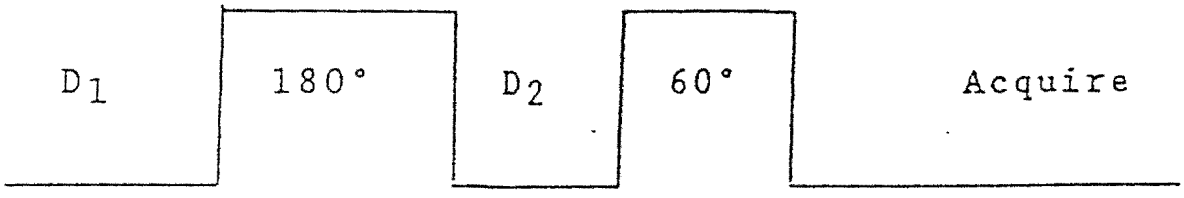

Table 1

^{7}Li MIR Parameters

180^{o} Pulse width/μs	60
60^{o} Pulse width/μs	20
D1 delay/s	60 (3 x longest T_1)
D2 delay/s	11.5
Pre-acquisition delay array/s	0,300,300,300,300,300,300
Probe Temperature/^{o}C	37
Line Broadening/Hz	5

0.72 s repetition time. The probe temperature was 25°C. ^{31}P NMR spectra of ATP in RBC and model systems were obtained using a 45° pulse width with an acquisition time of 1.5 s, the probe being maintained at 37°C.

III.2.2 Atomic Absorption Studies

AAS studies were performed on a Perkin-Elmer spectrophotometer, model 5000, equipped with a graphite furnace. Determinations of Li^+-Na^+ exchange rates by AAS were obtained by following established procedures (11,12).

III.2.3 Osmometer

The osmolarity of the suspension medium used for all the RBC samples was adjusted to 300 ± 5 mOsm with glucose, using a Wescor Vapor Pressure Osmometer.

III.2.4 Centrifuge

Blood processing and resealed RBC ghosts were prepared at 4°C using a Dupont model RC-5B refrigerated centrifuge, which was equipped with a Sorvall SS-34 rotor. A Savant refrigerated centrifuge, model HSC10000, was also used in washing blood.

III.2.5 Cell Volume Measurements

RBC volume changes were monitored using a Coulter Counter (CC), Model ZM. A 1:20,000 sample dilution of samples was made in the Na^+, Choline or Mg^{2+} media. The dilution medium used depended on the experiments performed. The dilution factor was taken into account in analysing the reported data.

III.2.6 Scanning Electron Microscopy

Scanning electron micrographs were obtained using an ISI SX-30 scanning electron microscope, operating at 15 kV. RBC diameter measurements on SEM micrographs were performed using the image analyzing system Bio-Quant II, interfaced with an Apple IIe computer.

III.2.7 Potentiometric Titrations

Potentiometric titrations were carried out with an Orion pH meter model 701A. 6 mM tetramethylammonium triphosphate and 3 mM $Dy(PPP)_2^{7-}$ (in tetramethylammonium form) were titrated with standard 0.1 M NaOH. The shift reagent was titrated in the presence and absence of 100 mM LiCl. Protonation constants were obtained through a computer program which used a simplex non-linear regression algorithm for fitting the potentiometric curves (103).

III.3 Sample Preparation

III.3.1 Preparation of Shift Reagents

The shift reagents containing the ligands $TTHA^{6-}$, HCA^{3-}, NTA^{3-}, and DPA^{2-} were freshly prepared by in situ methods previously described (65-68), with the exception that tetramethylammonium hydroxide was used as a base. With this modified procedure, these shift reagents were in the form of tetramethylammonium salts. This was done so that the bulky counter cation would be less competitive with alkali and alkaline-earth metal cations being studied.

Tetramethylammonium Dy(III) or Tm(III) triphosphate were prepared by the following method. Recrystallized Na_5PPP was passed down a cation-exchange Dowex-50 column loaded with tetramethylammonium chloride. The tetramethylammonium triphosphate thus obtained was recrystallized five times and was checked by ^{23}Na NMR and AAS for any residual sodium. Sodium content of tetramethylammonium triphosphate was estimated to be less than 9% of sodium present in Na_5PPP. The tetramethylammonium form of shift reagents $Dy(PPP)_2^{7-}$ and $Tm(PPP)_2^{7-}$ were obtained from the respective dysprosium and thulium chlorides by an in situ reaction with tetramethylammonium triphosphate.

The shift reagents containing the ligands $DOTP^{8-}$ and $NOTP^{6-}$ were prepared using the procedure of Sherry et al. (104).

The HEPES buffer, which was used in all the experiments, was adjusted to

physiological pH range with tetramethylammonium chloride. Ionic contributions from LiCl or NaCl, shift reagent, HEPES, and tetramethylammonium hydroxide used in adjusting pH, were taken into account in estimating the amount of tetramethylammonium chloride required to adjust the solution to a constant ionic strength.

III.3.2 Preparation of Li^+-loaded RBCs

Freshly packed RBCs or whole blood samples were washed three times with isotonic 5 mM sodium phosphate - 150 mM NaCl buffer, pH 7.4, by centrifugation at 2000 g for 6 minutes at 4^oC using a Savant refrigerated centrifuge.

Li^+ loading of RBCs were done by different procedures depending on the nature of experiments for which it was being used. Li^+ loaded RBCs for transport measurements were obtained by incubating RBCs (50% hematocrit) with 150 mM LiCl, 10 mM glucose, 10 mM HEPES, pH 7.4 at 37^oC for 3 hours. Intracellular Li^+ concentration in RBC was approximately 1 mM. The Li^+ loaded RBCs were washed five times with washing buffer (112.5 mM choline chloride, 85 mM sucrose, 10 mM glucose, 10 mM HEPES pH 7.4) at 4^oC by centrifugation at 2000g for 6 minutes. This procedure helps to remove all extracellular Li^+. Li^+-loaded RBCs were suspended at 13% hematocrit in the media immediately before transport measurements.

RBCs were incubated with different levels of Li^+ for SEM experiments, according to a modification of the procedure of Zimmermann and Soumpasis (105). RBCs at 5% hematocrit were suspended in an isotonic medium containing varying concentrations of LiCl (1.5 mM to 140 mM), 10 mM glucose, and 20 mM HEPES at pH 7.4, and incubated at 37^oC for 1 hour. The Li^+-loaded cells were then washed twice and resuspended in an isotonic solution containing varying concentrations of LiCl as indicated above. Osmolarity was adjusted to 300 $\pm$ 5 mosM using NaCl. The concentration of NaCl used depended on the concentration of LiCl.

For experiments designed to study the competition between Li^+ and Mg^{2+} in

RBCs, LiCl loading of RBCs was achieved by incubating the cells in a medium containing 40 mM LiCl, 100 mM NaCl, 5 mM KCl, 10 mM glucose, and 20 mM HEPES, pH 7.2 at 37° C for 12 hours. An intracellular RBC Li^+ concentration of 3 mM was achieved by this loading procedure. Using these loading conditions, no Li^+-induced hydrolysis of ATP in RBCs was detected by ^{31}P NMR. Mg^{2+} levels were also measured in suspension media before and after Li^+ loading. The RBC Li^+ loading procedure outlined above does not induce Mg^{2+} leak since the Mg^{2+} concentration, measured by optical absorbance using antipyrylazo-III (106) and atomic absorption, was the same in suspension media of Li^+-loaded RBC and Li^+-free control samples. The intracellular pH in Li^+-loaded and Li^+-free RBCs was monitored by measuring the separation between the P_i and P_α resonances. The pH was found to be 7.2 ± 0.1 and thus, Li^+ loading of RBC had no significant effect on intracellular pH.

III.3.3 Preparation of Resealed RBC Ghosts

The resealed RBC ghosts were prepared by lysing cells in a hypotonic buffer as per the procedure in reference 107. Briefly, one volume of washed RBCs was diluted four fold with 5 mM sodium phosphate buffer, pH 8 (5P8 buffer). The RBC ghosts were isolated by lysing and washing RBCs several times (at least five times) in 5P8 buffer by centrifugation at 38,720g for 8 minutes at 4°C on a Sorvall RC-5B high speed centrifuge. The white ghosts obtained were then washed with 5P8 buffer containing 1 mM $MgCl_2$.

Resealed Li^+ or Mg^{2+} loaded resealed RBC ghosts were obtained by incubating the ghosts in 5P8 buffer containing Li^+ or Mg^{2+} at four times the desired intracellular concentration. Resealed RBC ghosts were prepared and loaded with antipyrylazo-III according to the procedure of Yingst and Hoffman (106). The ghosts were suspended in the desired media prior to analysis.

III.3.4 Determination Li^+-Na^+ Countertransport Rates

The Li^+-loaded packed RBCs either from hypertensive patients or normotensive controls were suspended in isotonic media containing either 150 mM NaCl, 10 mM glucose, 0.1 mM ouabain, 10 mM TRIS-Cl pH 7.4 or 75 mM $MgCl_2$, 85 mM sucrose, 10 mM glucose, 0.1 mM ouabain, 10 mM TRIS-Cl pH 7.4. Ouabain inhibited any Li^+ transport through Na^+,K^+-ATPase (108). In experiments involving shift reagents choline chloride was used instead of $MgCl_2$. The $MgCl_2$ or choline chloride suspension medium allows the determination of the contribution of the leak pathway towards Li^+ efflux (41). The rate of Li^+ transport measured in the Na^+ medium is made up of two components: the Na^+-Li^+ countertransport and the leak pathways. The reported rates of Na^+-Li^+ countertransport were obtained by subtracting the measured rates in Na^+ and Mg^{2+} media (17,46).

III.3.5 SEM and Coulter counter measurements

0.05 ml of the Li^+-free and the Li^+-loaded RBC suspensions with and without shift reagents from the above preparation (section III.3.2) were placed on a 10 x 10 mm cover slip. After the RBCs were allowed to settle for 20 seconds, they were covered with a solution containing 3% glutaraldehyde, 3% paraformaldehyde in 0.1 M cacodylate buffer at pH 7.5 and rinsed thoroughly in this fixation solution. Post fixation was done in 1% OsO_4 at pH 7.5. After dehydration in ethanol, critical point drying was performed in liquid CO_2. The specimens were sputted with gold-palladium alloy to a thickness of about 30 nm in argon atmosphere using Hummer VI sputtering system from Analtech Ltd. Photographs were taken with an ISI SX-30 scanning electron microscope at 15 kV. Size measurements of RBCs were performed on SEM pictures using the image analyzing system Bio-Quant II, interfaced with an Apple IIe computer. SEM data for each entry in Table IV and Table V were obtained on six samples. About 8 to 10 pictures were taken for each sample.

III.4 Data Analysis

III.4.1 Determination of Li^+ Concentrations By ^7Li NMR

The RBC intra- and extracellular ^7Li NMR resonance areas determined by the shift reagent measured were recorded directly by integrating the spectra. The MIR approach helps to measure the intracellular Li^+ resonance areas directly. The resonance areas of the extracellular Li^+ were measured from the difference spectra obtained from the standard single pulse and MIR spectra of the same sample. The details of the MIR pulse sequence have been described in references 46 and 109.

The intracellular Li^+ concentration can be obtained from the ^7Li NMR resonance areas using the following equations:

$$A = A_{obs} / (f_{in} \cdot C_1) \qquad [1]$$

$$f_{in} = A_{in} / (A_{std} \cdot C_1) \qquad [2]$$

$$f_{out} = C_1 \cdot A_{out} / (Astd) \qquad [3]$$

where A_{in} and A_{out} represent the areas of known intra- and extracellular Li^+ concentrations (in mM) in isotonic RBC suspensions, A_{std} is the peak area for the same Li^+ concentration as in A_{in} and A_{out} except that there was no RBCs in the suspension medium. The fractional intra- and extracellular NMR windows are represented by f_{in} and f_{out}, respectively. The standard single pulse sequence was used to measure A_{std} and A_{out}, while the MIR pulse sequence was used for obtaining A_{in}. Since the intracellular Li^+ areas (A_{obs} and A_{in}) obtained by MIR sequence represent 80% of the total resonance area, hence a correction factor C_1 was incorporated in the above equations. The extracellular Li^+ peak area obtained by MIR spectral subtraction is overestimated by 20%, hence the correction factor C_1 was also used. While using a single pulse sequence the value of correction factor C_1 was equal to 1. The fractional NMR windows, f_{in} and f_{out}, are a measure of apparent hematocrit in the NMR window. The apparent hematocrit measured by NMR is described in great detail in reference 109.

For an RBC suspension, the observed intracellular Li^+ areas (A_{obs}) are corrected

(A) for the intracellular volume as shown in the equation below:

$$A = A_{obs} \times (A_{std} / A_{in}) \qquad [4]$$

RBCs were loaded with varying concentrations of intracellular Li^+ (0.2-3.5 mM) and suspended in an isotonic buffer at 13% hematocrit. The intracellular ^7Li NMR resonances of RBC samples were compared with standard aqueous solutions of LiCl (0.2-3.5 mM). The intracellular Li^+ concentrations were also determined by AA and compared with those obtained by NMR. In all the Li^+ calibration curves, a pulse width corresponding to 60^o was used.

III.4.2 Determination of Li^+ Concentrations by AAS

Li^+-loaded RBC containing suspension was centrifuged at 2000 g for 6 min at 4^oC. The packed cells were separated from the suspension medium. Prior to AA analysis an aliquot (50 μl) of packed Li^+-loaded RBCs (98 $\pm$ 2% hematocrit) were lysed by dilution with deionized water up to 25 times its original volume. The supernatant was diluted, if necessary, with deionized water.

Li^+ standards for calibration purposes were obtained on samples similar to RBC lysates and supernatants. In order to determine intracellular Li^+ concentrations, the standards were prepared by lysing 50 μl of Li^+-free packed RBCs as given above, except that the resulting lysate contained varying concentrations (0.2-0.42 μg/ml) of LiCl. The standards for determination of Li^+ in the supernatant were prepared in sodium or choline medium containing 0.2-42 μg/ml of LiCl. Absorption measurements were obtained by injecting 10 μl of the samples prepared above into the graphite furnace. Three independent measurements were made on each sample. Also the samples were prepared in triplicate.

The calibration curves for sodium and choline media were obtained by plotting the absorbance against Li^+ concentrations. The concentrations of Li^+ in RBC lysates or supernatants were obtained using the appropriate calibration curves,

hematocrit and dilution factors as shown in the equations below:

$$[Li^+]_{RBC} = \frac{[Li^+]_a \text{ x dilution factor}}{\text{(hematocrit) x (Mol wt of LiCl)}} \quad [7]$$

$$[Li^+]_S = \frac{[Li^+]_a \text{ x dilution factor}}{\text{(1 - hematocrit) x (Mol wt LiCl)}} \quad [8]$$

where $[Li^+]_{RBC}$, $[Li^+]_a$, and $[Li^+]s$ corrrespond to intracellular RBC Li^+ concentration, Li^+ concentration from AA calibration graph, and Li^+ concentration in the supernatant respectively.

III.4.3 Determinations of Rate Constants for Na^+-Li^+ Countertransport

The first order rate constant for the Na^+-Li^+ countertransport pathway was also estimated from MIR data. The rate constant for Li^+ efflux can be obtained from the equation given below.

$$\ln [Li^+]_t / [Li^+]_0 = kt$$

where $[Li^+]_0$ and $[Li^+]_t$ correspond to Li^+ concentrations at time zero and at different intervals of time, respectively. k denotes the first order rate constant. A plot of ln $\{[Li^+]_t / [Li^+]_0\}$ versus time is linear with a slope of k. The rate constant k is obtained for Li^+ efflux in Na^+- and Mg^{2+}-media. Subtracting the rate constant obtained for Li^+ efflux in Mg^{2+} medium from that obtained in Na^+-medium gives the rate constant for the Na^+-Li^+ countertransport pathway.

III.4.4 Statistical Analysis of Data

The statistical significance of the data obtained in this study has been analysed using a student t-test. The confidence levels are indicated as footnotes to the tables.

CHAPTER IV

RESULTS

IV.1 Characterization And Comparison of Aminocarboxylate Shift Reagents With Triphosphate Shift Reagent

IV.1.1 $^{7}Li^{+}$ NMR Paramagnetic Shifts Induced By Aminocarboxylate Complexes of Dysprosium And Thulium

The efficacy of the dysprosium and thulium chelates (Figure 2) as shift reagents for $^{7}Li^{+}$ NMR studies was tested. For these experiments, the following parameters were held constant: LiCl concentration at 5 mM, pH at 7.5, and the ionic strength at 0.36. Ten different shift reagents were tested, varying their concentrations from 3 to 30 mM.

The shift values are plotted against the stoichiometric mole ratio of shift reagent to Li^{+}, ρ, in Figure 4. The shifts induced in the $^{7}Li^{+}$ NMR resonance by $Dy(PPP)_2^{7-}$, $Tm(PPP)_2^{7-}$ and $Dy(TTHA)^{3-}$ are significantly larger than those induced by $Dy(HCA)_3^{3-}$, $Tm(HCA)_3^{3-}$, $Dy(NTA)_2^{3-}$, $Tm(NTA)_2^{3-}$, $Dy(DPA)_3^{3-}$, $Tm(DPA)_3^{3-}$ and $Tm(TTHA)^{3-}$, under similar conditions. Slightly larger shifts may have been observed if the solution were free of added salt. However, the shifts are close to their maximum value since a bulky, non-competitive organic counter cation, tetramethylammonium, was used.

Figure 4. Dependence of paramagnetic $^{7}Li^{+}$ NMR shifts induced by several shift reagents on [shift reagent]/[Li^{+}] ratio. Full and dotted lines indicate data for Dy3+ and Tm^{3+} shift reagents, respectively. The symbols for the ligands PPP^{5-} (○), $TTHA3^{-}$ (+), NTA^{3-} (▽), DPA^{2-} (△), and HCA^{2-} (X) are indicated in parenthesis. Each point represents the average of $^{7}Li^{+}$ NMR measurements on three separate samples. In all cases, the agreement was within 0.02 ppm. Li^{+} concentration was held constant at 5 mM while the shift reagent concentrations varied. All solutions were buffered with 50 mM HEPES and also contained 10 mM glucose and 17% D_2O. The pH was adjusted to 7.5 with tetramethylammonium hydroxide. Ionic strength was adjusted to 0.36 with tetramethylammonium chloride so that all samples had the same ionic strength as that of 30 mM $Dy(PPP)_2^{7-}$. NMR conditions are described in experimental section.

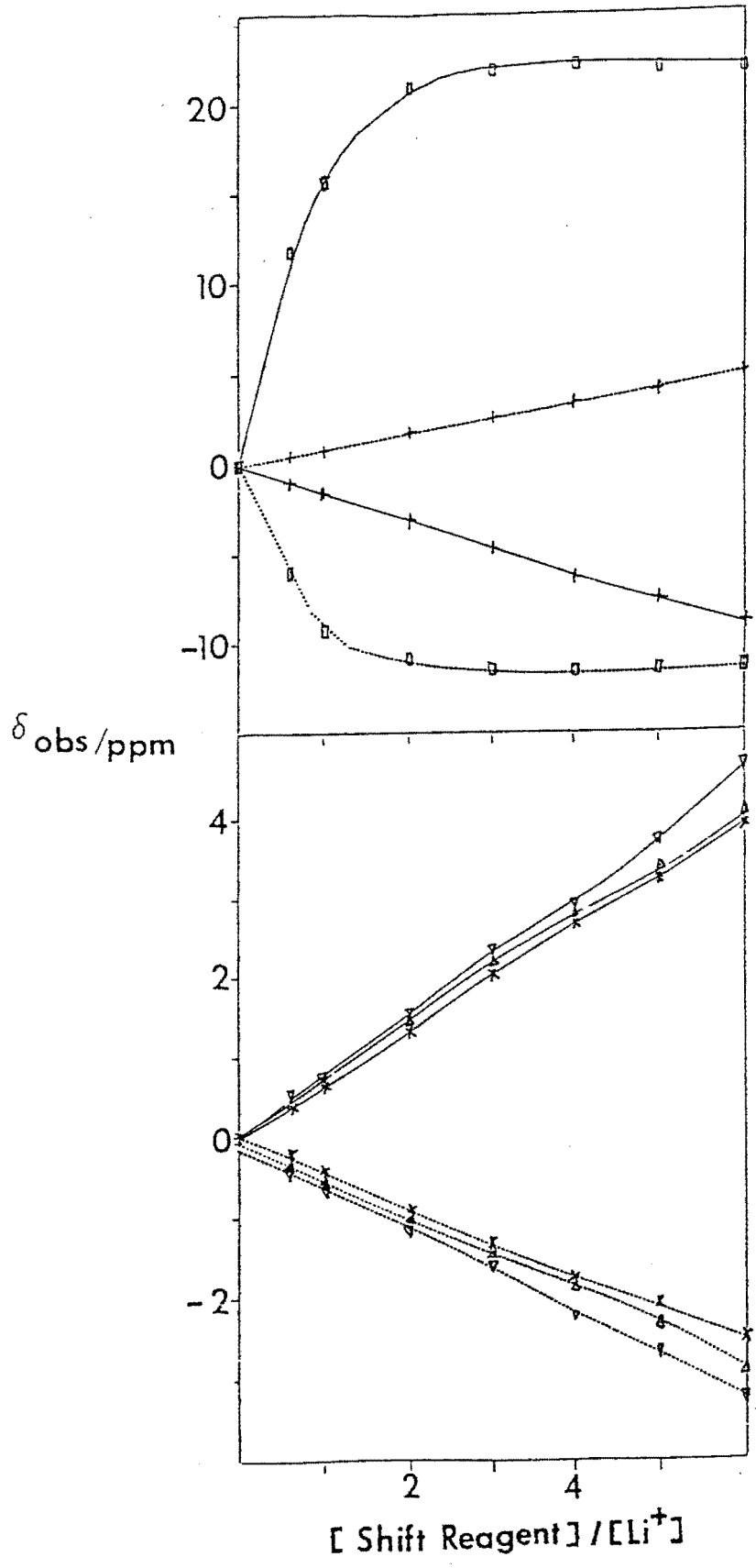
20
10
0
-10
δ obs /ppm
4
2
0
-2
2
4
[Shift Reagent] / [Li+]

Much larger $^{7}Li^{+}$ NMR shifts can be obtained at alkaline pH with the chelidamate shift reagents (data not shown). The enhanced shifts at alkaline pH are due to the increased electrostatic interaction between Li^{+} and the shift reagent, $Dy(CA)_3^{6-}$ or $Tm(CA)_3^{6-}$, resulting from the deprotonation of the chelidamate ligands above pH 8 (67). Similar observations were reported for $^{23}Na^{+}$ NMR shifts (68). Based on these studies alone, we conclude that $Dy(PPP)_2^{7-}$, $Tm(PPP)_2^{7-}$ and $Dy(TTHA)^{3-}$ are the preferred shift reagents among those tested for $^{7}Li^{+}$ NMR studies under physiological conditions.

IV.1.2 pH Dependence of $^{7}Li^{+}$ And $^{23}Na^{+}$ NMR Isotropic Shifts

As shown in Figure 5, the $^{7}Li^{+}$ shifts induced by $Dy(PPP)_2^{7-}$ and $Tm(PPP)_2^{7-}$ show a very strong pH dependence while the shift induced by $Dy(TTHA)^{3-}$ is quite independent of pH between 6 and 8.5. The decreased $^{7}Li^{+}$ NMR shifts observed above pH 8 for the triphosphate shift reagents may be due to increased competition for Li^{+} ions from the tetramethylammonium cations, which were increasing in concentration since tetramethylammonium hydroxide was used to adjust the pH. More likely, the decreased shifts are due to OH^{-} ions replacing the PPP^{5-} ligand at alkaline pH, leading to the formation of $Dy(OH)_3$ (68), as a precipitate of $Dy(OH)_3$ was observed above pH 8.5. The maximum positive shift observed on the $Dy(PPP)_2^{7-}$ occurs at a higher pH than the maximum negative shift on the $Tm(PPP)_2^{7-}$. This behavior may be related to the lower affinity of Dy^{3+} complexes for OH^{-} relative to the Tm^{3+} analog (70). However, the most important region from a physiological standpoint is that below pH 8, where the pH dependence of the paramagnetic shifts afforded by the triphosphate shift reagents is more noticeable.

The titration of 5 mM $Dy(PPP)_2^{7-}$ with excess Li^{+} or Na^{+} at pH 5.5 and 7.5 was monitored by ^{7}Li or ^{23}Na NMR spectroscopy, respectively (Figure 6). Li^{+} or Na^{+} were found to bind biphasically to the shift reagent at both pH values studied.

Figure 5. pH dependence of paramagnetic shifts afforded by $Dy(PPP)_2^{7-}$ (□), $Dy(TTHA)^{3-}$ (+), and $Tm(PPP)_2^{7-}$ (◇). Li^+ concentration was held constant at 5 mM in the three curves. The $Dy(PPP)_2^{7-}$ was kept constant at 5 mM while $Dy(TTHA)^{3-}$ and $Tm(PPP)_2^{7-}$ were held at 15 mM. The reported pH values are not corrected for the deuterium isotope effect. The pH dependence of $^7Li^+$ shifts was found to be reversible by adding tetramethylammonium hydroxide and HCl above and below pH 7.5, respectively.

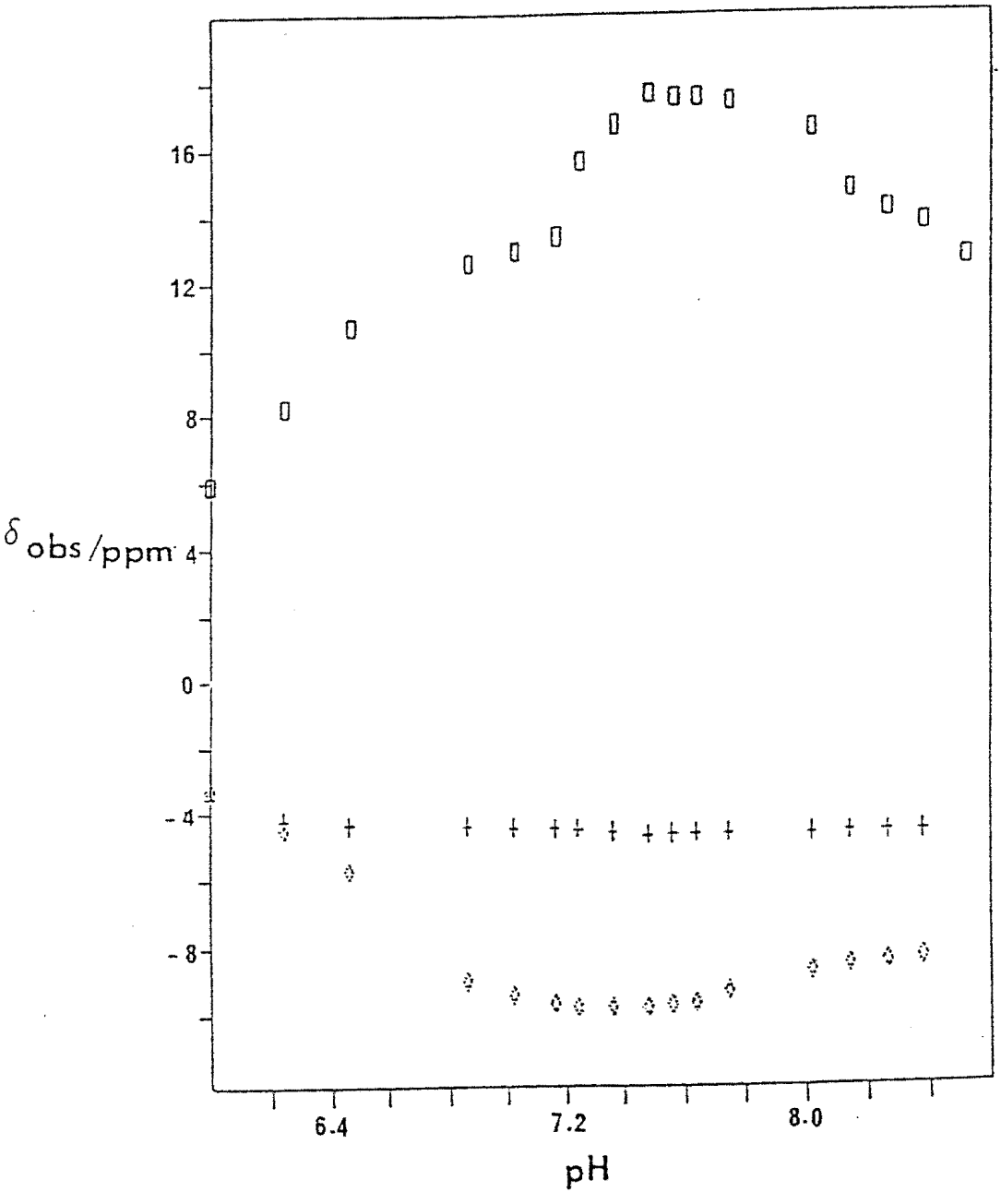
16
12
8
4
0
-4
-8
δ obs /ppm
6.4
7.2
8.0
pH

Figure 6. Titration of $^{7}Li^{+}$ (closed symbols) and $^{23}Na^{+}$ (open symbols) NMR paramagnetic shifts at pH 7.5 (squares) and 5.5 (triangles). $Dy(PPP)_2^{7-}$ concentration was held constant at 5 mM and Li^{+} or Na^{+} concentration was varied. The shift reagent used was in the tetramethylammonium form.

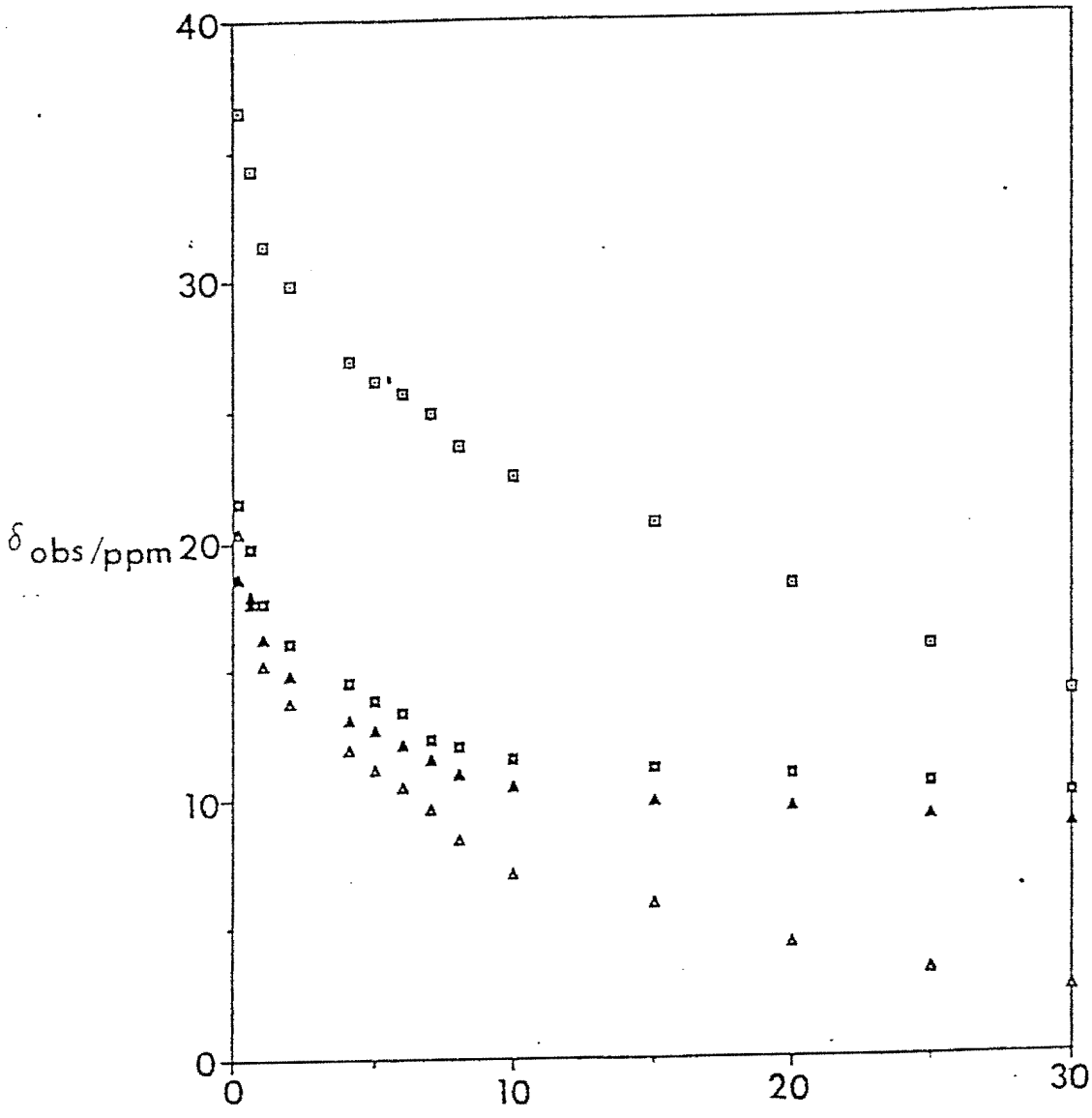
40
30
20
10
0
δ obs /ppm
0
10
20
30
[M+]/[Shift reagent]

Extrapolation of the linear portions of the curves results in breaks at $[M^+]$/[shift reagent] ratios of approximately 5 and 7 at pH 5.5 and 7.5, respectively. We conclude that up to seven Li^+ (or Na^+) ions are required to saturate all the binding sites on the shift reagent species, $Dy(PPP)_2^{7-}$, $DyH(PPP)_2^{6-}$, and $DyH_2(PPP)_2^{5-}$, present at pH 7.5 (110). At pH 5.5, the major species present in solution are $DyH_2(PPP)_2^{5-}$ and $Dy(PPP)^{2-}$ (110). Thus, the smaller number of cations bound at pH 5.5 (Figure 6) and the decreased $^7Li^+$ shifts below pH 7.0 (Figure 5) are presumably due to the presence of species with reduced negative charge at lower pH.

The $^7Li^+$ (or $^{23}Na^+$) paramagnetic shifts are maximized at $[M^+]$/[shift reagent] ratios of less than 1. This observation is evidence for a preferred Li^+ binding site in the second coordination sphere of the shift reagent (Figure 7.B) (69). However, solution structures that involve a preferential binding site for Li^+ in close proximity to the lanthanide ion (Figures 7.A and 7.C) (68,111) cannot be ruled out. Figure 6 shows that gradual decreases in $^7Li^+$ (and $^{23}Na^+$) shifts continue to occur after a ratio of 1. These results are in agreement with multinuclear NMR studies on dysprosium (III) triphosphate (69) carried out at pH 7.5 that suggest a solution structure where alkali countercations are present in the second coordination sphere of the complex thereby neutralizing its -7 charge (Figure 7.B). Thus, the first equivalent of Li^+ added to $Dy(PPP)_2^{7-}$ at pH 7.5 occupies a preferential binding site with a specific θ value and therefore a specific pseudo-contact shift. Further addition of Li^+ leads to exchange between the Li^+ on the preferred site and those on other locations (Figure 7.B). Each Li^+ location has its own θ and corresponding pseudo-contact shift. Averaging leads to a decrease of the $(3\cos^2\theta - 1)/r^3$ term and therefore to a decrease of the $^7Li^+$ paramagnetic shift. After the addition of a maximum of seven Li^+ ions depending on the species present at pH 7.5, further addition of Li^+ results in cation exchange between Li^+ in the second coordination sphere and the bulk solution. This results in an asymptotical decrease in

Figure 7. Hypothetical solution structures for $Dy(PPP)_2^{7-}$ based on studies reported in refs. 68 (A), 69 (B), and 111 (C).

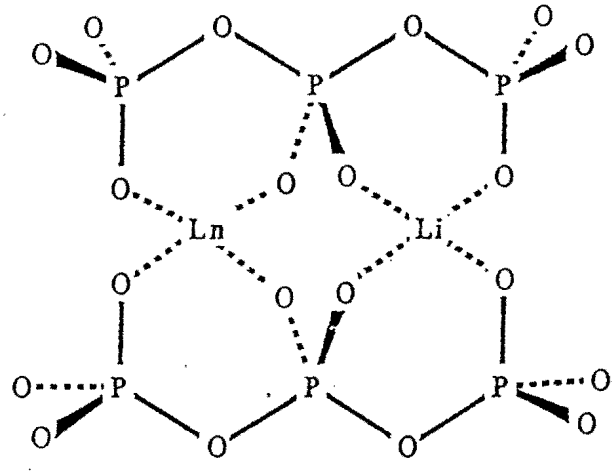

A

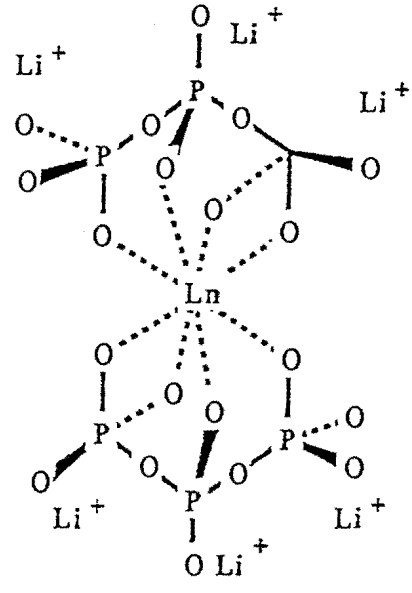

B

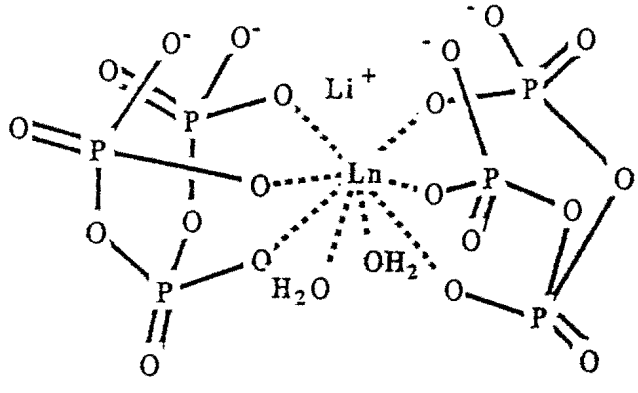

C

$^{7}Li^{+}$ paramagnetic shift down to zero.

Based on plots of $\delta_{obs}/[Li^{+}]$ vs. δ_{obs} of the linear portions of the curves at pH 7.5 for $[Li^{+}]/[\text{shift reagent}] \leq 2$ or ≥ 10, respectively, the first and last Li^{+} association constants were calculated to be approximately 740 and 136 M^{-1} (r = 0.98). The last Na^{+} association constant at pH 7.5 (135 M^{-1}) is of the same order of magnitude as those obtained previously by an independent ^{23}Na NMR study (120-360 M^{-1}) (111). The changes of $^{7}Li^{+}$ NMR shifts were less drastic in similar experiments performed with $Dy(TTHA)^{3-}$ (data not shown), indicating weaker binding ($K < 50$ M^{-1}) of Li^{+} to this shift reagent relative to $Dy(PPP)_2^{7-}$. We further investigated the pH dependence of the shifts induced by the triphosphate shift reagents by potentiometric and ^{31}P NMR titrations.

IV.1.3 Potentiometric Titration Studies of $Dy(PPP)_2^{7-}$

Table II compares protonation constants obtained from potentiometric titrations of PPP^{5-}, and of $Dy(PPP)_2^{7-}$ in the presence and absence of Li^{+}. Dy^{3+} binding considerably lowers the pKa's of the ligand due to competition between metal and hydrogen ions. This observation agrees with a previous report on the protonation of metal chelates of triphosphate with lanthanide ions (110). The binding of Ca^{2+} and Mg^{2+} is also known to lower the pKa_1 value of PPP^{5-} to 6.0 and 5.5, respectively (112,113). The presence of excess Li^{+} ions was found to decrease pKa_1 of $Dy(PPP)_2^{7-}$ by 0.5 units, while they do not significantly affect the subsequent pKa's. Similarly binding of Li^{+} is known to lower the pKa_1 value of the free ligand from 8.9 to 6.8 (110,113). Thus, at least one Li^{+} ion may preferentially coordinate to one of the outer phosphate groups undergoing deprotonation.

Table II also indicates the presence of more than one pKa of $Dy(PPP)_2^{7-}$ in the region where the $^{7}Li^{+}$ NMR chemical shift is strongly pH dependent. The uptake of

Table II

Protonation constants obtained by potentiometric titrations of tetramethylammonium salts of PPP^{5-} and $Dy(PPP)_2^{7-}$

	$(NMe_4)_5PPP$		$(NMe_4)_7Dy(PPP)_2$	
	I = 0[a]	I = 0.1[b]	No LiCl	100 mM LiCl
pKa_1	8.90	8.63	6.67	6.19
pKa_2	6.26	6.01	4.97	4.94
pKa_3	2.30	c	3.22	3.44
pKa_4	low	c	1.60	1.57
pKa_5	low	c	c	c

[a]Data from ref 110; [b]This work; [c]Not determined.

approximately two protons per shift reagent molecule below pH 5 implies that its approximate overall charge is decreased at lower pH. One would expect a decrease in the number of Li^+ (or other cations) binding sites at pH 5.5 as a result of lower charge, if the mechanism of interaction between Li^+ and the shift reagent were predominantly electrostatic.

IV.1.4 ^{31}P NMR titration studies of $Dy(PPP)_2^{7-}$

^{31}P NMR spectra of $Dy(PPP)_2^{7-}$ at pH 6.5, 7.4, and 8.3 in the absence of LiCl (Figure 8) exhibit an $A(X_2)$ type spectrum indicating that the outer phosphates of the triphosphate ligands are equivalent at all measured pH values. The chemical shift position of the α,γ-resonances is in general more sensitive to pH than that of the β-resonance (Table III). This observation is in agreement with preferential protonation of $Dy(PPP)_2^{7-}$ at the terminal phosphate groups (110,112-114). While the chemical shift position of the β-resonance of $Dy(PPP)_2^{7-}$ is virtually unaffected by the addition of Li^+, that of the α,γ-resonances is shifted downfield. From these results alone, one cannot conclude that Li^+ (or H^+) preferentially binds to the outer phosphate groups since ^{31}P complexation shifts are rather complex in nature. They depend not only on direct coordination effects (for example, inductive or cation charge effects) but also on indirect effects, such as changes in O-P-O torsional angles (115). Moreover, Li^+ binding to the triphosphate complex could also change the Dy^{3+} dipolar contribution to the ^{31}P shift.

The effect of pH on the linewidths of the ^{31}P NMR resonances is more significant than that observed on the chemical shifts (Table III). The linewidths of the ^{31}P NMR resonances corresponding to the two outer phosphates increase more drastically at pH 6.5 than does that of the central phosphate. Moreover, the linewidths of all phosphate resonances from the shift reagent are broader in the presence of Li^+ ions. The line broadening observed at pH 6.5 or upon addition of Li^+ ions is due to a

Figure 8. ^{31}P NMR (121.4 MHz, 25°C) spectra of $Dy(PPP)_2^{7-}$ at pH 8.3 (A), 7.4 (B), and 6.5 (C) in the absence of LiCl. The shift reagent in the tetramethylammonium form was used at a concentration of 5 mM and the ratio of Dy^{3+} to triphosphate ligand was 1:2. Line broadening of 25 Hz was used.

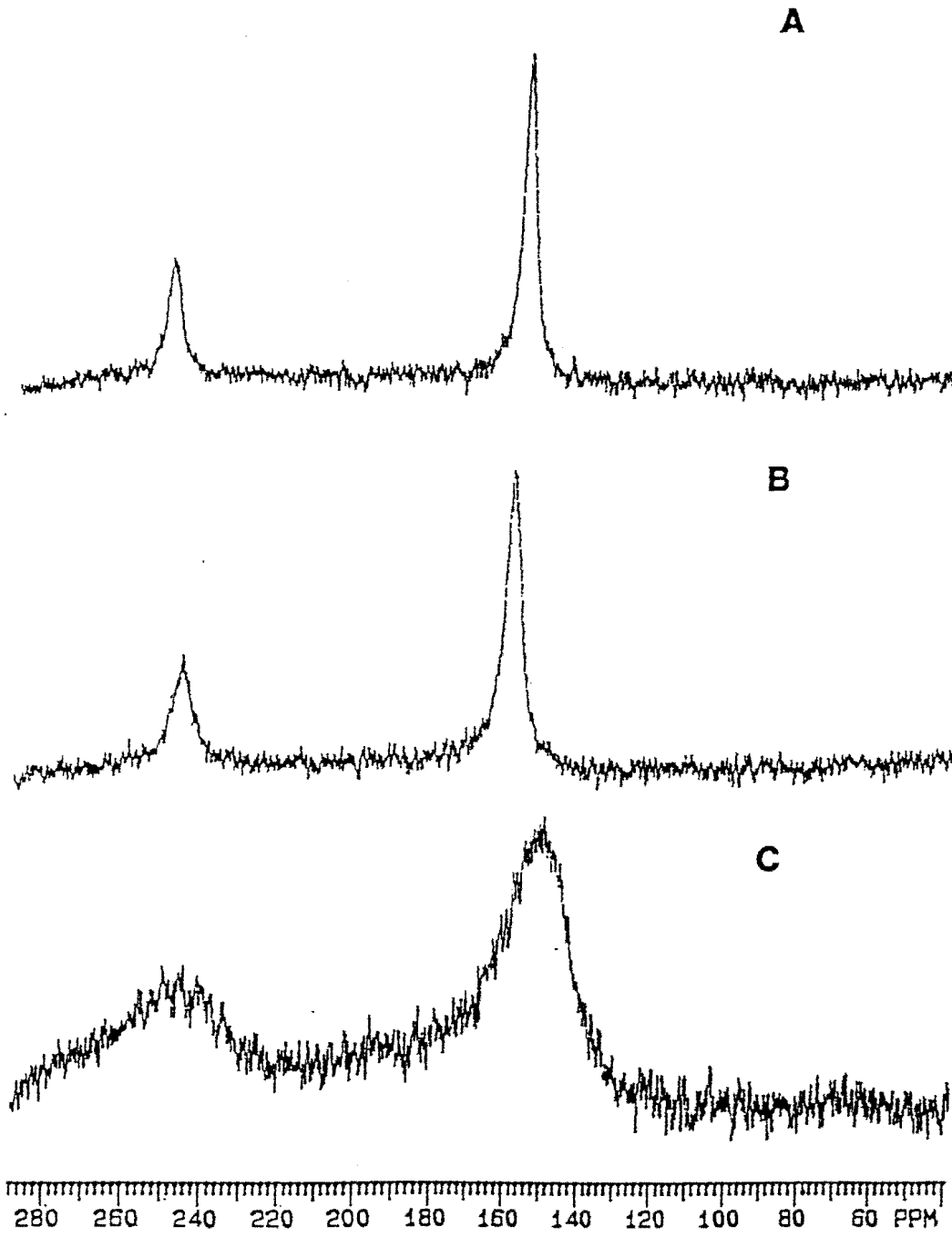
A
B
C
280
260
240
220
200
180
160
140
120
100
80
60
PPM

Table III

^{31}P NMR chemical shifts and linewidths of α,γ- and β-phosphate resonances of $Dy(PPP)_2^{7-}$ in the absence and presence of 100 mM LiCl

$[Dy^{3+}]/[PPP^{5-}]$	1:2			1:4		
pH	6.5	7.4	8.3	6.5	7.4	8.3
A. without LiCl						
α,γ $\delta(\Delta\nu_{1/2})^a$	156(646)	160(473)	157(378)	148(987)	151(633)	152(473)
β	243(898)	248(492)	250(428)	238(1132)	241(696)	242(497)
B. with 100 mM LiCl						
α,γ $\delta(\Delta\nu_{1/2})^a$	139(800)	152(586)	142(575)	b	141(803)	147(663)
β	b	247(548)	245(632)	b	238(897)	240(682)

[a]Chemical shifts and linewidths measured in ppm and Hz, respectively. [b]Resonance too broad to be measured accurately.

shorter τ_{cpx}, the residence time of the ligand in the complexed state. Since the outer phosphate groups of $Dy(PPP)_2^{7-}$ are preferentially protonated or bound to Li^+, (110,112-114) one would expect the interaction between protonated α,γ-phosphates and the Dy^{3+} ion at low pH and/or in the presence of Li^+ ions to be weaker than the corresponding one with deprotonated β-phosphates. Hence the shorter residence times and wider linewidths for the α,γ-resonances relative to those of the β-resonance.

Below pH 6.0, the chemical shifts of the α,γ-phosphate resonances start changing drastically and eventually coalesce at approximately pH 3.0 (111). For Dy(III) triphosphate, the chemical shift difference between bound and free phosphate resonances is larger for the central phosphate than for the outer phosphate resonances (111). Thus, upon lowering the pH below 6.0 there will be a relatively large increase in the linewidth of the β-phosphate resonance while a change in chemical shift will be first observed for the α,γ-phosphate resonance. However, the approach to coalescence, and its effect on linewidths and chemical shift positions, is not likely to be felt at the three pH values reported here.

Two different $[Dy^{3+}]$/[ligand] ratios, 1:2 and 1:4, respectively, were studied (Table III). In both cases, significant line broadening occurred at pH 6.5 and/or upon addition of Li^+ ions. The stability constants for $Dy(PPP)_2^{7-}$and $Dy(HPPP)_2^{5-}$ were previously measured at 35°C and found to be 9.5 and 7.2 (in logK units), respectively (110). Thus, for the metal/ligand ratios used in these experiments, the 1:2 Dy^{3+}-PPP complex will be the predominant species present in solution and a ligand exchange mechanism (69) may be operating:

$$Dy(PPP)_2^{7-} \rightarrow Dy(PPP)^{2-} + PPP^{5-}$$

High $[H^+]$ will favor the dissociation of $Dy(PPP)2^{7-}$ because of the weaker interaction between the protonated triphosphate ligand and the Dy^{3+} ion. Addition of Li^+ is also expected to facilitate ligand exchange mechanism since it can stabilize the negatively

charged species. Thus, one can conclude that the line broadening observed on the ^{31}P signals of the triphosphate ligand in the presence of Li^+ and at low pH is dominated by intermolecular ligand exchange processes and cannot be used unambiguously to construe any information about intramolecular exchange processes, like those presumably involved in Li^+ (and H^+) binding.

IV.1.5 Competition Between Li^+ And Other Cations For Aminocarboxylate Shift Reagents

Polyvalent cations present in solution can drastically decrease the $^7Li^+$ NMR paramagnetic shift by competing effectively with Li^+ for the same shift reagent. In physiological solutions, the divalent cations most likely to be encountered are Ca^{2+} and Mg^{2+}. Figure 9 shows the effects of Ca^{2+} and Mg^{2+} on the absolute magnitudes of the $^7Li^+$ NMR shifts induced by $Dy(PPP)_2^{7-}$ and $Dy(TTHA)^{3-}$. For physiologically relevant concentrations of Ca^{2+} and Mg^{2+} (less than 2 mM, in general) the shifts induced by $Dy(PPP)_2^{7-}$ are significantly larger than those produced by $Dy(TTHA)^{3-}$. Overall, the shifts induced by either shift reagent are sensitive to the presence of Ca^{2+} or Mg^{2+}, with those caused by $Dy(PPP)_2^{7-}$ being extremely sensitive to the presence of these two cations, when compared to $Dy(TTHA)^{3-}$. In physiological solutions, Na^+ and K^+ are encountered in much higher concentrations compared to Li^+. As observed with divalent cations, the shifts induced by either shift reagent are also sensitive to the presence of K^+ or Na^+ (Figure 10). Likewise, the shifts caused by $Dy(PPP)_2^{7-}$ are more sensitive to the presence of monovalent cations than $Dy(TTHA)^{3-}$. In the competition experiments involving Na^+ and K^+, there is a sluggish decrease in $^7Li^+$ paramagnetic shifts even in the presence of excess Na^+ or K^+. By contrast, there is a steep decrease in $^7Li^+$ shifts even in the presence of low concentrations of Ca^{2+} and Mg^{2+}. Assuming that the Li^+ ion populates the preferential binding site on the triphosphate shift reagent, in the presence of other monovalent cations Li^+ will be forced to exchange with other sites in

Figure 9. Competition between Ca^{2+} (□) or Mg^{2+} (+) and Li^{+} for $Dy(PPP)_2^{7-}$ (full lines) and $Dy(TTHA)^{3-}$ (dotted lines). The shift reagents' counter cation was tetramethylammonium ion. LiCl concentration was held constant at 5 mM. The concentration of $Dy(PPP)_2^{7-}$ was 5 mM while that of $Dy(TTHA)^{3-}$ was 15 mM, otherwise the experimental conditions were the same as for Figure 7. In $Dy(PPP)_2^{7-}$ solutions, precipitation was observed when the concentration of Mg^{2+} or Ca^{2+} rose above 3 mM or 2 mM, respectively.

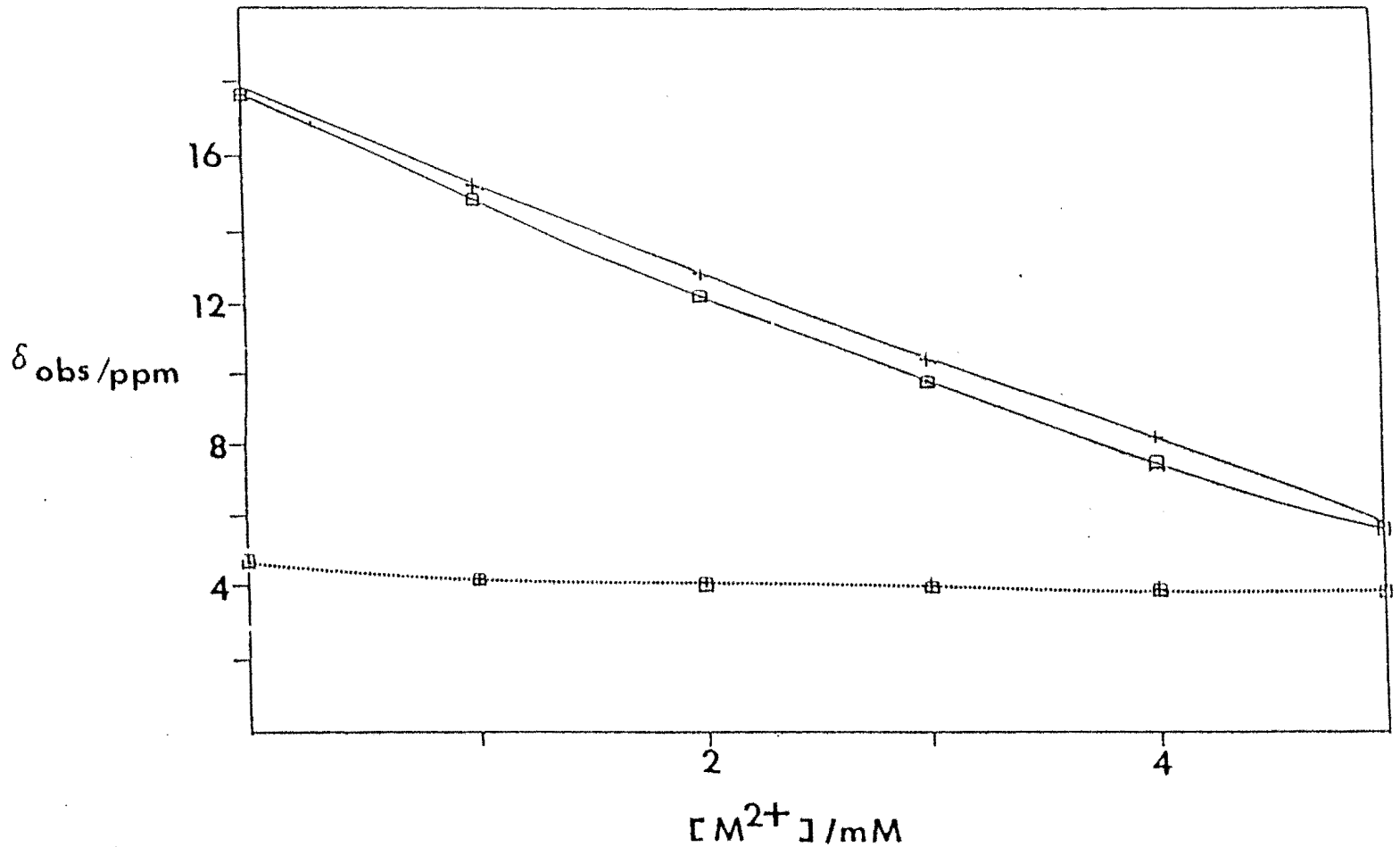
16
12
8
4
δ_{obs} /ppm
2
4
[M^{2+}] /mM

Figure 10. Competition between Na^+ (□) or K^+ (+) and Li^+ for $Dy(PPP)_2^{7-}$ (full lines) and $Dy(TTHA)^{3-}$ (dotted lines). Same experimental conditions as for Figure 9.

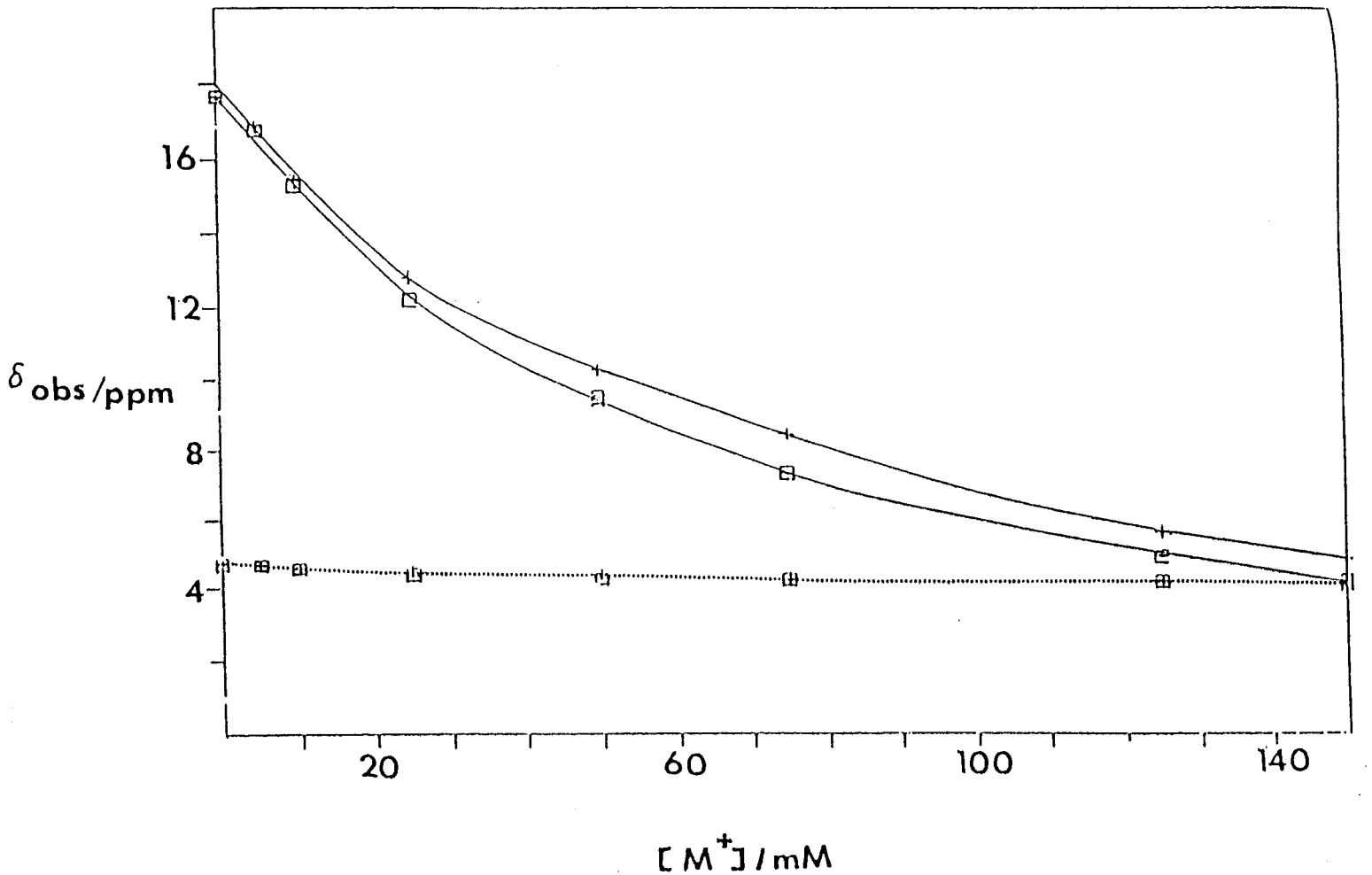
16
12
8
4
δ obs /ppm
20
60
100
140
[M+] / mM

the second coordination sphere of the shift reagent having different θ values. As a consequence, the term $(3 \cos^2 \theta - 1)/r^3$ will be averaged out and the induced $^7Li^+$ paramagnetic shift will decrease.

A quantitative interpretation of the competition between Li^+ and other cations for $Dy(PPP)_2^{7-}$ is difficult to obtain as a result of the complex solution chemistry of this shift reagent. However, based on the results depicted on Figures 9 and 10, the relative order of cation competition for $Dy(PPP)_2^{7-}$ at pH 7.5 is predicted to be $Ca^{2+} \geq Mg^{2+} > Li^+ > Na^+ \geq K^+$. The decreasing order of association constants for monovalent cations follows the increasing order of ionic radii lending support to an electrostatic model. As expected the competition between divalent cations and Li^+ is much larger than that observed with monovalent cations. Ca^{2+} competition is slightly larger than that provided by Mg^{2+} despite the fact that Ca^{2+} has a larger ionic radius and a smaller affinity for PPP^{5-} relative to Mg^{2+} (112). This indicates that a different mechanism (see infra) may significantly contribute toward the competition reaction between divalent cations and Li^+.

The addition of Ca^{2+} to $Dy(PPP)_2^{7-}$ was monitored by ^{31}P NMR (Figure 11). We observed a decrease in the intensity of the resonances of Dy^{3+}-complexed phosphates (Figure 11.A) accompanied by the formation of unshifted but broadened triphosphate resonances (Figure 11.B). The chemical shifts of the latter resonances match those of $CaPPP^{3-}$ (Figure 11.C) and are different from any tetramethylammonium triphosphate present in slow exchange prior to addition of Ca^{2+} (Figure 11.D). Similar ^{31}P NMR observations were found upon addition of Mg^{2+} salts to $Dy(PPP)_2^{7-}$. By contrast, no changes were observed on the ^{31}P NMR spectrum of $Dy(PPP)_2^{7-}$ upon addition of Na^+ and K^+ ions.

These observations indicate two distinct classes of competition mechanisms for divalent and monovalent cations. Divalent cations can compete with the Ln^{3+} ion

Figure 11. ^{31}P NMR (121.4 MHz, 25° C) spectra of: (A) 5 mM $Dy(PPP)_2^{7-}$ at pH 7.4. The shift reagent was in the tetramethylammonium form and a Dy^{3+} to ligand ratio of 1:2 was used. Line broadening of 25 Hz was used. (B) Same as in A except that 1 mM $CaCl_2$ was also present. The third sharp resonance from the right present in the B insert is due to inorganic phosphate resulting from Ca^{2+}-catalyzed triphosphate hydrolysis. (C) 5 mM $(NMe_4)_5PPP$ and 5 mM $CaCl_2$ at pH 7.4. (D) 5 mM $(NMe_4)_5PPP$ at pH 7.4.

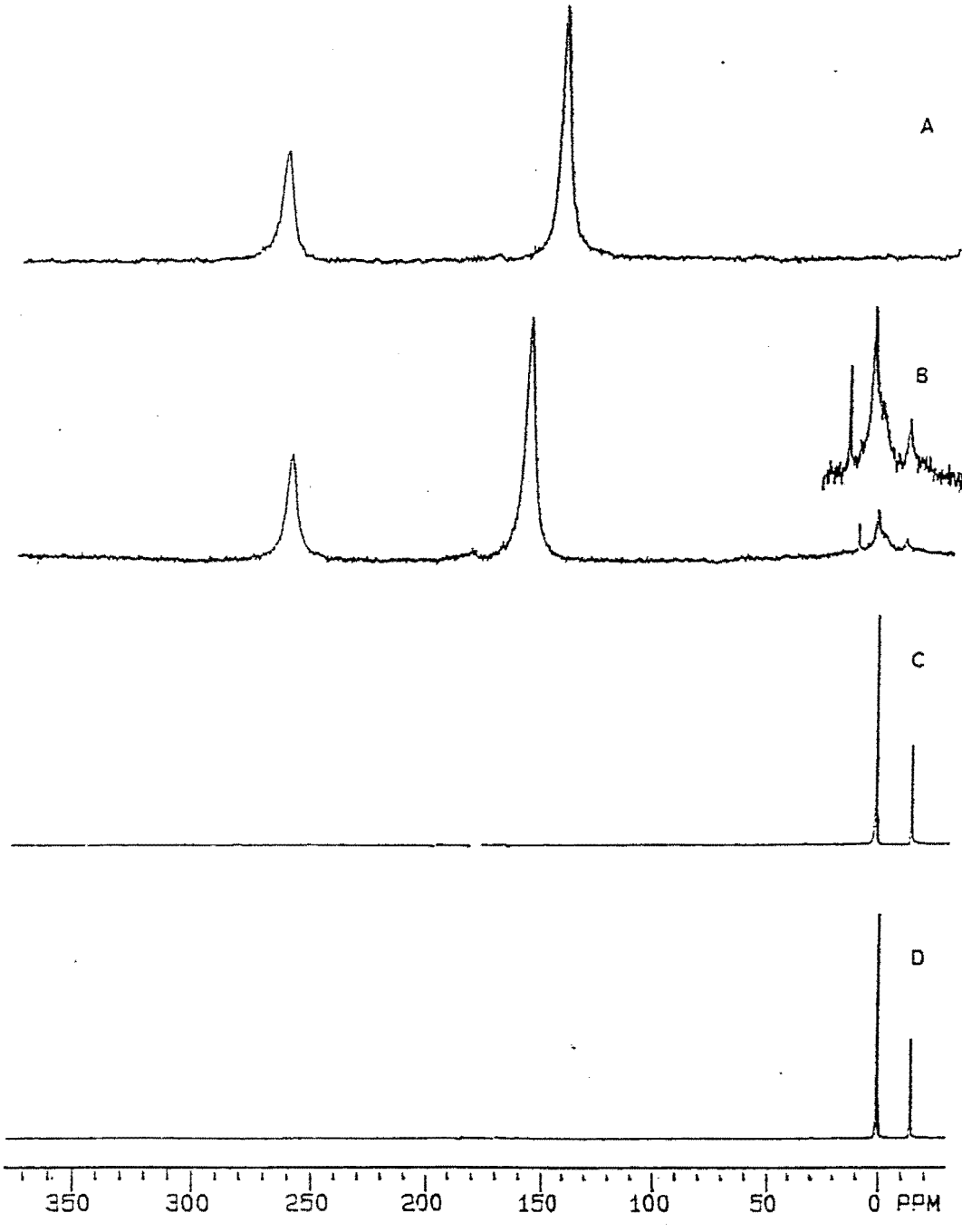
A
B
C
D
350
300
250
200
150
100
50
0 PPM

for the ligand in a scrambling type reaction, or alternatively, they can compete with the monovalent cations for the second coordination sphere of the shift reagents. The ^{31}P NMR studies (Figure 11) indicate that the scrambling mechanism is operating to a large extent when $Ln(PPP)_2^{7-}$ is present along with Ca^{2+} or Mg^{2+}. On the other hand, Na^+ and K^+ ions effectively compete for Li^+ binding sites in the second coordination sphere of the triphosphate complex. Analogous ^{13}C NMR studies on the $Dy(TTHA)^{3-}$ shift reagent suggested that this complex is not susceptible to the ligand scrambling reaction since no new unshifted ligand resonances were found upon addition of Ca^{2+} (data not shown). Thus, the small decrease observed in the $^7Li^+$ NMR shifts induced by $Dy(TTHA)^{3-}$ (Figure 9) is probably due to simple competition between Ca^{2+} or Mg^{2+} and Li^+. It is important to note that complexes of the type LnL^{3-n} (where Ln^{3+} and L^{n-} represent the lanthanide ion and ligand, respectively) are more resistant to ligand scrambling reactions than those with a stoichiometry of the type LnL_2^{3-2n} or LnL_3^{3-3n} since the trivalent lanthanide ions have higher affinities than di- and monovalent cations for most ligands. The ligand affinity of the lanthanide ion is enhanced in cases where only one polydentate ligand is coordinated, as in $Dy(TTHA)^{3-}$.

IV.2 Characterization and Comparison of Phosphonate Shift Reagents With Triphosphate Shift Reagent.

IV.2.1 $^7Li^+$ and $^{23}Na^+$ Paramagnetic Shifts Induced By Phosphonate Complexes of Dysprosium

The efficacy of phosphonate complexes of dysprosium as shift reagents for $^7Li^+$ and $^{23}Na^+$ NMR studies were tested under constant ionic strength conditions, at pH 7.5. The concentration of LiCl or NaCl were held constant at 5 mM and the ionic strength at 0.36. The shift reagent concentrations varied from 3 to 30 mM. The paramagnetic shifts induced by the phosphonate complexes are plotted against the stoichiometric mole ratio of shift reagent to Li^+ or Na^+, ρ, in Figure 12. The shifts

Figure 12. Dependence of paramagnetic $^{7}Li^{+}$ and $^{23}Na^{+}$ NMR shifts induced by several shift reagents on [shift reagent]/[Li^{+} or Na^{+}] ratio. Full and dotted lines indicate data for Na^{+} and Li^{+}, respectively. The symbols for the ligands $Dy(PcPcP)_2^{7-}$ (□), $Dy(DTPP)^{6-}$ (X), $Dy(DOTP)^{5-}$ (◇), Dy(NTP) (Δ), and Dy(NOTP) (▽) are indicated in parenthesis. Each point represents the average of $^{23}Na^{+}$ or $^{7}Li^{+}$ NMR measurements on three separate samples. In all cases, the agreement was within 0.02 ppm. Li^{+} concentration was held constant at 5 mM while the shift reagent concentrations varied. All solutions were buffered with 50 mM HEPES and also contained 10 mM glucose and 17% D_2O. The pH was adjusted to 7.5 with tetramethylammonium hydroxide. Ionic strength was adjusted to 0.36 with tetramethylammonium chloride so that all samples had the same ionic strength as that of 30 mM $Dy(PcPcP)_2^{7-}$. NMR conditions are described in experimental section.

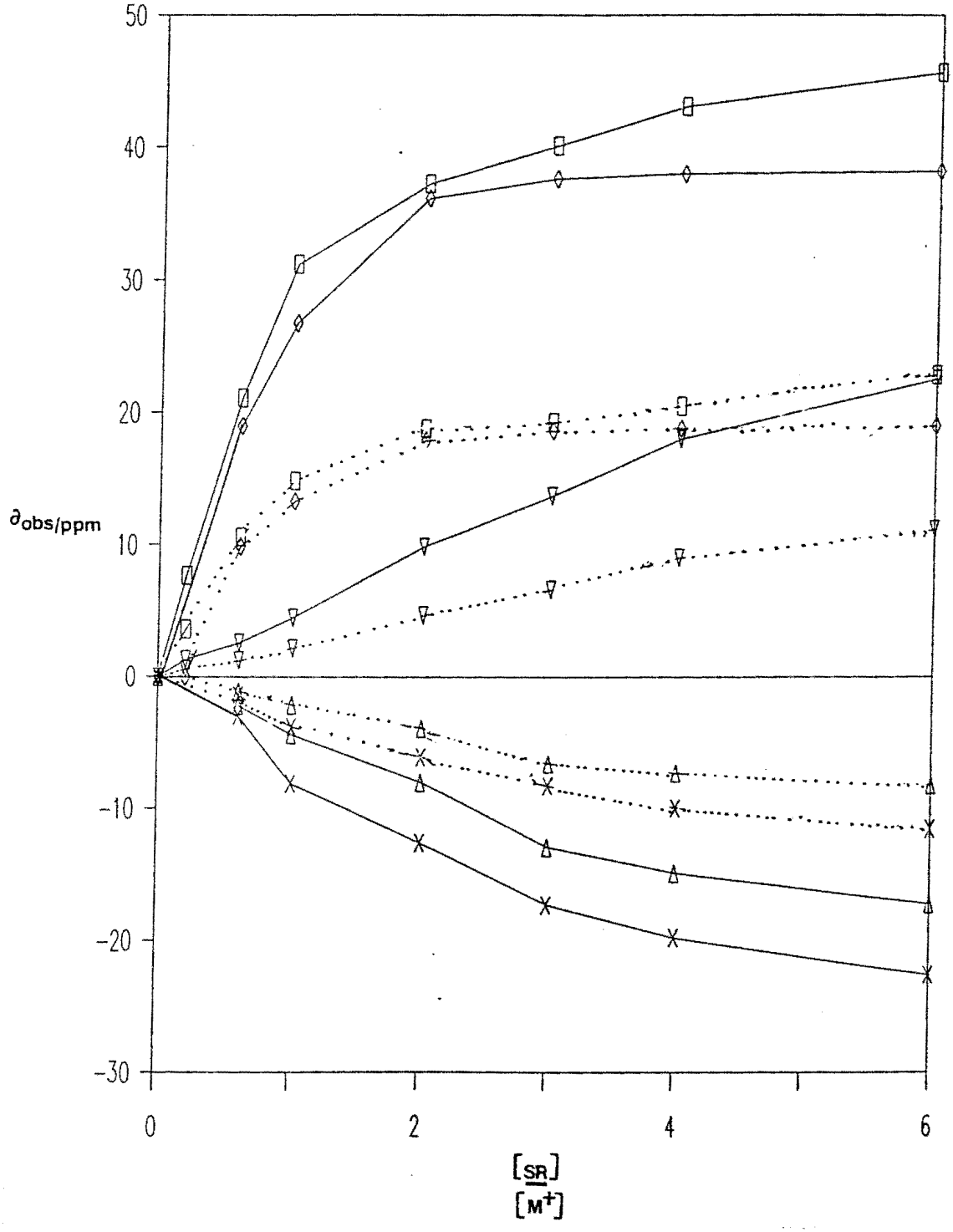
50
40
30
20
10
0
-10
-20
-30
0
2
4
6
∂obs/ppm
[SR]
[M+]

induced in the $^{7}Li^{+}$ and $^{23}Na^{+}$ NMR resonances by $Dy(PcPcP)_2^{7-}$ and $Dy(DOTP)^{5-}$ are significantly larger than those induced by $Dy(NTP)^{3-}$, $Dy(NOTP)^{3-}$, and $Dy(DTPP)^{6-}$, under similar conditions. The observed induced shifts may have been slightly larger if the solution were free of added salt. However, the shifts are close to their maximum value since a bulky, non-competitive organic counter cation, tetramethylammonium, was used. Based on these studies $Dy(PcPcP)_2^{7-}$ and $Dy(DOTP)^{5-}$ were chosen for further characterization for NMR studies under physiological conditions.

IV.2.2 pH Dependence of $^{7}Li^{+}$ NMR Shifts Induced By Phosphonate Shift Reagents

The pH dependence of $^{7}Li^{+}$ shifts induced by $Dy(PcPcP)_2^{7-}$ and $Dy(DOTP)^{5-}$are shown in Figure 13. These reagents are compared with $Dy(PPP)_2^{7-}$. The shifts exhibited by $Dy(PcPcP)_2^{7-}$ and $Dy(DOTP)^{5-}$ are dependent on pH between 6 and 8.5. The pH dependence of shifts induced by the above shift reagents are not as severe as in the case of $Dy(PPP)_2^{7-}$, but still are significant. The decreased $^{7}Li^{+}$ NMR shifts observed below pH 7 for $Dy(PcPcP)_2^{7-}$ may be due to protonation of the complex. In the case of $Dy(DOTP)^{5-}$, the decrease in shifts is due to protonation of the complex in this pH range (104). The protonation constants corresponding to the formation of $DyH(DOTP)^{4-}$ and $DyH_2(DOTP)^{3-}$ are 5.7 and 4.6, respectively (104).

IV.2.3 Competition Between Li^{+} and Other Cations for Phosphonate Shift Reagents

In physiological solutions, the divalent cations Ca^{2+} and Mg^{2+} can effectively compete with Li^{+} for the shift reagent and drastically decrease the $^{7}Li^{+}$ NMR isotropic shifts. Figure 14 shows the effects of Ca^{2+} and Mg^{2+} on the absolute magnitudes of the $^{7}Li^{+}$ shifts induced by $Dy(PPP)_2^{7-}$ and $Dy(PcPcP)_2^{7-}$. The shifts induced by $Dy(PcPcP)_2^{7-}$ are somewhat less sensisitve to Ca^{2+} and Mg^{2+} than those afforded by $Dy(PPP)_2^{7-}$ and yet more sensitive than those yielded by $Dy(TTHA)^{3-}$.

Figure 13. pH dependence of paramagnetic shifts afforded by $Dy(DOTP)^{5-}$ (△), $Dy(PPP)_2^{7-}$ (□) and $Dy(PcPcP)_2^{7-}$ (◇). Li^+ concentration was held constant at 5 mM in the three curves. The concentrations of $Dy(DOTP)^{5-}$, $Dy(PPP)_2^{7-}$ and $Dy(PcPcP)_2^{7-}$ were kept constant at 5 mM. The reported pH values are not corrected for the deuterium isotope effect. The pH dependence of $^7Li^+$ shifts was found to be reversible by adding tetramethylammonium hydroxide and HCl above and below pH 7.5, respectively.

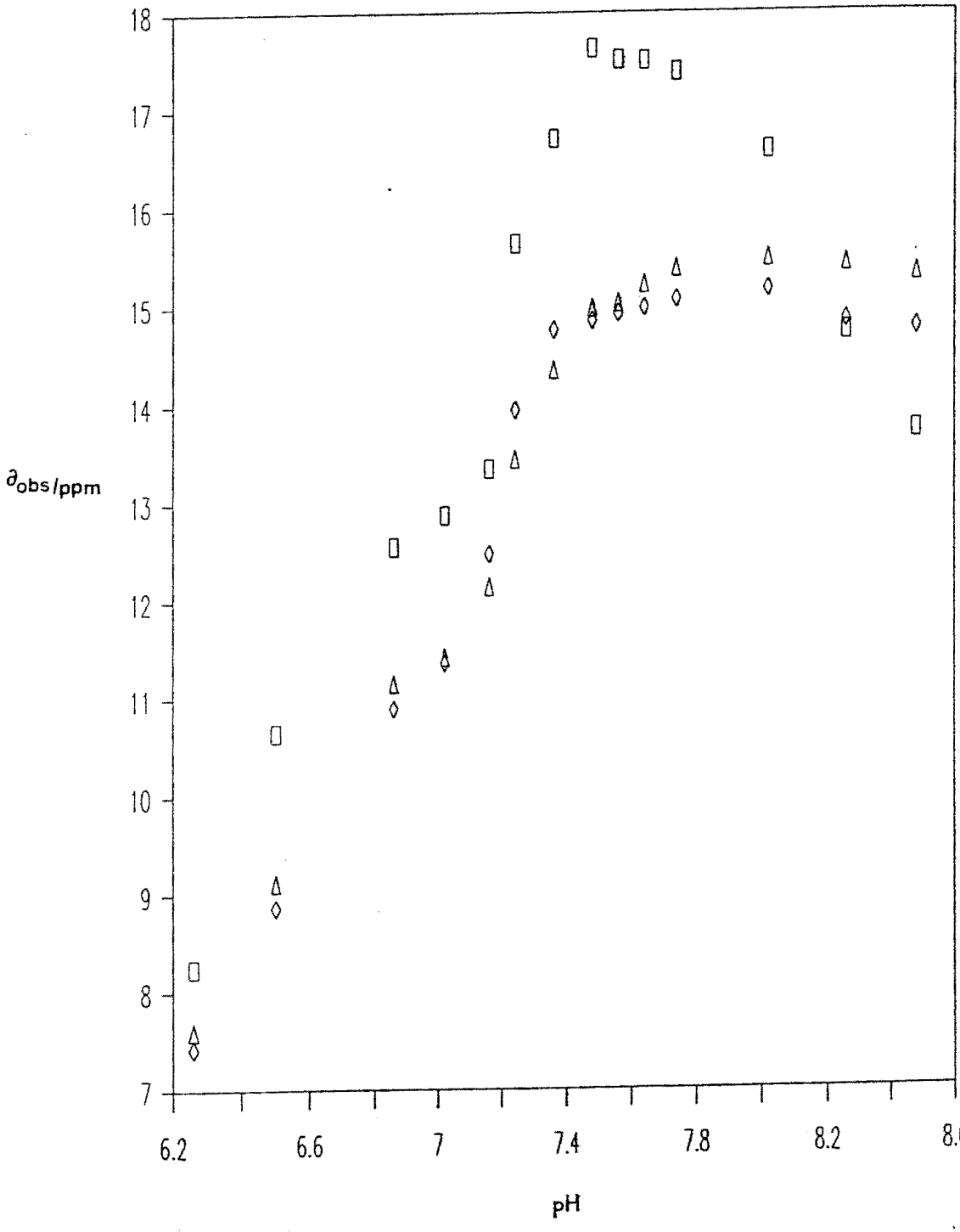
18
17
16
15
14
13
12
11
10
9
8
7
∂_{obs}/ppm
6.2
6.6
7
7.4
7.8
8.2
8.6
pH

Figure 14 Competition between Ca^{2+} (□) or Mg^{2+} (▲) and Li^{+} for $Dy(PcPcP)_2^{7-}$ (open symbols) and $Dy(DOTP)^{5-}$ (closed symbols). The shift reagents' counter cation was tetramethylammonium ion. LiCl concentration was held constant at 5 mM. The concentrations of $Dy(DOTP)^{5-}$ and $Dy(PcPcP)_2^{7-}$ were maintained at 5 mM.

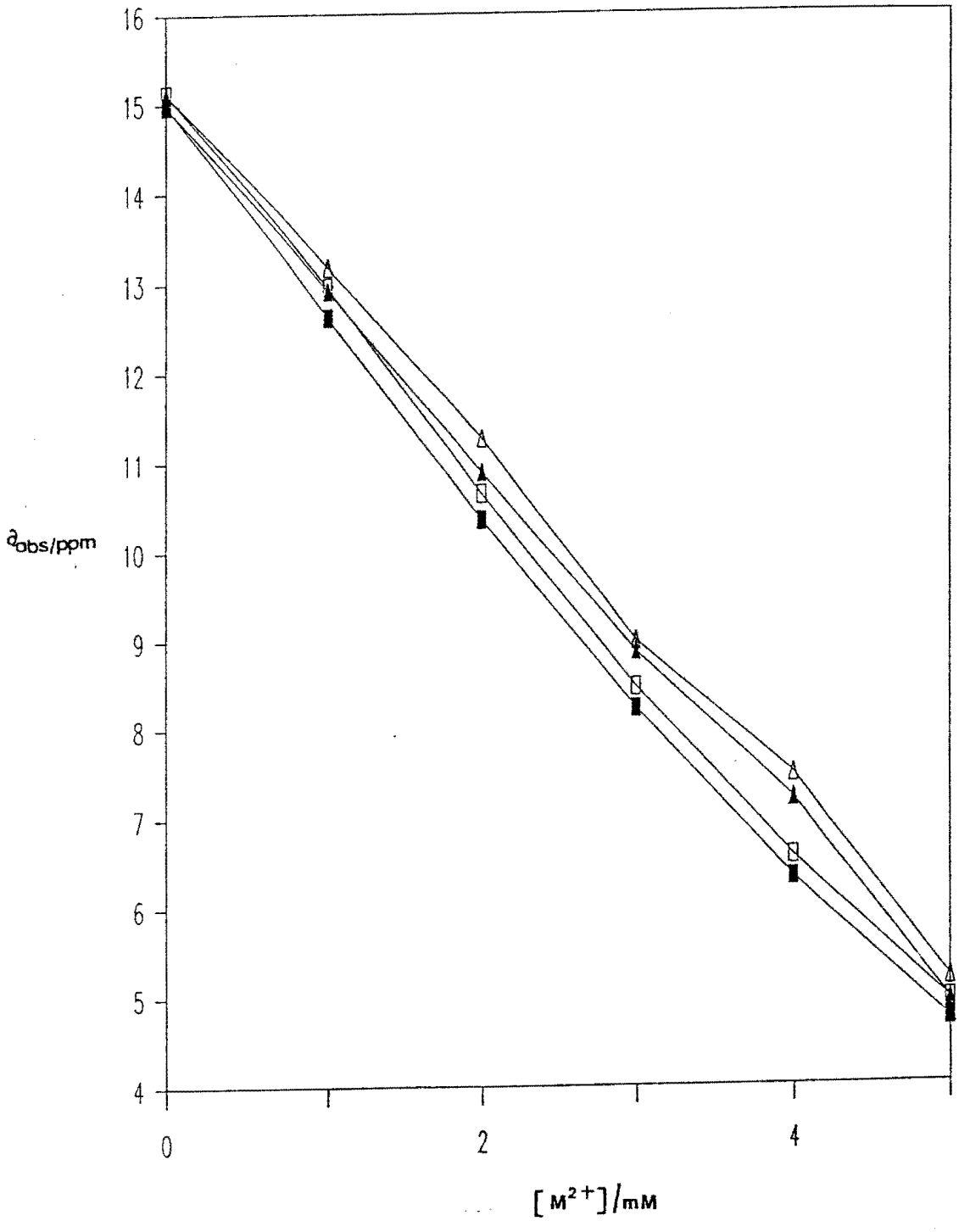
16
15
14
13
12
11
10
9
8
7
6
5
4
$\delta_{obs/ppm}$
0
2
4
$[M^{2+}]/mM$

Monovalent cations present in physiological solutions can effectively compete with Li^+ for the shift reagent. Moreover, Na^+ and K^+ are present at much higher concentrations compared to Li^+. Since the shift reagents are known to bind monovalent cations with a fairly weak labile interaction, it was therefore necessary to investigate the effects of Na^+ and K^+ on the absolute magnitudes of the shifts induced in the $^7Li^+$ NMR resonances. Figure 15 compares the effects of these ions on the shifts induced in the $^7Li^+$ resonance by $Dy(PPP)_2^{7-}$ and $Dy(PcPcP)_2^{7-}$. The shifts caused by $Dy(PcPcP)_2^{7-}$ are less sensitive to the presence of monovalent cations than $Dy(PPP)_2^{7-}$. The decrease in shifts are more pronounced in the presence of divalent cations than monovalent cations. In any case, the $^7Li^+$ shifts induced by shift reagents are still quite substantial despite the presence of competing cations like Na^+, K^+, Ca^{2+}, and Mg^{2+}.

IV.2.4 Hydrolytic Stability of Phosphonate Shift Reagents in Biological Sysytems Containing Phosphatases

Figure 16 depicts the time dependencies of the ^{31}P NMR spectra of solutions of $Dy(PcPcP)_2^{7-}$and $Dy(PPP)_2^{7-}$ in the presence of rat liver homogenates containing alkaline phosphatase. The ^{31}P NMR spectra of $Dy(PcPcP)_2^{7-}$ clearly indicates that the shift reagent is not hydrolysed when incorporated in the suspension containing rat liver homogenates. The hydrolytic stability is presumably due to the lack of high energy P-O-P linkages in $Dy(PcPcP)_2^{7-}$. However, we do observe a decrease in intensities of the chelate resonances and increase in the intensities of the free ligand resonances suggesting that the complex is dissociating in solution to give Dy^{3+} and free ligand. The chemical inertness of the complex towards hydrolysis in the presence of rat liver homogenates is confirmed by the absence of ^{31}P NMR resonances typical of phosphonate degradation products. The inorganic phosphate resonance observed in the case of $Dy(PcPcP)_2^{7-}$ sample is an impurity present from the start. There was no

Figure 15. Competition between Na^+ (□) or K^+ (▲) and Li^+ for $Dy(PcPcP)_2^{7-}$ (open symbols) and $Dy(DOTP)^{5-}$ (closed symbols). Same experimental conditions as for Figure 14.

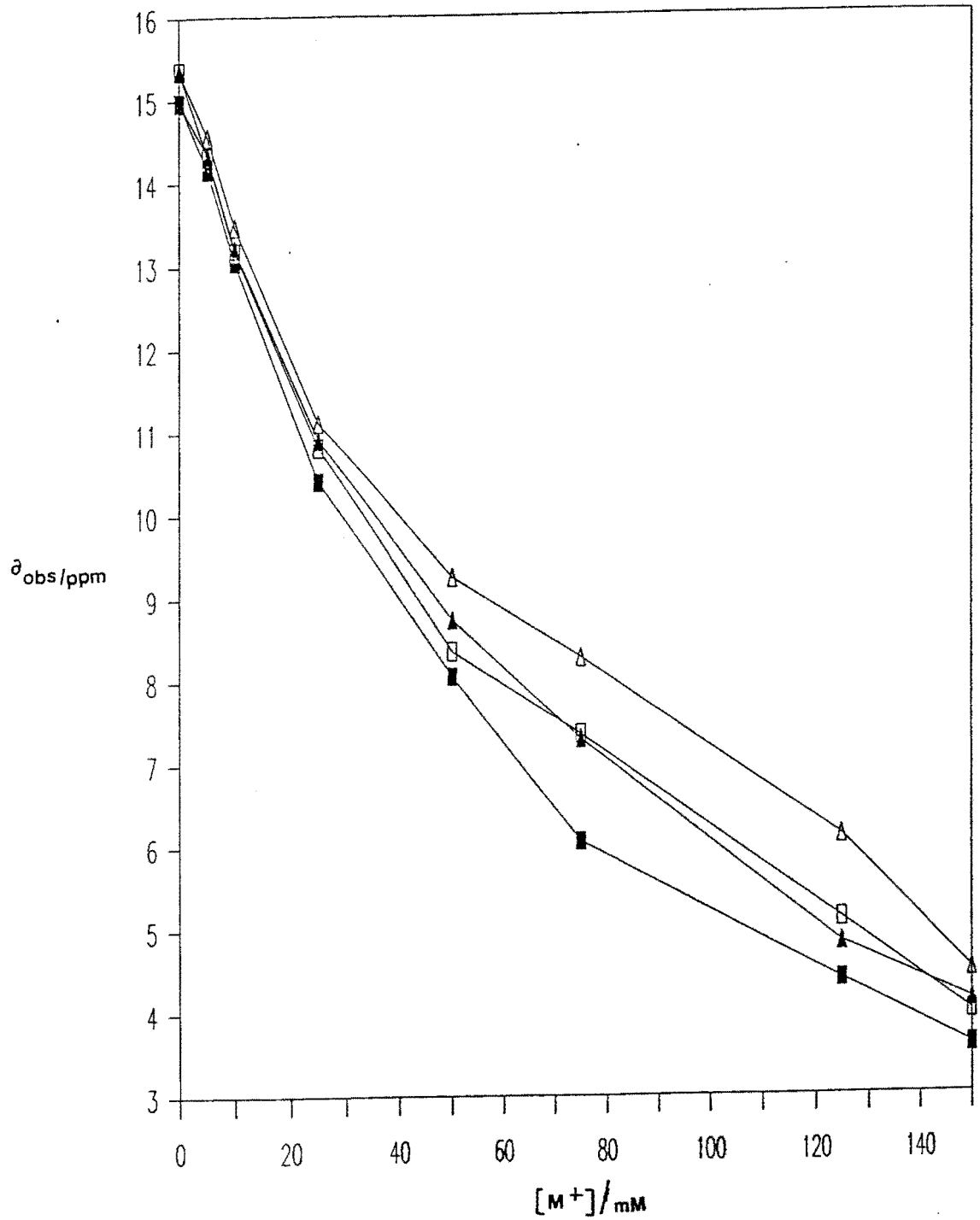
16
15
14
13
12
11
10
9
8
7
6
5
4
3
∂_{obs}/ppm
0
20
40
60
80
100
120
140
$[M^+]$/mM

Figure 16. Time dependence of ^{31}P NMR spectra of (A) 10 mM $Dy(PPP)_2^{7-}$ and (B) 10 mM $Dy(PcPcP)_2^{7-}$ in the presence of catalytic amounts of alkaline phosphatase from rat liver homogenates.

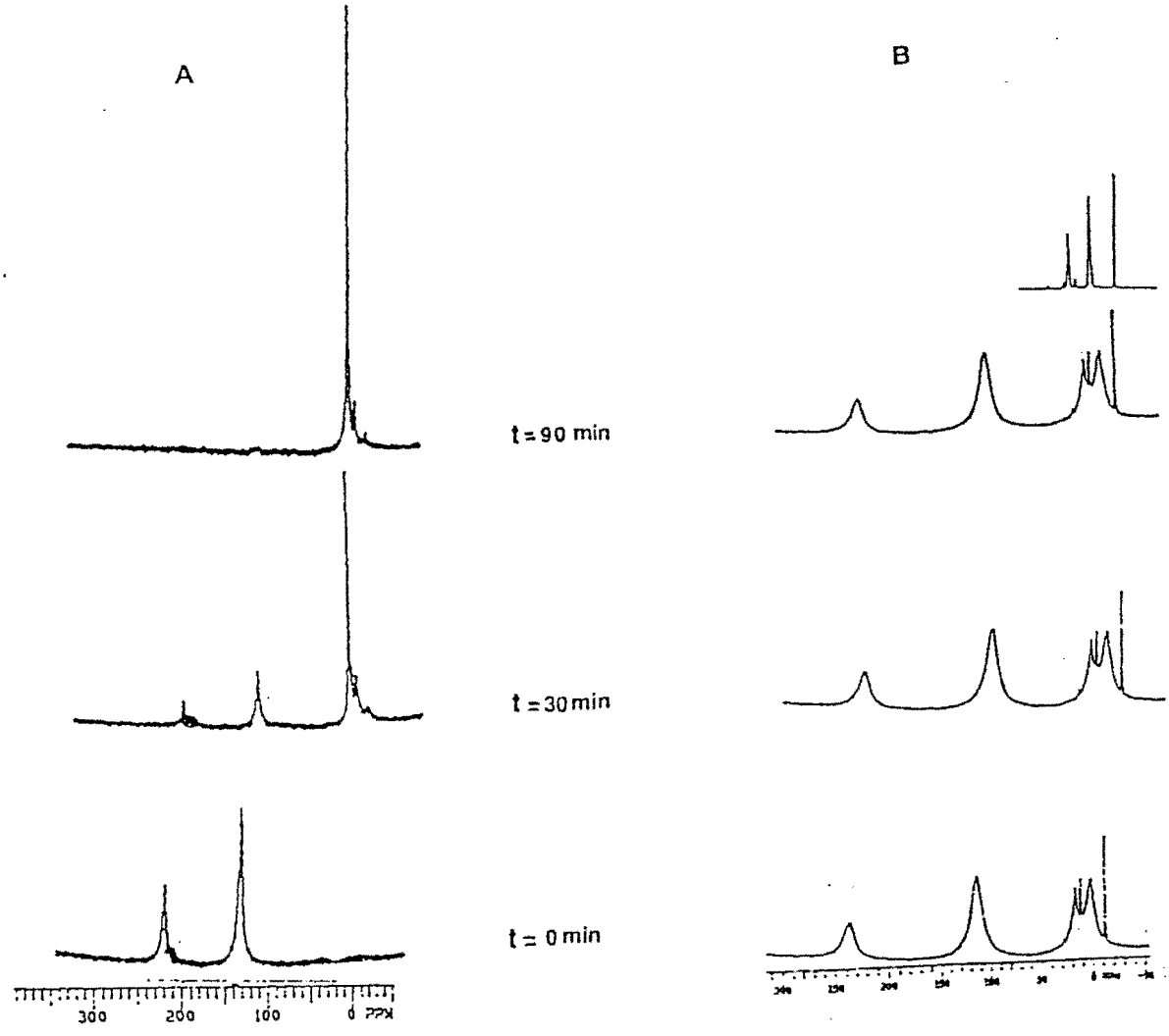
A
B
t = 90 min
t = 30 min
t = 0 min
300
200
100
0 PPM

change in the area of inorganic phosphate resonance. An inset of the spectra of free ligand $PcPcP^{5-}$ (Figure 16.B) also indicated the presence of inorganic phosphate, thus confirming that inorganic phosphate was an impurity and not a degradation product. The chelate $Dy(PPP)_2^{7-}$ is hydrolysed very rapidly when placed in the suspension containing rat liver homogenates. The P-O-P bonds in $Dy(PPP)_2^{7-}$ are very susceptible to attack by alkaline phosphatase and pyrophosphatases (117). Compared to $Dy(PPP)_2^{7-}$, $Dy(PcPcP)_2^{7-}$ is chemically inert towards hydrolysis by alkaline phosphatase as seen in this study.

IV.2.5 Application of Shift Reagents to The Study of Li^+ Transport in RBC

Li^+ transport has been traditionally studied by atomic absorption and flame spectrophotometries (47,48). These two methods involve invasive procedures since physical separation of RBCs and plasma is required prior to chemical analysis. Crucial information on ion binding to RBC membranes is lost by these techniques. There is therefore a need for the development of a time-efficient, non-invasive method that enables visualization of Li^+ transport in its time scale and simultaneously provides information at a molecular level about any specific ion interactions with membrane components and/or metabolites. Metal NMR spectroscopy, with the aid of highly negatively charged shift reagents, has partially solved this problem for cations such as Li^+, Na^+, K^+, Rb^+ and Cs^+ (45,62,63,66-68). Figure 17 shows ^7Li NMR spectra of Li^+-loaded RBCs. Figure 17.a indicates that the intra- and extracellular Li^+ pools are not resolved in the ^7Li NMR spectrum of RBC suspensions in the absence of shift reagent. The two pools of Li^+ are not resolved by ^7Li NMR because Li^+ exists basically in the same chemical environment (as a hydrated ion) in the two cell compartments. In addition, the chemical shift range for ionic lithium is only 4 ppm and it is only weakly dependent on solvation and/or ligation (59). A ^7Li NMR technique involving the shift reagent $Dy(PPP)_2^{7-}$

Figure 17. (A) ^{7}Li NMR spectrum of packed Li^{+}-loaded RBCs in a suspension containing 3.5 mM LiCl, 5 mM KCl, 140 mM NaCl, 10 mM glucose, 10 mM HEPES, pH 7.5. Packed RBCs were incubated with 140 mM LiCl at 37°C for 12 hours prior to NMR measurements. Hematocrit was 13 %. 17% D_2O was present for field frequency lock. (B) ^{7}Li NMR spectrum of a similar RBC suspension as in A except that 3 mM $Dy(PPP)_2^{7-}$ was present in the suspension instead of 30 mM NaCl. (C) ^{7}Li NMR spectrum of a similar suspension as in A except that the suspension had 3 mM $Dy(PcPcP)_2^{7-}$ instead of 30 mM NaCl. (D) ^{7}Li NMR spectrum of the same RBC suspension as in A except 7 mM $Dy(TTHA)^{3-}$ was present in the suspension medium instead of 21 mM NaCl. (E) ^{7}Li NMR spectrum of RBC suspension as in A except that 5 mM $Dy(DOTP)^{5-}$ was present in the suspension medium. (F) ^{7}Li NMR spectrum of RBC suspension described in A except that the medium contained 7 mM $Tm(PPP)_2^{7-}$ instead of 70 mM NaCl. The spectra shown here are obtained in 32 transients. Line broadening of 5 Hz was used throughout. The inner pools of Li^{+} are indicated by the letters a through e and the outer pools by f through j.

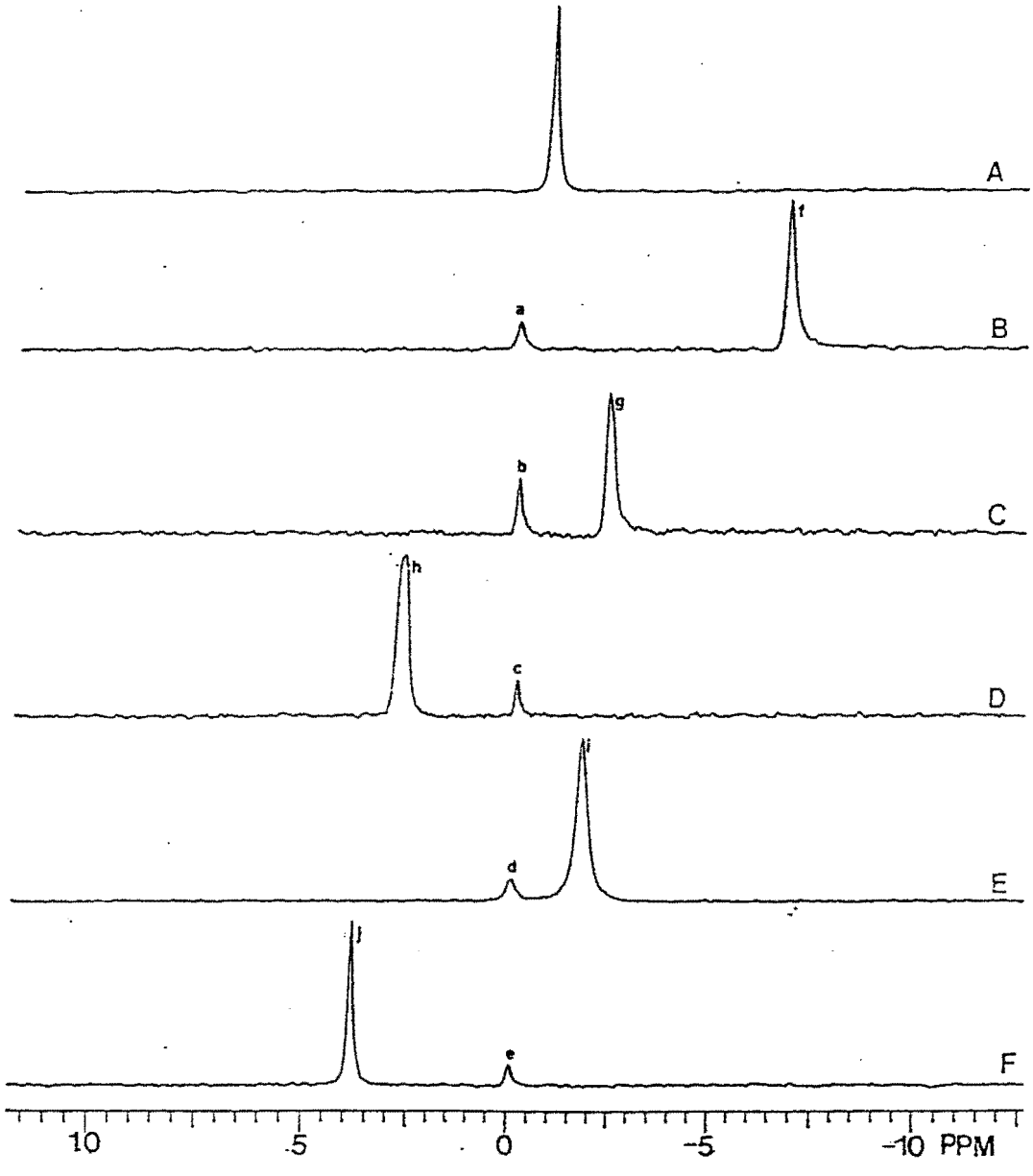
A
f
a
B
g
b
C
h
c
D
i
d
E
j
e
F
10
5
0
-5
-10 PPM

has been reported by us (45,46) to study Li^+ ion distribution in RBCs. The shift reagent remains outside the RBC and interacts electrostatically with the Li^+ ions in the suspension medium. Li^+ ions in contact with the shift reagent are paramagnetically shifted. Two ^7Li NMR resonances appear, the intracellular Li^+ resonance is unshifted while that of extracellular Li^+ is paramagnetically shifted by the shift reagent. Chemical shift separation of the two $^7Li^+$ resonances was achieved with 3 mM $Dy(PPP)_2^{7-}$ (Figure 17.B), 3 mM $Dy(PcPcP)_2^{7-}$ (Figure 17.C), 7 mM $Dy(TTHA)^{3-}$ (Figure 17.D), 5 mM $Dy(DOTP)^{5-}$ (Figure 17.E), and 7 mM $Tm(PPP)_2^{7-}$ (Figure 17.F). The shift reagents selected for this study gave the largest chemical shift separations between the two Li^+ ion pools for relatively low concentrations of shift reagent. The application of the shift reagents mentioned above for $^7Li^+$ and $^{23}Na^+$ NMR transport studies in cellular systems had been previously reported (45,60-62,66-68,104), except for $Dy(PcPcP)_2^{7-}$. To the best of our knowledge, only the Gd^{3+} analogue of the phosphonate shift reagent has been reported as a contrast agent for imaging studies (116).

IV.3 Effects of Lanthanide Shift Reagents

IV.3.1 Effect of Lanthanide Shift Reagents on Shape and Size of RBC

SEM pictures in Figure 18 show the effect of three negatively charged shift reagents, at concentrations typically used in metal NMR experiments, on the morphology of RBCs. At these low concentrations even the most highly charged shift reagents do not have a noticeable effect on the shape and size of RBCs, which appear as discocytes. However, at higher concentrations of $Dy(PPP)_2^{7-}$ and $Dy(TTHA)^{3-}$ these shift reagents seem to have a sizeable effect, producing echinocytes (see Figures 18.e and 18.f). SEM pictures for the shift reagents, 5 mM $Tm(PPP)_2^{7-}$ and 3 mM $Dy(PcPcP)_2^{7-}$, showed identical results (data not shown). Data on the average diameter of RBCs obtained from SEM and Coulter counter (CC) measurements are given in Table IV. Although the trend

Figure 18. Comparison of SEM pictures of (a) control RBCs and (b) 3 mM $Dy(PPP)_2^{7-}$, (c) 5 mM $Dy(DOTP)^{5-}$, (d) 10 mM $Dy(TTHA)^{3-}$, and (e) 15 mM $Dy(PPP)_2^{7-}$ (f) 20 mM $Dy(TTHA)^{3-}$ treated RBCs. Osmolarity was adjusted to 300 $\pm$ 5 mosM. pH of all the samples were maintained at 7.5. Pictures shown here are magnified 1500 times. Details of the incubating medium are described under Materials and Methods. The scale bar represents 10 μm.

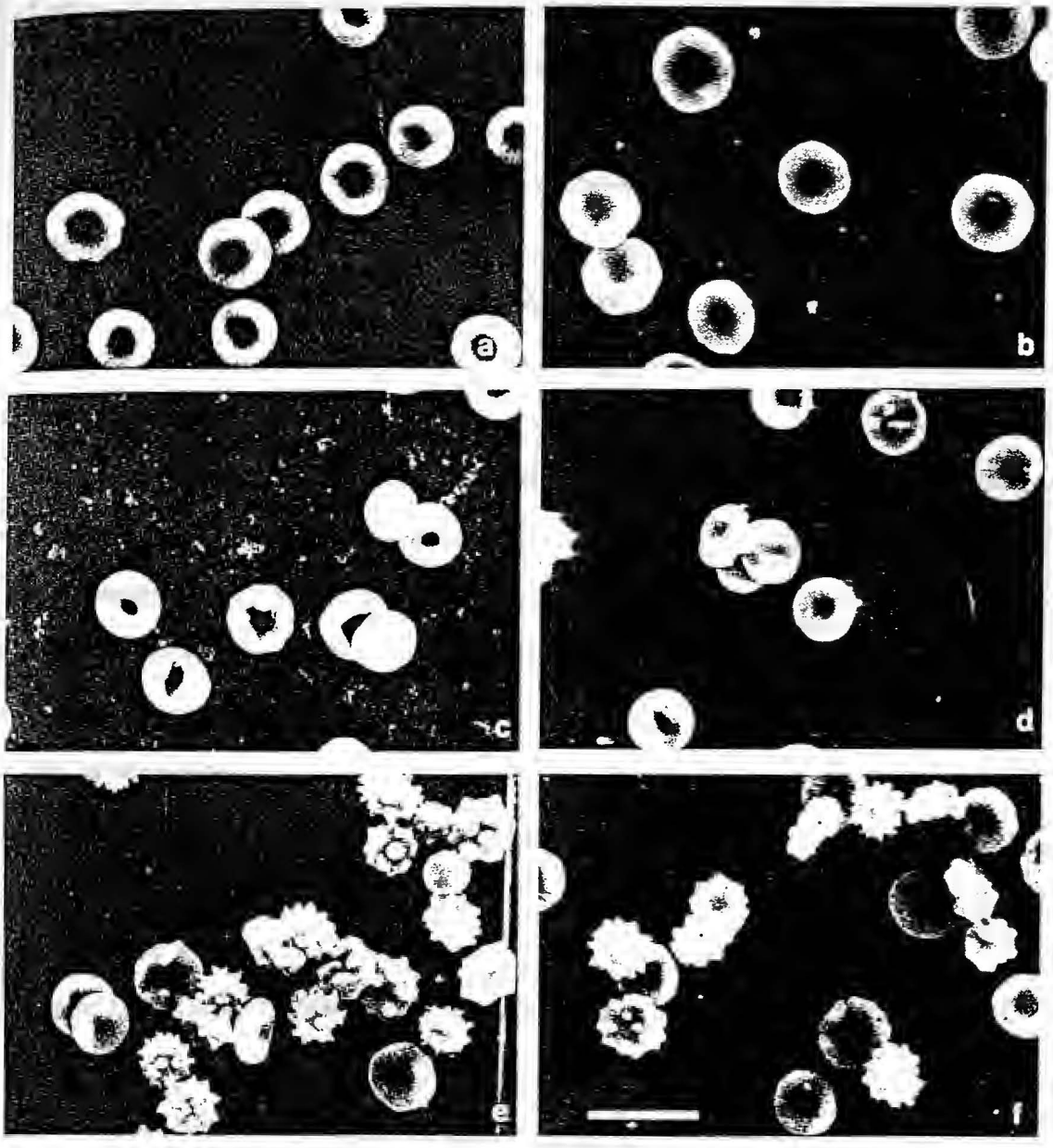
a
b
c
d
e
f

Table IV

Comparison of average RBC diameter obtained for Li^+-free RBC treated with various lanthanide shift reagents. The diameter was obtained using SEM[a] and CC.[b]

Sample	n	Average diameter/μm[a]	Average diameter/μm[b]
RBC controls	636	7.56 ± 0.14	5.38 ± 0.14
RBC treated with 3 mM $Dy(PPP)_2^{7-}$	892	7.64 ± 0.21	5.56 ± 0.09
RBC treated with 5 mM $Tm(PPP)_2^{7-}$	720	7.61 ± 0.18	5.52 ± 0.12
RBC treated with 3 mM $Dy(PcPcP)_2^{7-}$	667	7.68 ± 0.12	5.59 ± 0.06
RBC treated with 10 mM $Dy(TTHA)^{3-}$	718	7.55 ± 0.16	5.40 ± 0.11
RBC treated with 5 mM $Dy(DOTP)^{5-}$	694	7.59 ± 0.12	5.46 ± 0.12

Values are expressed as mean ± standard error of the mean. $p > 0.001$. No significant changes in diameter of RBCs were observed on shift reagent treatment.

is the same for both data sets, the average cell diameters measured by the two techniques for each shift reagent suspension do not agree. This discrepancy has to do with the nature of the two sets of measurements. The CC values shown in Table IV are calculated from the volume measurements assuming spherical shape for RBC. Thus, the CC values are clearly underestimated as a result of the assumption made on this calculation.

Size measurements of RBCs after preparation for SEM must be interpreted with caution. Because of fixation, dehydration, and drying, shrinkage of cells is always to be expected. In the pictures presented here a diameter of about 7.6 μm is measured in RBC controls (NaCl treated cells). Therefore, the specific effects of different shift reagent treatments must be interpreted relative to control samples. In order to probe if the SEM measurements were indeed valid, we also observed RBCs using phase contrast microscope prior to fixing. The shapes of cells observed before and after fixing are essentially the same. This procedure helps to identify if there are any errors due to fixation of red cells.

IV.3.2 Effect of Li^+ on Shape and Size of RBC

In order to differentiate the effects of the anionic shift reagents from those of the cations on the morphology of RBC, the specific effect of the Li^+ ion was further investigated because of its unusual hydration properties (105). Figure 19 shows the effect of the presence and absence of Li^+ in the suspension medium on shape and size of RBC. The intracellular Li^+ concentration in sample 19.B was measured by atomic absorption to be 0.48 mM and thus, it is representative of the deformations that RBCs from bipolar patients may be subject to during lithium therapy (27). As the concentration of Li^+ increases from 1.5 mM to 140 mM, the tendency to crenation increases in RBC. Table V gives the average diameter of Li^+ treated cells by SEM and CC, respectively. Li^+ treated RBCs are significantly larger than the normal RBCs. Li^+

Figure 19. SEM pictures obtained for (a) RBCs incubated with 5 mM LiCl and (b) RBC controls. pH was maintained at 7.4 and the osmolarity of all samples were maintained at 300 ± 5 mosM. Magnification and SEM conditions were the same as for Figure 18.

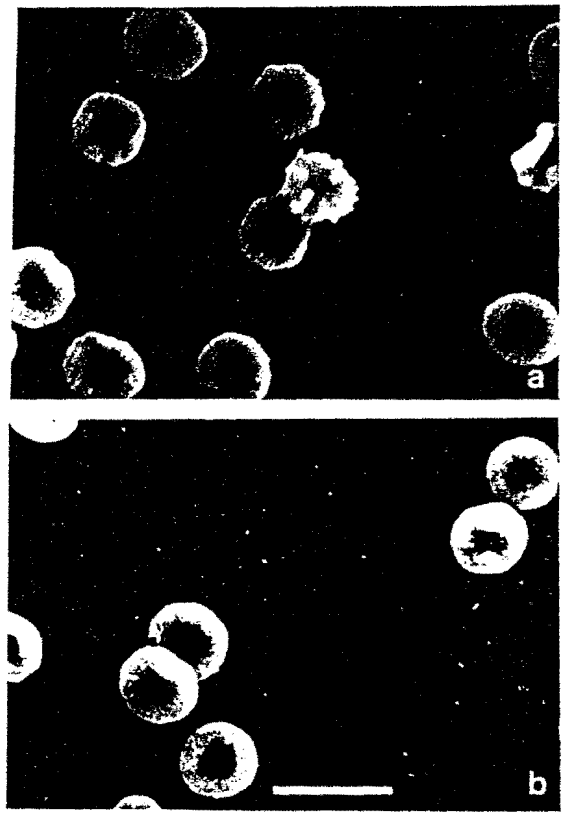
a
b

Table V

Comparison of average diameter of Li^+ and Dy^{3+} treated RBC obtained by SEM[a] and CC.[b]

Sample	n	Average diameter/μm[a]	Average diameter/μm[b]
RBC control	636	7.56 ± 0.14	5.38 ± 0.14
RBC treated with 1.5 mM LiCl	720	7.96 ± 0.22	5.62 ± 0.08
RBC treated with 5 mM LiCl	692	8.12 ± 0.12	6.07 ± 0.18
RBC treated with 140 mM LiCl	768	8.48 ± 0.10	6.36 ± 0.11
RBC treated with 0.06 mM $DyCl_3$	732	7.62 ± 0.10	5.39 ± 0.12

Values are expressed as mean ± standard error of the mean. LiCl and $DyCl_3$ treated RBCs were compared with RBC control. $p < 0.001$ for RBCs treated with 5 mM or 140 mM LiCl. $p > 0.001$ for RBCs treated with 1.5 mM LiCl or 0.06 mM $DyCl_3$. Significant changes in diameter of RBCs were observed on treatment with 5 mM LiCl or 140 mM LiCl.

treated RBCs also exhibit diminished biconcavity and tendency to crenate.

Some of the shift reagents used, in particular the triphosphate complexes (117,118), are subject to hydrolytic instability. As a result, some Dy^{3+} ion could diffuse into the RBCs and thus, exert an effect on the cell morphology. Based on the fact that the affinity constants for the Dy^{3+} and Tm^{3+} complexes of the aforementioned ligands are all below -3 (log pKa units) (103,110,119), the effect of 0.06 mM of $DyCl_3$ on the size and shape of RBC was also investigated (Table V). $DyCl_3$ at such a low concentrations has very little effect on size and morphology of RBCs which is in good agreement with literature reports (120,121).

IV.3.3 Effect of Lanthanide Shift Reagents on Na^+-Li^+ Exchange by ^7Li NMR Spectroscopy

In order to find out whether the presence of shift reagents in the cell suspension had a significant effect on the ion distribution in RBCs, we investigated the effect of LSRs on Na^+-Li^+ exchange in RBCs by ^7Li NMR spectroscopy. Intracellular Li^+ concentrations were calculated from the peak area of the intracellular Li^+ NMR resonance using previously described methods (46). Li^+-loaded RBCs were suspended in either a Na^+- or choline containing medium. From the data obtained in the choline medium, the rate for the Li^+ leak pathway was calculated. The rate obtained for the Na^+-suspension medium represents both the leak and Na^+-Li^+ exchange pathways. By subtracting these two values, we determined the contribution of the Na^+-Li^+ exchange pathway in Li^+-loaded RBCs (17,46). Table VI shows a comparison of Na^+-Li^+ exchange rates for Li^+-loaded RBCs determined by atomic absorption (AA) and ^7Li NMR methods. It is important to note that the NMR measurements are generally carried out on intact RBC suspensions while the AA measurements require cell lysis prior to chemical analysis. Since the determination of intracellular Li^+ concentration by the ^7Li NMR method required the addition of a shift reagent to the suspension medium, AA measurements

Table VI

Comparison of Na^+-Li^+ exchange rates in mmoles of Li^+ / (L RBCs x hour) of Li^+-loaded RBCs obtained in the presence and absence of shift reagents by AA and ^7Li NMR

sample	n	AA	NMR
control[a]	12	0.19 ± 0.04	---
7 mM $Dy(TTHA)^{3-}$	3	0.21 ± 0.02	0.22 ± 0.02
5 mM $Dy(DOTP)^{5-}$	6	0.25 ± 0.01	0.26 ± 0.02
3 mM $Dy(PPP)_2^{7-}$[b]	12	0.27 ± 0.04	0.28 ± 0.02
3 mM $Dy(PcPcP)_2^{7-}$[b]	12	0.28 ± 0.02	0.29 ± 0.03

[a] No shift reagent in this sample.
[b] The difference between Na^+-Li^+ countertransport rates measured in the presence and absence of 3 mM $Dy(PPP)_2^{7-}$ or 3 mM $Dy(PcPcP)_2^{7-}$ is significant up to a 99% confidence level.

were also taken on RBC samples which had been pretreated with LSR. The use of shift reagents $Dy(PPP)_2^{7-}$, $Dy(PcPcP)_2^{7-}$, $Dy(DOTP)^{5-}$, and $Tm(PPP)_2^{7-}$ effected an enhancement in the measured rates of Na^+-Li^+ exchange in RBCs. The effect was not significant with $Dy(TTHA)^{3-}$. These observations are in agreement with the known higher affinity of the triphosphate type shift reagents for metal cations relative to $Dy(TTHA)^{3-}$ (66-68).

IV.3.4 Effect of Lanthanide Shift Reagents on RBC Membrane Potential

Figure 20 and Table VII displays the effect of lanthanide shift reagents on RBC membrane potential. The membrane potential was obtained using the equations described by Kirk et al. (122). The described procedure involves incorporation of hypophosphite ion in the cell suspension. Hypophosphite ion crosses the cell membrane via the anion exchange protein, and the intra- and extracellular populations of the ion gives rise to separate ^{31}P NMR resonances. The relative areas of the two peaks (I_i / I_o) corresponds to the relative distribution of the intra- and extracellular hypophosphite populations. As described in reference 122, the concentration distribution ratio for the hypophosphite ion is given by the following equation:

$$r(H_2PO_2^-) = (I_i / I_o)((1-H_t)/\alpha H_t) \qquad [5]$$

where α is equivalent to the gravimetrically determined fractional water volume of the cell (123). Also it was assumed that for red cells membrane permeability of Cl^- is much larger than either K^+ or Na^+ and therefore the Nernst equation was simplified to

$$V_m = (RT/F) \ln r(Cl^-) \qquad [6]$$

where R is the gas constant, T is the absolute temperature and F is the Faraday constant. In the event of $H_2PO_2^-$ incorporation in cell suspension, it was assumed that $r(H_2PO_2^-)$ was equivalent to $r(Cl^-)$ (122). Hence the equation [6] modifies to

$$V_m = (RT/F) \ln r(H_2PO_2^-) \qquad [7]$$

RBCs in isotonic suspension medium consistently yielded a membrane potential estimate

Figure 20. Proton-decoupled ^{31}P NMR spectra of (A) RBCs (45% hematocrit) in a suspension medium containing 130 mM NaCl, 15 mM hypophosphite, 10 mM glucose, 10 mM Tris-Cl, pH 7.4. (B) The sample was similar in composition as sample A except that an aliquot of $Dy(TTHA)^{3-}$ (300 mOsM) was added such the final concentration of $Dy(TTHA)^{3-}$ was 7 mM. (C) The sample was similar to sample to sample A except that an isotonic aliquot of $Dy(PPP)_2^{7-}$ was added to the suspension such that the final concentration of $Dy(PPP)_2^{7-}$ was 5 mM.

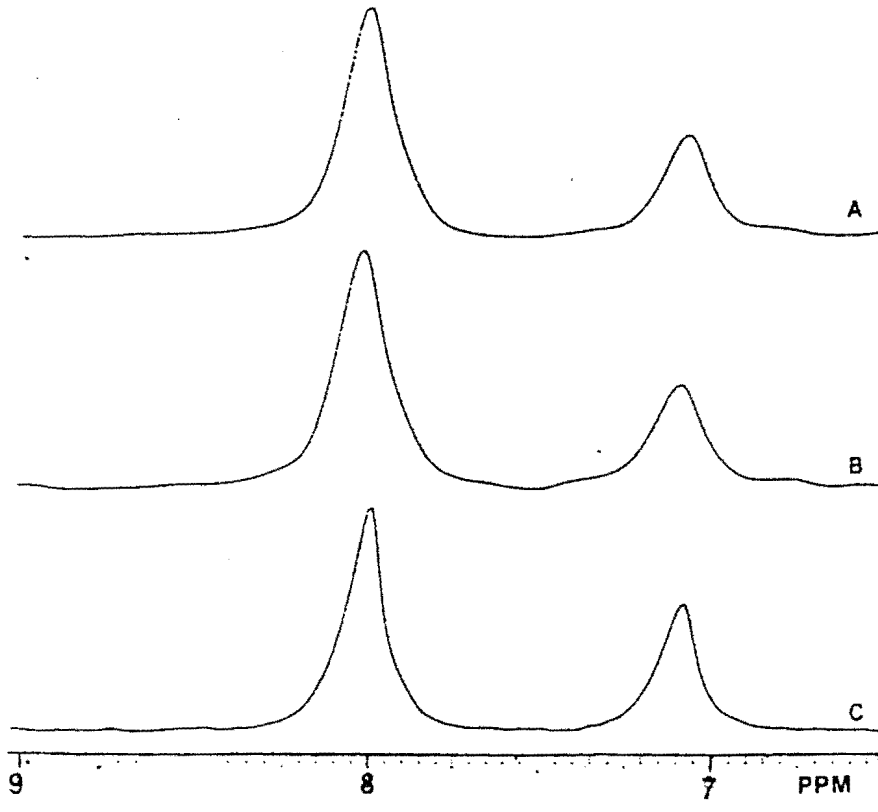
A
B
C
9
8
7
PPM

Table VII

Effect of various shift reagents on the membrane potential of RBCs obtained by ^{31}P NMR.[a,b]

Sample	n	$r(H_2PO_2^-)$	V_m / mV
RBC control	12	0.65 ± 0.04	- 11.42 ± 0.54
RBC treated with 7 mM $Dy(TTHA)^{3-}$	6	0.67 ± 0.03	- 10.28 ± 0.54
RBC treated with 5 mM $Dy(DOTP)^{5-}$	6	0.78 ± 0.05	- 6.38 ± 0.46
RBC treated with 5 mM $Dy(PPP)_2^{7-}$	9	0.92 ± 0.02	- 2.14 ± 0.56

[a]The relative distribution of the intra- and extracellular hypophosphite populations, $r(H_2PO_2^-)$, and the membrane potential, V_m, were calculated according to the equations (118): $r(H_2PO_2^-) = (I_i/I_o)[(1 - H_t)/\alpha H_t]$ and $V_m = (RT/F \ln r(H_2PO_2^-)$, where I_i and I_o are the areas of the intra- and extracellular $H_2PO_2^-$ ^{31}P NMR peaks, α is the gravimetrically determined fractional water volume of RBC (119), R is the gs constant, T is the absolute temperature, and F is the Faraday constant. [b]The effect of 5 mM $Tm(PPP)_2^{7-}$ on RBC membrane potential was briefly studied and was found to be similar (-1.98 ± 0.39, n = 3) to that of 5 mM $Dy(PPP)_2^{7-}$.

of around - 11 mV. This value is in good agreement with that obtained by others (122,124,125). Lithium loaded RBCs suspended in an isotonic suspension medium also yielded a membrane potential estimate around - 10 mV (n = 3) (data not shown) thereby indicating that Li^+ does not affect the membrane potential of RBC. In experiments involving the shift reagents, an aliquot of the isotonic shift reagent solution was added to the isotonic RBC suspension, such that the osmolarity of the sample did not change upon shift reagent addition. Of the studied shift reagents, $Dy(PPP)_2^{7-}$ induced significant changes in the membrane potential of RBCs. Addition of $Dy(PPP)_2^{7-}$ to the RBC suspension caused the membrane potential of RBC to change from -11 mV to -2 mV. $Dy(DOTP)^{5-}$ also caused significant changes in the membrane potential of RBC, while $Dy(TTHA)^{3-}$ had no significant effect.

In another set of experiments the extracellular NaCl was replaced iso-osmotically with $Na_7[Dy(PPP)_2]$. The membrane potential changed progressively from -11 mV in the absence of shift reagent to + 0.56 mV at an extracellular $Dy(PPP)_2^{7-}$ concentration of 5 mM. 5 mM $Tm(PPP)_2^{7-}$ caused a similar change in RBC membrane potential. These results along with those given above suggest that shift reagents are specifically affecting the membrane potential. Thus the shift reagent effect on membrane potential is not due to replacement of Cl^- in the shift reagent containing samples. These findings further confirm the ability of some shift reagents to affect the distribution of ions across the membrane.

The intracellular pH was maintained for all the samples shown in Table VII. The changes in intracellular pH of RBC were not significant upon the addition of shift reagents. Hence, the changes in membrane potential of RBC upon addition of shift reagents are shift reagent specific effects and not due to intracellular pH fluctuations.

The membrane potential of shift reagent treated RBCs were also determined using a ^{19}F NMR method (126). In this method 2 mM trifluoroacetate and 1.5 mM

trifluoroacetamide are incorporated in the suspension medium and their distribution across the RBC membrane is used in obtaining the membrane potential. The intensities of the intra- and extracellular trifluoroacetate and trifluoroacetamide are incorporated into the Nernst equation as given below:

$$V_m = \frac{RT}{F} \frac{[I_i(TFA)\ \ I_e(TFM)]}{[I_e(TFA)\ \ I_i(TFM)]}$$

where I_i and I_e correspond to the intra- and extracellular ^{19}F NMR resonances. Trifluoroacetate (TFA) and trifluoroacetamide (TFM) intra- and extracellular intensities are obtained in a single spectrum which then can be used to estimate the membrane potential. Table VIII shows the RBC membrane potential data obtained by the ^{19}F NMR method. The data obtained by this method agree well with those obtained by the ^{31}P NMR method using hypophosphite. It is clearly evident by two different NMR methods that the shift reagents, especially $Dy(PPP)_2^{7-}$, have a significant effect on the membrane potential of RBC. The extent to which the membrane potential is affected depends on the overall charge on the shift reagent. $Dy(PPP)_2^{7-}$, with a higher negative charge than $Dy(DOTP)^{5-}$ and $Dy(TTHA)^{3-}$, has the largest effect on the membrane potential of RBC. $Tm(PPP)_2^{7-}$ had a similar effect on membrane potential as $Dy(PPP)_2^{7-}$. Based on this study, $Dy(TTHA)^{3-}$ exhibits minimum delirious effect on RBC and thus can be considered to be the best shift reagent of those tested.

IV.4 Na^+-Li^+ Countertransport Measurements In RBCs From Hypertensive Patients And Normal Controls By MIR Pulse Sequence

Discrimination between the two pools of Li^+ ion in RBC by NMR spectroscopy can be achieved by incorporating lanthanide shift reagents in the suspension medium (Figure 21.A) (45,60). Although the shift reagent approach is excellent for monitoring Li^+ transport in biological systems (45), it was found that the

Table VIII

Effect of various shift reagents on the membrane potential of RBCs by ^{19}F NMR.

Sample[a]	n	V_m / mV
RBC control	3	-11.26 ± 0.32
RBC treated with 7 mM $Dy(TTHA)^{3-}$	3	-10.32 ± 0.27
RBC treated with 5 mM $Dy(DOTP)^{5-}$	3	-6.46 ± 0.32
RBC treated with 5 mM $Dy(PPP)_2^{7-}$	3	-1.98 ± 0.36

[a]The suspension media for RBC samples contained 145 mM NaCl, 10 mM HEPES pH 7.4, 10 mM glucose, 2 mM trifluoroacetate and 1.5 mM trifluoroacetamide. In shift reagents samples an aliquot of the isotonic shift reagent $Dy(PPP)_2^{7-}$ or $Dy(DOTP)^{5-}$ or $Dy(TTHA)^{3-}$ was added to obtain the desired concentration of the shift reagent.

Figure 21. (A) ^{7}Li NMR (116.5 MHz, 37°C) spectrum of Li^{+}-loaded RBC in a suspension containing 3.5 mM LiCl, 3 mM $Dy(PPP)_2^{7-}$, 5 mM KCl, 110 mM NaCl, 10 mM glucose, 50 mM HEPES, pH 7.4. Hematocrit was 13%. 17% D_2O was present for field frequency lock. The upfield signal depicts the extracellular Li^{+} pool. The flip angle was 45° and the acquisition time of 1 s was followed by a delay of 6.5 s. 8 scans were used resulting in a total accumulation time of approximately 1 min. (B) ^{7}Li NMR spectrum of a Li^{+}-loaded RBC suspension as in A except that 30 mM NaCl was present in the medium instead of 3 mM $Dy(PPP)_2^{7-}$. A single pulse sequence (D_1-60°-AQ) was employed consisting of a repetition rate D_1 of 50 s and a flip angle of 60° before spectral acquisition AQ of 1 s. The spectrum consists of two overlapped intra- and extracellular lithium pools. The spectrum was obtained after 8 scans, total time being 8.3 min. (C) ^{7}Li NMR spectrum of the same RBC suspension as in B except that a modified inversion recovery pulse sequence (D_1-180°-D_2-60°-AQ) was used. The spectrum C represents the intracellular $^{7}Li^{+}$ resonance. (D) The difference spectrum of Figures 21.B and 21.C. The spectrum D represents the extracellular $^{7}Li^{+}$ resonance. (E) ^{7}Li NMR spectrum of the suspension medium (no RBC) using the same MIR method as in C. Line broadening of 5 Hz was used for all spectra.

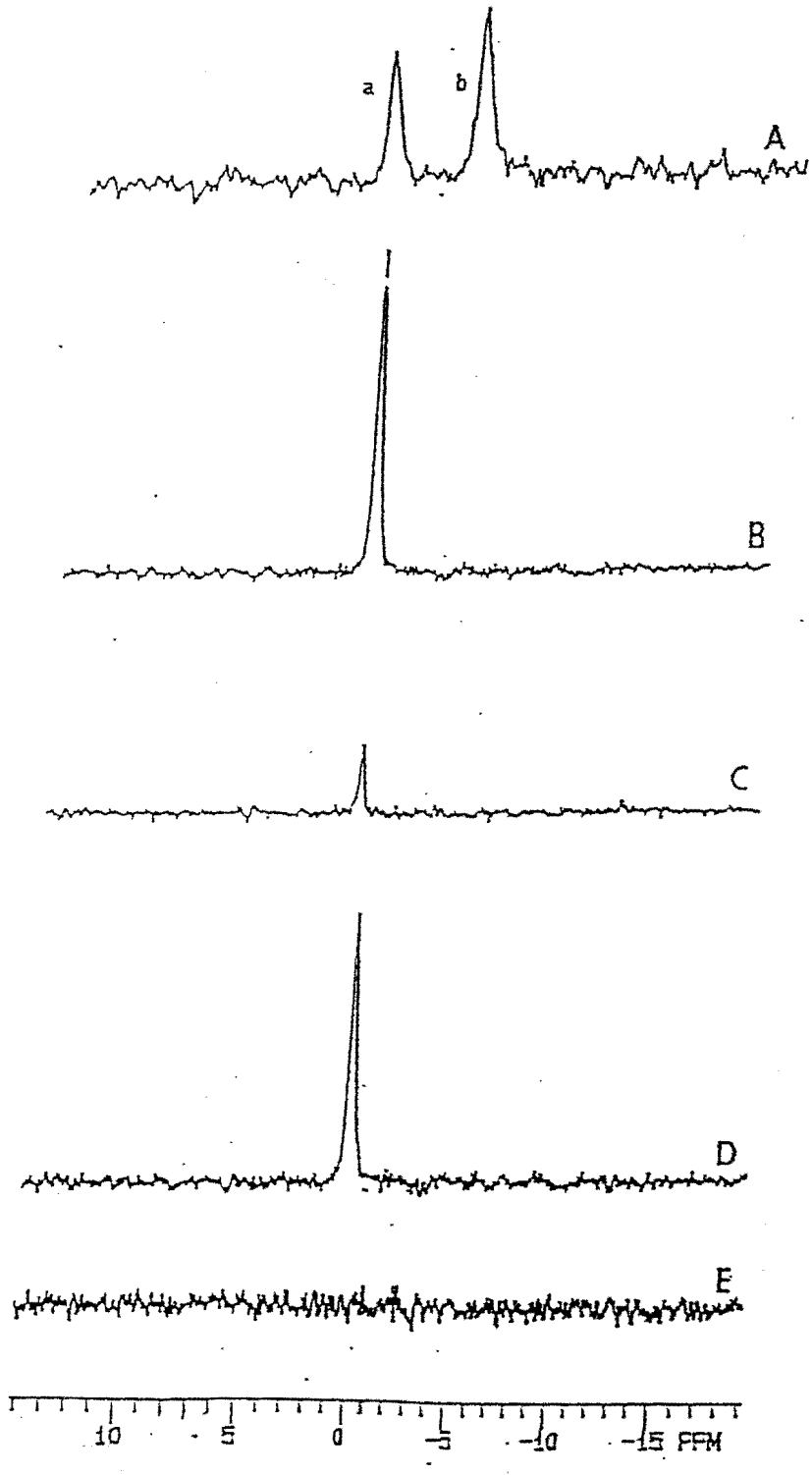
a
b
A
B
C
D
E
10
5
0
-5
-10
-15 PPM

presence of shift reagents in the plasma changes the ion distribution between the two cellular compartments (46). We have now developed a modified inversion recovery (MIR) method (46) that is able to discriminate between the two pools of Li^+ ion in RBC without involving any shift reagents. The pulse sequence takes advantage of the large difference in T_1 values for the intra- and extracellular $^7Li^+$ ions (4.9 and 16.5 s, respectively).

Figure 21.B shows the $^7Li^+$ NMR signal obtained using a single pulse sequence (D_1-60^o-AQ) on lithium loaded RBC in a suspension medium containing 3.5 mM lithium chloride. The signal obtained in Figure 21.B represents the overlapped intra- and extracellular $^7Li^+$ resonances. The delay time D_1 was arrayed at 5 s intervals in the range of 40 through 60 s. Maximal signal intensity was obtained for a value of $D \geq 48$ s. Thus, the 60^o flip angle and the delay between single pulses of 50 s used allows complete relaxation of both $^7Li^+$ NMR signals. The intracellular Li^+ pool can be selectively observed (fig 21.C) by employing the MIR pulse sequence (D_1-180^o-D_2-60^o-AQ) (46). Since the T_1 value of intracellular $^7Li^+$ is about 5 s, it will have sufficient time to relax completely after a delay D_2 of 11.5 s, while the extracellular $^7Li^+$ will not. The intracellular $^7Li^+$ resonance, which has longer T_1 value, can therefore be uniquely detected along the y-axis after a 60^o pulse. Several D_2 values were used (in the range 7 to 30 s) and the maximal intensity for the intracellular $^7Li^+$ NMR signal was obtained for D_2 = 11.5 s.

No signal is observed by recording the ^7Li NMR spectrum of the suspension medium (Figure 21.E) using the MIR pulse sequence (46). The inability to observe a $^7Li^+$ resonance for extracellular Li^+ for D_2 = 11.5 s indicates that the signal observed in Figure 21.C can only be due to the intracellular Li^+ pool and not a combination of intra- and extracellular signals. The intensities of intracellular $^7Li^+$ signal obtained by shift reagent method (Figure 21.A) and MIR method (Figure 21.C) are not the same

because it is known from previous studies that $Dy(PPP)_2^{7-}$ affects the Li^+ distribution ratios in RBCs (46, 109). The difference spectrum shown in Figure 21.D represents the extracellular Li^+ pool. The delay time D_2 for suppression of extracellular $^7Li^+$ resonance and the relaxation time T_1 of the extracellular Li^+ may be dependent on the composition of the suspension medium and temperature conditions employed during the measurements. Thus, it is important to keep the temperature regulated during the NMR experiments and check the D_2 parameter when using the MIR method for the first time with a different suspension medium and/or cellular system. However, we found D_2 to be the same (11.5 s) in NaCl and $MgCl_2$ suspensions of RBC at the temperature of 37° C.

The MIR pulse sequence was used to measure the rate of $^7Li^+$ transport of Li^+-loaded RBCs (normotensive and hypertensive) in NaCl and $MgCl_2$ media. The decrease in area of the intracellular $^7Li^+$ signal, due to Li^+ efflux, was monitored with time in both Na^+- and Mg^{2+}-media. The resonance areas measured in the NMR experiments can be expressed in terms of intra- and extracellular Li^+ concentrations as shown in the experimental section (Section III.4.1).

The changes in intracellular Li^+ concentrations in RBC of normotensives and hypertensives are plotted against time in Figure 22. The slope of the plot of intracellular Li^+ concentration vs. time in the $MgCl_2$ medium gives the rate for the Li^+ leak pathway. By subtracting these two values, we determined the contribution of the Na^+-Li^+ countertransport in Li^+-loaded RBCs. Table IX summarizes determinations of the rates of Na^+-Li^+ countertransport in RBC from normotensive and hypertensive subjects by atomic absorption and non-invasive ^7Li NMR techniques. The rates of RBC Na^+-Li^+ countertransport measured by the ^7Li NMR method correlated well with the measurements made by atomic absorption for both the hypertensive ($r = 0.964$) and control ($r = 0.961$) groups. A student t-test was employed to test the statistical significance of the difference in rates obtained for normotensive and hypertensive

Figure 22. Time dependence of intracellular lithium concentration obtained from $^{7}Li^{+}$ NMR signal intensities in Na^{+}- (triangles) and Mg^{2+}- (squares) media for hypertensive patient # 10 (filled symbols) and normotensive control # 10 (open symbols). Patient number refers to Table IX.

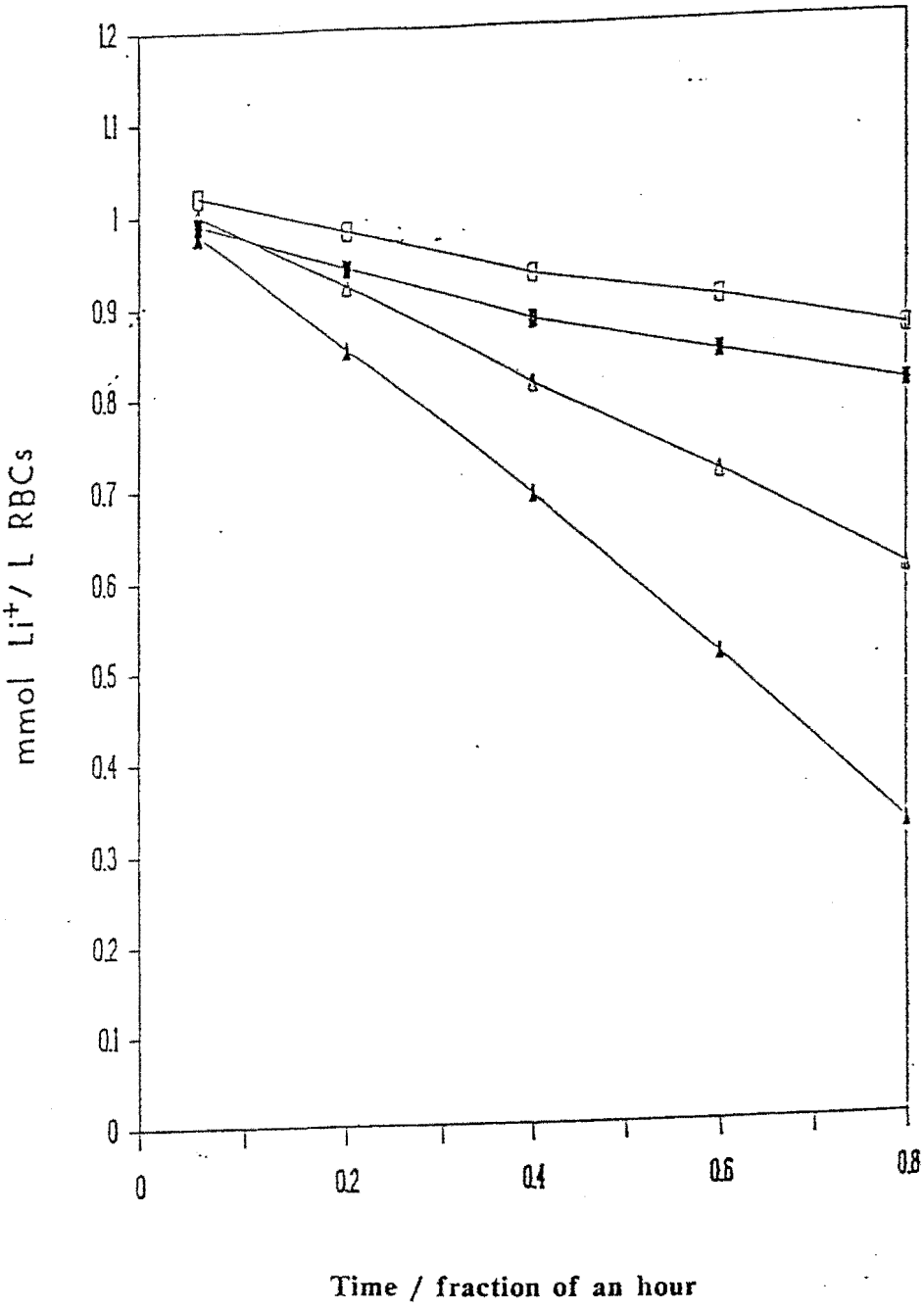
mmol Li+ / L RBCs
1.2
1.1
1
0.9
0.8
0.7
0.6
0.5
0.4
0.3
0.2
0.1
0
0
0.2
0.4
0.6
0.8
Time / fraction of an hour

Table IX

Comparison of Na^+-Li^+ countertransport rates in mmoles of Li^+ /(L RBCs x hour) and rate constant in h^{-1} obtained by atomic absorption (AA) and ^7Li NMR (MIR) methods on normotensives (NS) and hypertensives (HS).

Patient Number	Age, Race, Sex, Weight & Smoking*		Rates				Rate constant	
			AA		MIR		MIR	
	HS	NS	HS	NS	HS	NS	HS	NS
1	43W,F,244,S	35W,F,130,NS	0.46	0.20	0.47	0.20	0.56	0.17
2	50W,M,160,NS	30W,M,138,NS	0.52	0.23	0.51	0.24	0.59	0.18
3	50B,F,128,NS	47B,F,150,S	0.54	0.22	0.53	0.22	0.62	0.17
4	52W,M,283,NS	31W,M,175,NS	0.56	0.19	0.54	0.20	0.62	0.16
5	52W,F,253,NS	25W,F,115,NS	0.54	0.22	0.52	0.21	0.60	0.17
6	55W,M,214,NS	33W,M,160,NS	0.50	0.23	0.50	0.23	0.59	0.19
7	60W,F,133,NS	37W,F,120,NS	0.51	0.22	0.50	0.22	0.59	0.18
8	63W,M,196,NS	35W,M,148,NS	0.52	0.20	0.53	0.21	0.60	0.19
9	65W,F,139,NS	40W,F,125,NS	0.51	0.24	0.52	0.24	0.59	0.18
10	73W,M,228,S	50W,M,168,NS	0.62	0.25	0.61	0.26	0.71	0.20
Average#			0.53±0.02	0.22±0.02	0.51±0.04	0.21±0.02	0.61±0.01	0.18±0.01

*Abbreviations used are M-male, F-female, W-white, B-black, NS-non-smoker, S-smoker. #Values expressed as mean ± standard error of the mean. $p < 0.001$

patients. For both techniques, the rates of Na^+-Li^+ countertransport in RBC of hypertensive patients were found to be significantly higher (above the 99.9% confidence level) than those obtained from RBC of normotensives.

First order rate constants for Na^+-Li^+ countertransport pathway were also estimated from MIR data. Table IX reveals that the rate constants for the Na^+-Li^+ countertransport pathway are much higher in hypertensive ($k = 0.61 \pm 0.01\ h^{-1}$) than in normotensive RBCs ($k = 0.18 \pm 0.01\ h^{-1}$).

The differences in rate constant values between hypertensive and normotensive RBCs are much larger than those of rates. It is tempting to speculate that rate constant could be used as a marker to determine the extent of hypertension (i.e. borderline or chronic). After an extensive determination and analysis of rate constant for RBCs with varying degree of hypertension, it could be possible to predict the extent of hypertension in patients with fair precision. Table IX indicates that MIR method gives statistically reliable data for both rate constants and rates of Na^+-Li^+ countertransport. It may be possible to set up a reliable chart with values for rate constants for varying degrees of hypertension from MIR measurements.

It is important to stress that the atomic absorption method requires physical separation of RBC and plasma prior to chemical analysis. This procedure could lead to errors related to non-specific ion binding to membranes and additional ion transport during blood processing. Moreover, atomic absorption is time consuming and does not reveal any information on ion binding to membranes. The large variation in Li^+ transport rates for RBC of hypertensives obtained previously by atomic absorption was attributed to the heterogeneity the origin of hypertension (6,9,17). That conclusion was reached on the grounds that varying overlapping rates of Li^+ transport were found in RBC of patients from different countries and races (6,9,17). The limitations of the AA technique could have been responsible, at least in part, for some of these

discrepancies. However, we show in this study that by using a totally non-invasive method like ^{7}Li NMR spectroscopy, a statistically significant difference between rates of Li^+ transport in RBC of hypertensives relative to that observed in normal controls still exists.

IV.5 Competition Between Li^+ And Mg^{2+} In Human RBCs

Figure 23 displays the effect of the presence and absence of Li^+ on ^{31}P NMR resonances of ATP in Mg^{2+}-depleted and saturated RBCs. The chemical shift separation between the α and β phosphate resonances of ATP ($\delta_{\alpha\beta}$) in Li^+-loaded-Mg^{2+}-depleted RBCs (spectrum 23.D) is smaller than the values observed in free ATP solutions or Mg^{2+}-depleted cells (spectra 23.A and 23.B, respectively). However, the value of $\delta_{\alpha\beta}$ for Li^+-loaded-Mg^{2+}-depleted cells resembles that observed in Li^+-saturated ATP solutions (cf. spectra 23.C and 23.D) indicating that Li^+ loading has a significant effect on $\delta_{\alpha\beta}$ measured in Mg^{2+}-depleted RBCs. By contrast, $\delta_{\alpha\beta}$ is approximately the same in Mg^{2+}-saturated cells either in the presence or absence of Li^+ (spectra 23.E through 23.G). Mg^{2+}, because of its higher charge, has a higher affinity than Li^+ for ATP (39,127). Because of their relative affinities for ATP, the competition between Li^+ and Mg^{2+} in RBCs is better felt in Mg^{2+}-depleted than in Mg^{2+}-saturated cells.

The intracellular pH of Li^+-loaded and Li^+-free RBCs were monitored by ^{31}P NMR. The chemical shift separation between P_i and Pα (of ATP) was used as an indicator of intracellular pH in Li^+-loaded and Li^+-free RBCs. No significant changes in intracellular pH was observed in Li^+-loaded RBCs when compared with Li^+-free RBCs. The total intracellular Mg^{2+} concentration in Li^+-loaded and Li^+-free RBCs were measured by AA method as described in a published procedure (128). The total concentration of intracellular Mg^{2+} was 2.926 $\pm$ 0.008 mM (n = 3) and 2.922 $\pm$ 0.007 mM (n = 3) in Li^+-free RBCs and Li^+-loaded RBCs respectively. In Li^+-free and Li^+-loaded Mg^{2+}-saturated RBCs, the total intracellular Mg^{2+} was 9.829 $\pm$ 0.012 mM (n=3) and 9.802

Figure 23. ^{31}P NMR (121.4 MHz, 37° C) spectra of ATP under the following conditions: (A) 5 mM ATP in the Na^+ form. (B) RBC + 20 mM EDTA + 40 mg/L ionophore A23187 (Mg^{2+}-depleted cells). (C) 5 mM ATP + 5 mM LiCl. (D) Li^+-loaded RBC + 20 mM EDTA + 40 mg/L A23187 (Li^+-loaded-Mg^{2+}-depleted cells). (E) 5 mM ATP + 20 mM $MgCl_2$. (F) RBC + 20 mM $MgCl_2$ + 40 mg/L A23187 (Mg^{2+}-saturated cells). (G) Li^+-loaded RBC + 20 mM $MgCl_2$ + 40 mg/L A23187 (Li^+-loaded-Mg^{2+}-saturated cells). Following the incubation procedures indicated above, RBCs used in spectra B, D, F, and G were resuspended in the same medium containing containing 140 mM KCl, 10 mM glucose, and 10 mM Tris-Cl, pH 7.2. Line broadening of 5 Hz was used in all spectra. In sample D Li^+ was loaded to Mg^{2+} depleted RBC (EDTA would otherwise interfere with Li^+ loading), while in sample F Li^+ was loaded before saturating with Mg^{2+}. Going from left to right, the ^{31}P NMR signals are due to the γ ,α, and β phosphate resonances of ATP. The exchange broadening of the γ and β resonances of ATP present in spectra F and G is due to incomplete saturation of RBC with Mg^{2+}.

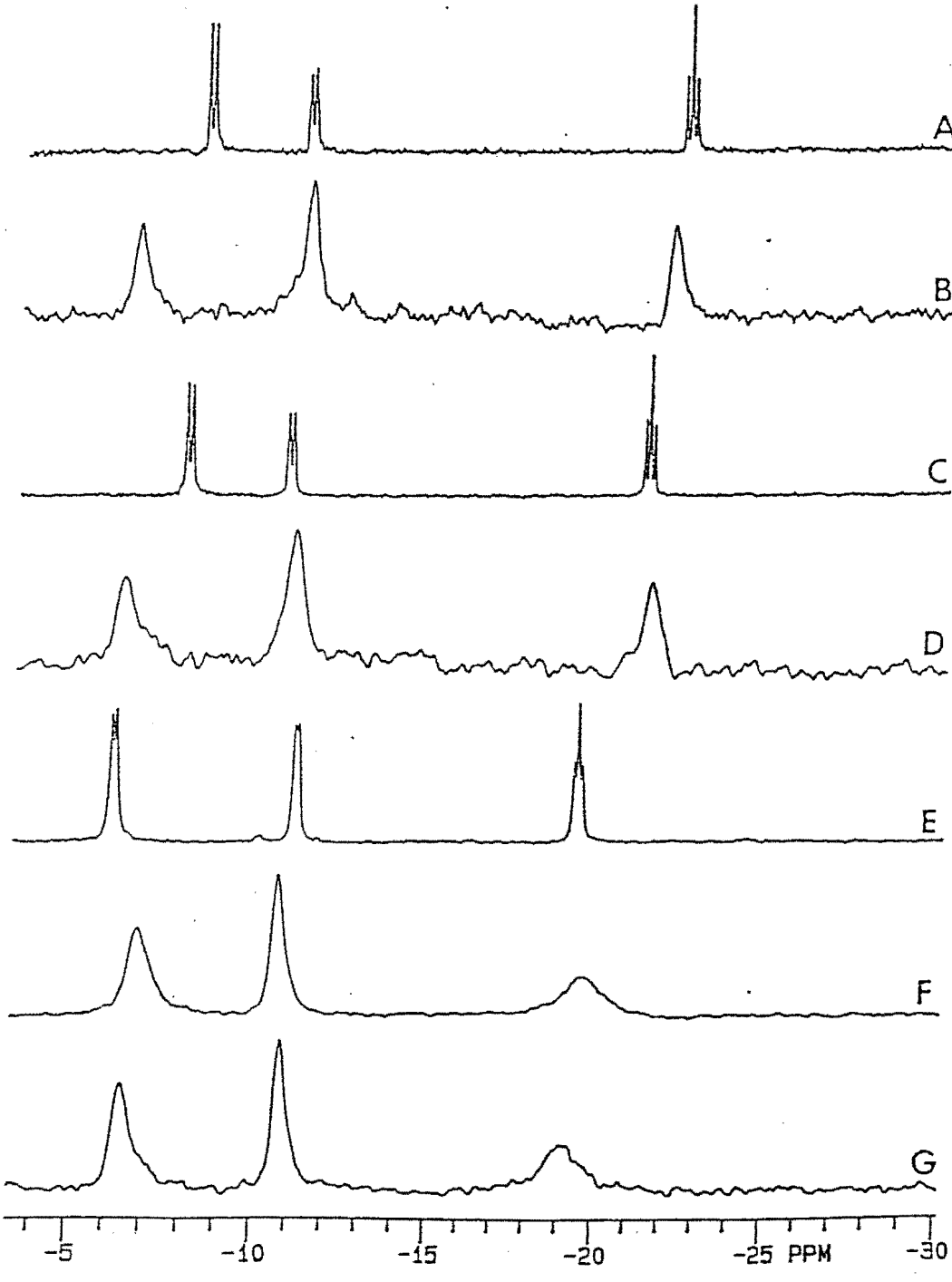
A
B
C
D
E
F
G
-5
-10
-15
-20
-25 PPM
-30

± 0.014 mM (n=3), respectively. Thus it is clear that Li^+ loading in RBCs did not stimulate Mg^{2+} efflux in RBCs.

Figure 24 shows the effect of Li^+ loading on the $\delta_{\alpha\beta}$ separation of ATP in RBCs containing normal intracellular Mg^{2+} levels. $\delta_{\alpha\beta}$ for Li^+-free RBCs was 8.54 ± 0.04 ppm (n = 14) while for Li^+-loaded RBCs it was 9.46 ± 0.06 ppm (n = 14). While the intracellular Mg^{2+} levels were manipulated in Figure 23 by addition of an ionophore, those in Figure 24 represent normal intracellular Mg^{2+} levels and yet, at an intracellular 3 mM Li^+ concentration, competition between the two metal ions occurs. Estimation of the ratio of free ATP to total ATP can be obtained from $\delta_{\alpha\beta}$ (129). This separation is greater for free ATP (spectrum 23.A) than for $MgATP^{2-}$ (spectrum 23.E), and for intermediate degrees of complexation, the observed separation represents a weighted average, since Mg^{2+} ions exchange rapidly between ATP molecules and solution on the NMR time scale. If Li^+ ions were to displace Mg^{2+} from ATP one would predict an increase in the ratio of free to Mg^{2+}-bound ATP and an increase in $\delta_{\alpha\beta}$, as observed.

We quantitated intracellular free Mg^{2+} concentrations using a combined ^{31}P NMR and optical absorbance spectroscopic approach as shown in Table X. Calibration graphs ($r > 0.98$) were constructed, in the presence and absence of Li^+, for samples A through C shown in Table X. These curves correlated $\delta_{\alpha\beta}$ obtained by ^{31}P NMR and intracellular free Mg^{2+} concentration obtained by optical spectroscopy both measured in antipyrylazo-III loaded resealed RBC ghost samples. Using these calibration graphs, the intracellular free Mg^{2+} concentrations in control RBCs and Li^+-loaded RBCs were estimated (sample D). It was found that the free intracellular Mg^{2+} concentration in RBCs decreased upon Li^+ loading. Model studies with ATP solutions containing the RBC components 2,3-diphosphoglycerate (DPG), and ADP (sample A) indicate that Li^+ displacement of Mg^{2+} from ATP could only account for a 0.3 ppm increase in $\delta_{\alpha\beta}$ as opposed to a 0.9 ppm increase observed in Li^+-loaded RBCs. Moreover, the free Mg^{2+}

Figure 24. ^{31}P NMR spectra of ATP in (A) Li^+-free RBCs and (B) 3 mM Li^+-loaded RBCs at 37^{o} C. The suspension medium for both samples contained 140 mM KCl, 10 mM glucose, and 10 mM Tris-Cl, pH 7.2. Line broadening of 5 Hz was used.

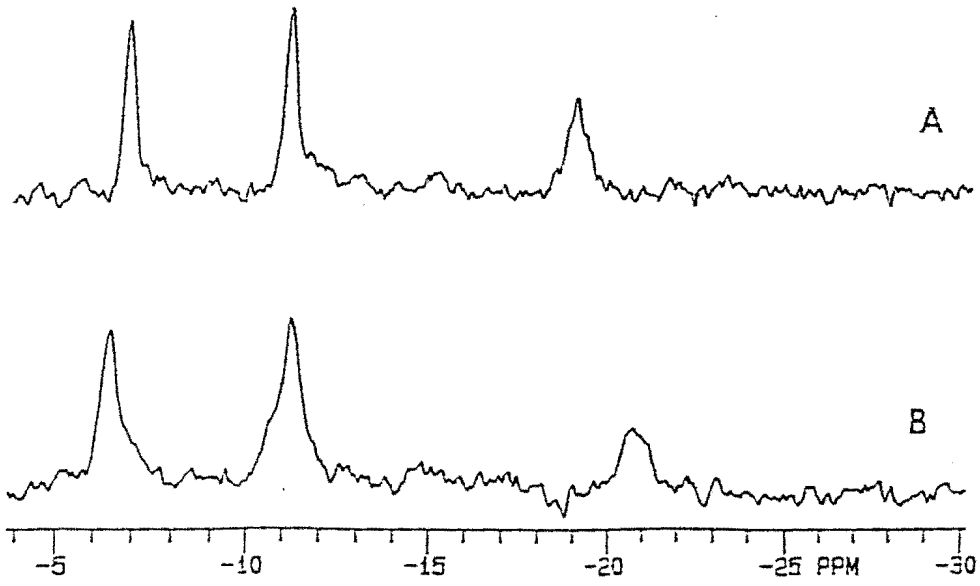
A
B
-5
-10
-15
-20
-25 PPM
-30

concentration increased in sample A and it decreased in intact RBCs. However, the presence of the RBC membrane (samples B and C) is able to mimic the effects occurring in intact RBCs. It is known that Li^+-loaded RBCs have larger volume than Li^+-free RBCs (105). The observed decrease in intracellular free Mg^{2+} is much greater than what would be expected due to dilution of intracellular compartment. The dilution effect would decrease the intracellular free Mg^{2+} concentration from 252 to 208 μM in Li^+-loaded RBCs. The intracellular free Mg^{2+} concentration obtained for Li^+-loaded RBCs were much lower, indicating that what is being observed is mostly due to competition between Li^+ and Mg^{2+} in Li^+-loaded RBCs. Thus, the decrease in intracellular free Mg^{2+} concentrations in Li^+-loaded RBCs is mostly due to displacement of Mg^{2+} from $MgATP^{2-}$and subsequent binding of Mg^{2+} to the RBC membrane. Similar observations of an increase in $\delta_{\alpha\beta}$ and a decrease in free intracellular Mg^{2+} concentration have been reported upon storage of RBCs (128,129). These changes may also be the result of enhanced Mg^{2+} binding to RBC membranes in stored blood but that possibility remains to be tested.

The equation of Gupta et al. (129) used to quantitate free intracellular Mg^{2+} concentration in intact RBCs needs to be modified in order to be applied to Li^+-loaded RBCs. The existing Gupta's equation predicts a free Mg^{2+} concentration of 156 μM ($\delta_{\alpha\beta}$ = 8.82 ppm) for an isolated system containing 2 mM ATP, 3 mM LiCl and 2.4 mM $MgCl_2$ (sample A), as opposed to 360 μM directly measured by the dye method. This calculation clearly indicates that information about free intracellular Li^+ concentration, along with K_{LiATP} affinity constant, will have to be incorporated into the original Gupta's equation in order to calculate free intracellular Mg^{2+} concentrations in Li^+-loaded RBCs. Obtaining free Li^+ concentration directly in the presence of other cations such as Mg^{2+} and Na^+ may be technically difficult. However, the recent development of a Li^+ ion selective electrode shows some promise in this respect (53,55). Moreover,

Table X

Effect of Li^+ on free Mg^{2+} concentrations in model systems and in RBCs obtained by ^{31}P NMR[a] and optical absorbance[b] techniques.

	No LiCl		with 3 mM LiCl	
	$\delta_{\alpha\beta}$/ppm[a]	$[Mg^{2+}]/\mu M$[b]	$\delta_{\alpha\beta}$/ppm[a]	$[Mg^{2+}]/\mu M$[b]
Sample A (n = 6) 2 mM ATP + 5.4 mM 2,3-DPG + 0.2 mm ADP + 2.4 mM $MgCl_2$	8.59 ± 0.06	324 ± 8	8.82 ± 0.02	356 ± 6
Sample B (n = 6) Resealed RBC membranes + 2 mM ATP + 2.4 mM $MgCl_2$	8.89 ± 0.04	386 ± 9	9.68 ± 0.06	288 ± 8
Sample C (n = 6) Resealed RBC membranes with 2 mM ATP + 2.4 mM MgCl2 + 5.4 mM 2,3-DPG + 0.2 mM ADP	8.66 ± 0.08	336 ± 16	9.52 ± 0.06	246 ± 18
Sample D (n = 14) Intact RBC	8.54 ± 0.04	252 ± 12	9.46 ± 0.06	146 ± 14

mixed ternary complexes such as Li-ATP-Mg could be present in solution. Their presence and influence (if any) on free Mg^{2+} concentration must also be taken into account.

Relaxation measurements shown in Table XI further confirm the competition between Li^+ and Mg^{2+} in RBCs and resealed RBC ghosts. It is well established that slow motions contribute only towards T_2 whereas fast motions contribute towards both T_1 and T_2 (102). The observation of a large difference between T_1 and T_2 suggests that the correlation times of Li^+ are relatively slow due to the interaction of Li^+ with the components in RBC and resealed RBC ghosts. When lithium ions are subject to electric field gardients in the membrane or are immobilized in the membrane, the relaxation time T_2 decreases more than T_1. The shorter the relaxation time the stronger the interaction of Li^+ with the membrane. Table XI shows that Mg^{2+} addition lengthens the relaxation times of $^7Li^+$ and that qualitatively, Mg^{2+} has a much higher binding affinity for the membrane than Li^+. This observation reinforces the ^{31}P NMR chemical shift data that Li^+ displaces Mg^{2+} form $MgATP^{2-}$ and that the released Mg^{2+} could be binding to the membrane.

Table XI

^{7}Li NMR Relaxation Time Measurements of Mg^{2+} Depleted And Mg^{2+} Saturated Li^{+}-Loaded RBCs

Sample	Total $[Mg^{2+}]$ / mM	T_1 / s	T_2 / s
(A) Li^{+}-loaded RBCs (n=3)			
Mg^{2+}-depleted	---	4.9 ± 0.1	0.082 ± 0.008
Normal	2.9 ± 0.1	6.6 ± 0.1	0.15 ± 0.01
Mg^{2+}-saturated	9.8 ±0.3	7.8 ± 0.2	0.28 ± 0.02
(B) Li^{+}loaded RBC ghosts (n=3)			
Mg^{2+}-depleted	---	9.8 ± 0.3	1.1 ± 0.2
Normal	2.9 ± 0.2	11.1 ± 0.2	1.9 ± 0.1
Mg^{2+}-saturated	9.8 ± 0.2	13.1 ± 0.5	2.4 ± 0.2

All samples were loaded with 3 mm LiCl.

CHAPTER V

DISCUSSION

Springer and coworkers (68) have hypothesized a solution structure (Figure 7.A) for the interaction of Na^+ with $Ln(PPP)_2^{7-}$ based on x-ray crystallographic studies of Na_5PPP (132). The paramagnetic effect of Gd^{3+} on the T_1 relaxation rate of the ^{23}Na nucleus in the $Na.Gd(PPP)_2^{6-}$ complex was also investigated by Gupta (133) and the Gd^{3+} to Na^+ distance was calculated to be 4 Å. Both the x-ray studies of Na_5PPP and the relaxation studies of $Gd(PPP)_2^{7-}$ suggest a specific Na^+ binding site close to the Ln^{3+} ion (Figure 7.A). More recently, a different structure for $Dy(PPP)_2^{7-}$ has been proposed that also entails a preferential binding site for Na^+ (Figure 7.C) (111). Although these two structures differ in the mode of Dy^{3+} coordination to PPP^{5-}, the distance between Dy^{3+} and Na^+ in both complexes is similar. Therefore, the dipolar shift, which is inversely proportional to the cube of the distance of the binding site from the paramagnetic center, would be similar for the two models (Figures 7.A and 7.C) assuming that the angular dependence of the dipolar shift is approximately the same.

The PPP^{5-} ligand can also act as a tetradentate ligand in $Ca(PPP)^{3-}$ and in $Nd(PPP)_2^{7-}$ (113,134). An alternative structure for $Ln(PPP)_2^{7-}$ based on a tetradentate PPP^{5-} ligand is also given in Figure 7.B, where no specific Na^+ or Li^+ binding site is present. Peters and coworkers (69) have investigated the solution structure of $Dy(PPP)_2^{7-}$ by multinuclear NMR spectroscopy and postulated a model for this shift reagent, similar to that of Figure 7.B, where cations compete for seven sites in the

second coordination sphere of the complex. The triphosphate ligand is coordinated to Dy^{3+} via two oxygens of one outer phosphate, one oxygen of the other outer phosphate, and one oxygen of the central phosphate group.

^{31}P NMR spectra of Dy^{3+}-complexed triphosphate are dependent on pH and addition of Li^+ ions (Figure 8 and Table III). However, chemical shift changes observed could not be unambiguously interpreted in terms of preferential Li^+ coordination or protonation to specific phosphate groups. Similarly, the linewidths changes caused by H^+ and Li^+ are primarily due to intermolecular ligand exchange processes and are not helpful in establishing which one of the three solution structures (Figure 7) for the interaction of Li^+ with $Dy(PPP)_2^{7-}$ is correct. ^{17}O NMR spectroscopy constitutes an alternative probe of the triphosphate ligand. Unfortunately, it would not help settle the issue of a preferential binding for Li^+ in $Dy(PPP)_2^{7-}$ since it was found that the triphosphate ligand is in slow exchange and that the ^{17}O NMR signals for the Dy^{3+}-complexed ligand are broadened beyond detection (69).

We found that pH has a dramatic effect on the shift the triphosphate reagent induces in the $^7Li^+$ NMR resonance. This behavior would be expected if H^+ and Li^+ were competing for the same phosphate binding sites on the dysprosium ligands. Since the $[Li^+]$/[shift reagent] ratio in the $Ln(PPP)_2Li_n^{n-7}$ complex is greater than 1:1 (Figure 6), the additional Li^+ ions could not occupy the same binding site as shown in Figures 7.A and 7.C, except on a time averaged basis.

Potentiometric equilibrium measurements carried out on the association of Dy^{3+} ion with protonated and deprotonated triphosphate anions have shown (110) that, in the pH region where $^7Li^+$ NMR shifts are highly pH dependent, various protonated complexed forms of the 1:2 complex exist at pH 7.5, such as $DyH(PPP)_2^{6-}$ and $DyH_2(PPP)_2^{5-}$. At pH 5.5, extensive dissociation into the 1:1 $Dy(PPP)^{3-}$ complex occurs. If the mechanism of interaction between Li^+ and the shift reagent is predominantly electrostatic, one

would expect a weaker interaction between Li^+ (or other cations) and the triphosphate shift reagent at low pH as a result of the lower negative charge of the species, $DyH_2(PPP)_2^{5-}$ and $Dy(PPP)^{3-}$, present in solution. We found by $^7Li^+$ NMR spectroscopy that up to seven Li^+ ions may saturate all the binding sites on the second coordination sphere of $Dy(PPP)_2^{7-}$ at pH 7.5 (Figure 6). Thus, our studies support a model for the solution structure of $Dy(PPP)_2^{7-}$ where up to seven Li^+ ions (at pH 7.5) are bound in the second coordination sphere of the complex (Figure 7.B). The first equivalent of Li^+ added to $Dy(PPP)_2^{7-}$ may occupy a preferential binding site with a specific θ value and therefore a specific pseudo-contact shift. Further addition of Li^+ leads to exchange between the Li^+ on the preferred site and those on other locations.

Although the pH dependence of $^7Li^+$ NMR shifts is a matter of concern in some studies, one could also take advantage of this property to estimate pH changes in biological systems. This is particularly important in the case of $^7Li^+$ NMR transport studies since there are examples of Li^+ transport that generate transmembrane proton gradients. For instance, Li^+-induced Cl^- transport in red blood cells suspended in a bicarbonate medium occurs via the anion-exchange, or band 3, protein and is accompanied by H^+ transport (108).

$Dy(PPP)_2^{7-}$, $Tm(PPP)_2^{7-}$, and $Dy(TTHA)^{3-}$ can induce very large shifts in the $^7Li^+$ NMR resonance (Figure 4). Under equivalent pH and ionic strength conditions, the shift induced by $Dy(PPP)_2^{7-}$ is much greater than that induced by other shift reagents used in this study. The high charge of these three complex ions certainly must serve to increase the fraction of Li^+ ions bound to these shift reagents. However, the nitrilotriacetate, dipicolinate, and chelidamate shift reagents all have an overall charge of -3 at the pH used in these studies and yet they give much smaller paramagnetic shifts than $Dy(TTHA)^{3-}$. These observations suggest a more specific type of interaction, other than electrostatic, at least in the case of $Dy(TTHA)^{3-}$.

Based on a charge effect alone, one might predict lower $^{7}Li^{+}$ NMR shifts for $Dy(TTHA)^{3-}$. The large shifts produced by $Dy(TTHA)^{3-}$ may result from some specific binding site for Li^{+}, possibly involving the carboxylate oxygen atoms (68). Two proposals for the solution structure of $Ln(TTHA)^{3-}$ complexes have been reported (119,135). Both studies agree that in the $TTHA^{6-}$ ligand one or more carboxylate groups remain uncoordinated to the lanthanide ion. The oxygen atoms in these uncoordinated carboxylate groups could serve as binding sites for Li^{+}, H^{+} or other metal cations. Since the potential Li^{+} (or H^{+}) binding sites would be further from the paramagnetic ions than the coordinated carboxylates, it is not surprising that the $^{7}Li^{+}$ NMR shifts induced by $Dy(TTHA)^{3-}$ are relatively smaller than those given by the triphosphate reagents and less pH dependent.

The results in Figure 4 indicate that the corresponding Dy(III) and Tm(III) complexes always shift the $^{7}Li^{+}$ NMR resonance in opposite directions, as predicted by dipolar shift theory (136). Provided that the paramagnetic shift is purely dipolar in nature and that all other factors are equal, the ratio of the shift induced by Dy(III) over that induced by Tm(III) should be -1.9. The ratio observed for the five ligands studied are in good agreement with this prediction. Similar observations were made for $^{23}Na^{+}$ NMR shifts (68). $Dy(TTHA)^{3-}$ causes $^{7}Li^{+}$ NMR shifts in the opposite direction from those caused by $Dy(PPP)_2^{7-}$. As reported by Chu et al. (68) this behavior has to do with the geometric relationships of the Li^{+} or Na^{+} binding sites on the two shift reagents to the symmetry elements of their respective asymmetric magnetic susceptibility tensors.

Although $Dy(PPP)_2^{7-}$ and $Tm(PPP)_2^{7-}$ induced the largest $^{7}Li^{+}$ NMR shifts, these shift reagents may not be the best for applications to certain biological systems. In addition to their strong pH dependence and extreme sensitivity to the presence of Na^{+}, K^{+}, Ca^{2+} or Mg^{2+}, there are problems with their hydrolytic instability (113,134).

Recently, the possibility of living cells using PPP^{5-} as an energy source has also been demonstrated (117,118). Our ^{31}P NMR studies also indicate that addition of Ca^{2+} to $Dy(PPP)_2^{7-}$ induces hydrolysis of the triphosphate ligand (Figure 11.B). However, the triphosphate shift reagents will continue to be useful in systems where inorganic pyrophosphatase activity is low, as in RBCs for example. Therefore, although the $Dy(TTHA)^{3-}$ complex produces smaller shifts compared to $Dy(PPP)_2^{7-}$, it stands as the most promising $^7Li^+$ NMR shift reagent for biological applications since it has a relatively low affinity for Li^+ and is fairly unaffected by pH changes and the presence of physiologically important cations such as Na^+, K^+, Ca^{2+} or Mg^{2+}.

The phosphonate shift reagents, specifically $Dy(DOTP)^{5-}$ and $Dy(PcPcP)^{7-}$, induce larger shifts in $^{23}Na^+$ and $^7Li^+$ NMR resonances compared to $Dy(TTHA)^{3-}$ but less than $Dy(PPP)_2^{7-}$. The logarithm of stability constants at 25°C for $Dy(TTHA)^{3-}$, $Dy(DOTP)^{5-}$, and $Dy(PPP)_2^{7-}$ are 16.80, 25.0, 9.2 respectively (104,110,135). It is evident that the shifts induced by lanthanide complexes are dependent more on the overall charge of shift reagents. But one has to compromise in choosing a shift reagent for the system of interest. Biological systems containing phosphatases rapidly hydrolyse $Dy(PPP)_2^{7-}$ (104,117,118). Moreover, for experiments that require monitoring transport for several hours, the stability of shift reagents $Dy(PPP)_2^{7-}$ and $Dy(PcPcP)_2^{7-}$ clearly indicates that they are not suited for this purpose.

The shift reagents $Dy(TTHA)^{3-}$, $Dy(DOTP)^{5-}$ and $Dy(PcPcP)_2^{7-}$, and $Dy(PPP)_2^{7-}$ (in order of preference) show great promise for probing Li^+ ion distribution in RBCs by ^7Li NMR spectroscopy. But because of the high negative charge on these shift reagents, the amount of extracellular Li^+ (and other cations) complexed to them is significant. Thus, these reagents may change the distribution of Li^+ (and of other cations) across the RBC membrane. During ion transport measurements, as shown in Table VI, this effect is much more complicated by the fact that the amount of Li^+

complexed to the shift reagent will vary and thus, it will be difficult to correct for the effects of complexation during an ion transport experiment. We found that this problem of complexation (45,46) is considerably reduced when a shift reagent like $Dy(TTHA)^{3-}$ is used (see table VI). It is well established from our studies (45,46) and those of others (66,104) that all the shift reagents used in this study, except $Dy(TTHA)^{3-}$, have high affinity for divalent alkaline earth cations specifically Ca^{2+} and Mg^{2+}. It appears from our results that the concentration of lanthanide shift reagents used in this study have very little effect on shape and size of RBCs. It has been proposed (137) that anionic drugs intercalate mainly into lipids in the exterior half of the bilayer and thereby induce cells to crenate.

The lanthanide shift reagents used in this study are inorganic complexes with high negative charges. Shift reagents are impermeable to the RBC membrane since the NMR resonances corresponding to the two metal ion pools never collapse into one. The probability of these shift reagents intercalating into the lipids in the exterior half of the bilayer and expanding the exterior layer relative to the cytoplasmic portion, is very unlikely. Preferential entry of the shift reagents into the outer leaflet of the membrane is not possible due to high repulsion of negative charges on shift reagents and the membrane.

The effect of shift reagents on ATP metabolism in RBCs was investigated using ^{31}P NMR by us (data not shown) and others (118). No significant decrease in ATP concentrations in RBC were observed for a time period of 4 hours at $37^{o}C$. During the transport measurement period of 1 hour the ATP concentration remained unaffected. Thus the alteration in spectrin phosphorylation due to ATP depletion is totally ruled out from the above experiments. On this basis one would expect to see very little changes in RBC shape.

SEM and ^{31}P NMR results complement each other in substantiating the above

speculation. Our findings on the effect of varying concentrations of Li^+ on shape and size of RBCs are in good agreement with those of Zimmermann and Soumpasis (105). The main difference between the two studies is that Zimmermann and Soumpasis only looked at the effect of Li^+ incubation at large concentrations (140 mM). We find that even incubation of RBCs with 5 mM LiCl results in considerable cell swelling comparable to that obtained with 140 mM LiCl incubation (Table V). The probable sites of interaction of Li^+ with the RBC membrane can be speculated based on the available knowledge on the composition and organization of red cell membrane and on the basis of the bilayer couple theory. Possible sites of Li^+ interaction in the RBC membrane are on the surface coat sialic carboxylate groups of glycoproteins, and to a lesser extent the hydroxyl groups of glycolipids, and on the inner leaflet of the membrane phosphate and carboxyl groups of phosphatidyl serine.

Phosphatidyl serine bears a net negative charge at neutral pH and therefore contributes to the resting potential of 10 mV negative inside across the membrane of red cells (124). Phosphatidyl choline and sphingomyelin on the outer surface and phosphatidyl ethanolamine on the inner leaflet have zwitterionic head groups and therefore should have a negligible influence on the effects observed. Inner sphere complexation of alkali metal ions depends on variations in cation charge density and decreases in the order $Li^+ > Na^+ > K^+ > Rb^+$. A similar complexation behavior for these ions is expected with RBC membrane components. Studies on monovalent cation association with phophatidyl serine bilayers (138,139) supports the speculation mentioned above.

Involvement of spectrin in maintaining the structural integrity of red cell shape is fairly well documented. Evidence for alterations in the spectrin phosphorylation due to Li^+ is lacking. Probability of Li^+ binding to spectrin and or indirect effect of Li^+ in affecting spectrin conformation thereby causing shape changes, cannot be ruled out (60).

It is possible that Li^+ binding to the probable sites in the membrane could weaken electrostatic membrane stretching, thus leading to swollen red cells. We also looked at the effects of micromolar quantities of free $DyCl_3$ on RBCs (data not shown) for a period of one hour. There were no shape and size changes observed which is in good agreement with those reported earlier (120,121).

Studies on the effect of cell impermeant shift reagents on RBC membrane potential suggest that the extent to which RBC membrane potential is affected depends on the charge of shift reagent (Table VII and VIII). The maximum changes in membrane potential were observed for $Dy(PPP)_2^{7-}$. $Dy(TTHA)^{3-}$ had negligible effect on RBC membrane potential while $Dy(DOTP)^{5-}$ had a substantial effect on RBC membrane potential of RBC. The shift reagents $Dy(PPP)_2^{7-}$ and $Dy(DOTP)^{5-}$ are likely to cause a larger reduction in $[Cl]_o$ than $Dy(TTHA)^{3-}$, thereby resulting in an increase in V_m. Similar observations on the effect of cell impermeant anion citrate on RBC membrane potential have been reported (122). In experiments performed under constant $[Cl]_o$, the effect of shift reagents $Dy(PPP)_2^{7-}$ and $Dy(DOTP)^{5-}$ on the membrane potential is still significant. It may be possible that shift reagents, being membrane impermeable, induce the Cl^- ions to readjust its equilibrium thereby causing changes in the membrane potential.

The relation of elevated RBC Na^+-Li^+ countertransport to the pathogenesis of essential hypertension is not quite clear. One hypothesis is that this abnormality in red cell action transport reflects an abnormality in sodium transport in vascular smooth-muscle cells that is somehow coupled to contraction and increased vascular resistance (17). Marche et al. (140) have shown that the change in phosphoinositide metabolism in RBC of hypertensives could be viewed as an intrinsic membrane defect. This membrane abnormality may be associated with functional alterations of Ca^{2+} fluxes which in hypertensives may result in enhanced intracellular Ca^{2+} level. Inositol lipids, and

particularly polyphosphoinositides, via their metabolic pathways, are involved in the regulation of intracellular Ca^{2+} levels during receptor induced cell activation (141). In erythrocytes, these lipids are located on the inner leaflet of the membrane and their Ca^{2+} binding properties permit them to contribute to the buffering of intracellular Ca^{2+}. Fluorescence studies have revealed the presence of structural alterations at the lipid level in the erythrocyte membrane of essential hypertensives (142). Other studies have also shown that phosphoinositides participate in maintaining the fluidity of membranes and hence influence the transport of monovalent and divalent cations (143). This could possibly explain the higher rates of Na^+-Li^+ countertransport obtained in RBCs of hypertensive subjects.

In contrast to the vast literature available on the validity of Li^+/Na^+ transport rates as a possible genetic marker for essential hypertension, not much is known about the interactions of Li^+/Na^+ in RBCs. At present, studies are in progress to understand the effects of Li^+ and Na^+ ions on the dynamics of erythrocyte membranes from normotensive and hypertensive RBCs. ^{23}Na NMR investigations by Urry et al. (64) have revealed a decrease in sodium binding to erythrocyte membranes of hypertensive patients.

Interaction of Li^+ with normal RBCs membranes has been investigated by ^7Li NMR (60,109) and fluorescence (144) spectroscopies. ^7Li NMR (60,109) studies revealed large differences in the spin-lattice (T_1 = 5s) and spin-spin (T_2 = 0.15s) relaxation times for intracellular Li^+ in normal RBCs. It was speculated that the large difference in relaxation times was due to diffusion of Li^+ across the heterogeneous electrostatic field gradients generated by the spectrin-actin network of the RBC membrane. More details on the mode of Li^+ and/ or Na^+ binding to hypertensive RBC membranes remain unearthed. NMR relaxation times (T_1 and T_2) of Li^+ and or Na^+ in RBCs of hypertensive patients would help to enhance our understanding of the existing

abnormality in Na^+-Li^+ countertransport rates.

We report on the application of a new NMR method to the measurement of rates of Na^+-Li^+ countertransport in RBCs. This method does not suffer from the limitations present in the AA technique or NMR methods involving shift reagents. Because of the ability to provide mechanistic information at a molecular level, easy visualization of Li^+ pools, total non-invasiveness, and time efficiency, the MIR approach described here is likely to become the method of choice for establishing the significance, if any, of lithium transport studies in hypertension.

The observed competition between Li^+ and Mg^{2+} in Li^+-loaded RBCs clearly suggests that Li^+ is displacing Mg^{2+} from ATP and that the released Mg^{2+} is being bound to the membrane. The phospholipids phosphatidylserine, phosphatidylcholine, phosphatidylinositol, phosphatidylethanolamine, and sphingomyelin are potential binding sites with higher affinity for Mg^{2+} compared to Li^+. Also, hemoglobin and spectrin-actin are known to bind Mg^{2+} fairly strongly. Since the efflux for Mg^{2+} in RBCs is extremely slow (practically no efflux) under standard conditions, the released Mg^{2+} in Li^+-loaded RBCs is forced to bind to the above mentioned sites in the membrane. Further experiments need to be performed in order to confirm the above speculation. The above approach could be used to understand the basis for low intracellular free magnesium concentrations in hypertensive RBCs and during blood storage.

BIBLIOGRAPHY

1. Genest J (1983) Personal views on the mechanisms of essential hypertension. In Genest J, Kuchel O, and Carter M (eds.), in " Hypertension, Pathophysiology and Treatment ", second edition, McGraw Hill, New York, p 599.
2. Annest JL, Sing CF, Biron P, and Mongeau JG (1979) Familial aggregation of blood pressure and weight in adoptive families. II. Estimation of relative contribution of genetic and common environmental factors to blood pressure correlations between family members. Am J Epidemol 110 : 492.
3. Morton NE, Gulbrandsen CL, Rao DC, Rhoads GG, and Kagon A (1980) Determinants of blood pressure in Japanese-American families. Human Genet 53 : 216.
4. Wolstenholm G, and Cameron, M (eds.) (1954) CIBA foundation symposium on hypertension. Little Brown and Co., New York, p 1.
5. Weinshilboum RM (1979) Hypertension: A biochemical genetic approach. In Sing C, and Solnick M (eds.), " Genetic analysis of common diseases: Application to predictive factors in coronary disease ", Alan R. Liss, Inc., New York, p 675.
6. Garay R, de Mendonca M, and Meyer P (1982) Erythrocyte Na^+ transport systems in human and experimental genetic hypertension. In Bonne-Tamir B, Cohen T, and Goodman RM (eds.), " Human Genetics, Part B ", Alan R. Liss, Inc., New York, p 127.
7. Glynn IM and Karlish SJ (1975) The sodium pump. Ann Rev Physiol 37 : 13.
8. Langford HG, Canessa M, and Watson RL (1983) A salt-sensitive population subset with distinct red blood cell Na and K fluxes. Clin Res 31 : 537a.
9. Boerwinkle E, Turner ST, and Sing CF (1984) The role of the genetics of sodium lithium countertransport in the determination of blood pressure variability in the

population at large. In " The Red Cell: Sixth Ann Arbor Conference ", Alan R. Liss, Inc., New York, p 479.

10. Wiley JS and Cooper RA (1974) A furosemide-sensitive cotransport of Na plus K in the human red blood cell. J Clin Invest 53 : 745.

11. Adragna N, Canessa M, Solomon H, Slater E, and Tosteson DC (1982) Red cell lithium-sodium countertransport and Na-K cotransport in patients with essential hypertension. Hypertension 4 : 795.

12. Smith JB, Price AL, and Williams RR (1984) A reproducible sodium-lithium countertransport assay: The outcome of changing key laboratory parameters. Clin Chim Acta 122 : 327.

13. Garay RP, Dagher G, Pernollet MG, Devinck MA, and Meyer P (1980) Inherited defect in Na-K cotransport system in erythrocytes from essential hypertensive patients. Nature 284 : 281.

14. Pandey GN, Sarkadi B, and Haas M (1978) Lithium transport pathways in human red blood cells. J Gen Physiol 72 : 233.

15. Haas M, Schooler J, and Tosteson DC (1975) Coupling of lithium to sodium transport in human red cells. Nature, 258 : 425.

16. Sarkadi B, Alifimoff JK, Gunn RB and Tosteson DC (1978) Kinetics and stoichiometry of Na-dependent Li transport in human red blood cells. J Gen Physiol 72 : 249.

17. Canessa M, Adragna N, Solomon HS, Connolly TM, and Tosteson DC (1980) Increased sodium-lithium countertransport in red cells of patients with essential hypertension. N Engl J Med 302 : 772.

18. Canessa M, Adragna N, Bize I, Connolly TM, Solomon MS, Williams G, Slater E, and Tosteson DC (1980) In Intracellular Electrolytes and Arterial Hypertension (Zumkley H, and Losse H, eds.), Georg Thieme Verlag, New York, p 239.

19. Morgan K, Brown RC, Spurlock G, Southgate K, and Mir MA (1986) Inhibitin: A specific inhibitor of sodium/sodium exchange in erythrocytes. J Clin Invest 77 : 1132.

20. Morgan K, Spurlock G, Collins PA, and Mir MA (1989) Interaction of inhibitin with the humanerythrocyte $Na^+(Li^+)_i$ / Na_o^+ exchanger. Biochim Biophys Acta 979 : 53.

21. Cusi D, Barlassina C, Ferrandi M, Lupi P, Ferrari P, and Bianchi G (1981) Familial aggregation of cation transport abnormalities and essential hypertension. Clin Exp Hypertens 3 : 871.

22. Williams RR, Hunt SC, Kuida H, Smith JB, and ASH KO (1983) Sodium-lithium countertransport in erythrocytes of hypertension prone families in Utah. Am J Epidemiol 118 : 338.

23. Pandey GN and Davis JM (1980) Biology of lithium. Adv Exper Med Biol 127 : 15.

24. Egeland JA, Gerhard DS, Pauls DL, Sussex JN, Kidd KK, Allen CR, Hostetter AM, and Housman DE (1987) Bipolar affective disorders linked to DNA markers on chromosome 11. Nature 325 : 783.

25. Hodgkinson S, Sherrington R, Gurling H, Marchbanks R, Reeders S, Mallet J, McInnis M, Peturson H, and Brynjolfsson J (1987) Molecular genetic evidence for heterogenity in manic depression. Nature 325 : 805.

26. Baron M, Risch N, Hamburger R, Mandel B, Kushner S, Newman M, Drumer D, and Belmaker RH (1987) Genetic linkage between X-chromosome markers and bipolar affective illness. Nature 326 : 289.

27. Pandey GN, Ostrow DG, Haas M, Dorus E, Casper RC, Davis JM and Tosteson DC (1977) Abnormal sodium and lithium transport in erythrocytes of a manic patient and some members of his family. Proc Natl Acad Sci USA 74 : 3607.

28. Mallinger AG, Mallinger J, Himmelloch JM, Rossi Aand Hanin I (1983) Essential hypertension and membrane lithium transport in depressed patients. Psychiatry Res 10 : 11.

29. Dagher G, Gay C, Brossard M, Feray JC, Olie JP, Garay RP, Loo H and Meyer P (1984) Lithium, sodium and potassium transport in erythrocytes of manic-depressive patients. Acta Psychiatr Scand 69:24.

30. (a) Egeland JA, Kidd JR, Frazer A, Kidd KK, and Neuhauser VI (1984) Amish study V: Lithium-sodium countertransport and catechol o-methyltransferase in pedigrees of bipolar probands. Am J Psychiatry 141 : 1049.

(b) Richelson E, Snyder K, Carlson J, Johnson M, Turner S, Lumry A, Boerwinkle E, and Sing CF (1986) Lithuim ion transport in erythrocytes of randomly selected blood donors and manic-depressive patients: lack of association with affective illness. Am J Psychiatry 143 : 457.

31. Sachs J, Faler LD, Rabson E (1982) Proton hydroxyl transport in gastric and intestinal epithelia. J Membr Biol 64 : 123.

32. Aronson PS (1982) Sodium-lithium countertransport in essential hypertension. N Engl J Med 307 : 317.

33. Funder J, Weith JO, Jensen HA, Ibsen KK (1984) The sodium/lithium exchange mechanism in essential hypertension: is it a sodium/proton exchanger. In: Villareal H and Sambi MP (eds) "Topics in Pathophysiology of hypertension", Martinus Nijhoff Publishers, Boston, p 147.

34. Escobales N, Canessa M (1985) Ca^{2+}-activated Na^{+} fluxes in human red cells. Amiloride sensitivity. J Biol Chem 260 : 11914.

35. Escobales N, Canessa M (1986) Amiloride sensitive Na^{+} transport in human red cells: evidence for a Na:H exchange system. J Membr Biol 90 : 21.

36. Canessa M, Spalvins A (1987) Kinetic effects of internal and external H^{+} on Li/H

and Li/Na exchange of human red cells. Biophys J 51 : 567a.

37. Canessa M, Spalvins A, Escobales N (1986) Li_o/H_i and Li_i/Na_o exchange in human red cells: effect of H^+ gradients. Biophys J 49 : 141a.

38. Canessa M, Morgan K, Semplicini A (1988) Genetic differences in lithium-sodium exchange and regulation of the sodium-hydrogen exchanger in essential hypertension. J Cardiovasc Pharmacol 12 : 592.

39. Frausto Da Silva JJR and Williams RJP (1976) Possible mechanism for the biological action of lithium. Nature 263, 237.

40. Aronoff MS, Evens RG, and Durell J (1971) Effect of lithium salts on electrolyte metabolism. J. Psychiatr. Res. 8 : 139.

41. Frizel DA, Coppen A, and Marks V (1969) Plasma magnesium and calcium in depression. Br J Psychiatry 115 : 1375.

42. Pavlinic D, Langer R, Lenhard L, and Deftos L (1979) Magnesium in affective disorders. Biol.Psychiatry 14 : 657.

43. Resnick LM, Gupta RK, and Laragh JH (1984) Intracellular free magnesium in erythrocytes in essential hypertension: relation to blood pressure and serum divalent cations. Proc. Natl. Acad. Sci. USA 81 : 6511.

44. Altura BM, and Altura BT (1978) Magnesium and vascular tone and reactivity. Blood Vessels 15 : 5.

45. Espanol MT, and Mota de Freitas D (1987) ^7Li NMR studies of lithium transport in human erythrocytes. Inorg Chem 26 : 4356.

46. Espanol MT, Ramasamy R, and Mota de Freitas D (1989) Measurement of lithium transport across human erythrocyte membranes by ^7Li NMR spectroscopy. In Butterfield DA (ed.): "Biological and Synthetic Membranes", Alan R. Liss, New York, p 33.

47. Trevisan M, Ostrow D, Cooper R, Kiang L, Sparks S, Stamler J (1981)

Methodological assesment of assays for red cell sodium concentration and sodium-dependent lithium efflux. Clin Chim Acta 116 : 319.

48. Blijenberg BG and Leijinse B (1968) The determination of lithium in serum by atomic absorption and flame emission spectroscopy. Clin Chim Acta 19 : 97.

49. Xie YX and Christian GD (1987) Measurement of serum lithium levels. In Johnson FN (ed.): "Depression and Mania", IRL Press, Oxford, p 78.

50. Kimura K (1985) Highly selective crown ether dyes for extraction photometry. Chemistry Lett, 1239.

51. Wheeling K and Christian GD (1984) Spectrofluorimetric determination of serum lithium using 1,8-dihydroxyanthraquinone. Anal Lett 17 : 217.

52. Pacey GE, Wu YP, and Sasaki K (1987) Selective determination of lithium in biological fluids using flow injection analysis. Anal Biochem 160 : 243.

53. Gadzepko VPY, Hungerford JM, Kadry AM, Ibrahim YA, Xie RY, and Christian GD (1986) Comparitive study of neutral carriers in polymeric lithium ion selective electrodes. Anal Chem 58 : 1948.

54. Sakamoto H, Kimura K, and Shono T (1987) Lithium separation and enrichment by proton-driven cation transport through liquid membranes of lipophilic crown nitrophenols. Anal Chem 59 : 1513.

55. Metzger E, Dohener R, Simon W, Voderschmitt DJ, and Gautschi K (1987) Lithium / sodium ion concentration measurements in blood serum with lithium and sodium ion selective liquid membrane electrodes. Anal Chem 59 : 1600.

56. Xie RY and Christian GD (1986) Serum lithium analysis by coated wire lithium ion selective electrodes in a flow injection analysis dialysis system. Anal Chem 58 : 1806.

57. Vartsky D, LoMonte A, Ellis KJ, Yasumura S, and Cohn SH (1988) A method for *in vivo* measurement of lithium in body. In Birch NJ (ed.): "Lithium: Inorganic

Pharmacology and Psychiatric Use", IRL Press, Oxford, p 297.

58. Thellier M, Wissocq J-C, and Monnier A (1988) Methods for studying the distribution and transport of lithium. In Birch NJ (ed.): "Lithium: Inorganic Pharmacology and Psychiatric Use", IRL Press, Oxford, p 271.

59. Detellier C (1983) Alkali Metals. In Laszlo P (ed.): "NMR of Newly Accessible Nuclei", vol 2, Academic Press, New York, p 105.

60. Pettegrew JW, Post JFM, Panchalingam K, Withers G, and Wossener DE (1987) ^{7}Li NMR study of normal human erythrocytes. J Magn Reson 71 : 504.

61. Gupta RJ and Gupta P (1982) Direct observation of resolved resonances from intra- and extracellular sodium-23 ions in NMR studies of intact cells and tissues using dysprosium (III) tripolyphosphate as paramagnetic shift reagent. J Magn Reson 47 : 344.

62. Brophy PJ, Hayer MK, and Ridell FG (1983) Measurement of intracellular potassium concentrations by NMR. Biochem J 210 : 961.

63. Davis DG, Murphy E, and London RE (1988) Uptake of cesium ios by human erythrocytes and perfused rat heart: A cesium-133 NMR study. Biochemistry 27 : 3547.

64. Urry DW, Trapane TL, Andrews SK, Long MM, Overbeck HW, and Oparil S (1980) NMRobservation of altered sodium interaction with human erythrocyte membranes of essential hypertensives. Biochem Biophys Res Commun 96 : 514.

65. Hinckley CC (1969) Paramagnetic shifts in solutions of cholesterol and the dipyridine adduct of trisdipivalomethanatoeuropium (III). A shift reagent. J Am Chem Soc 91 : 5160.

66. Pike MM and Springer CS (1982) Aqueous shift reagents for high resolution cationic magnetic resonance. J Magn Reson 46 348.

67. Pike MM, Yarmush DM, Balschi JA, Leninski RE, and Springer CS (1983) Aqueous

shift reagents for high resolution cationic nuclear magnetic resonance. II. Mg-25, K-39, and Na-23 resonances shifted by chelidamate complexes of dysprosium (III) and thulium (III). Inorg Chem 22 : 2388.

68. Chu SC, Pike MM, Fossel ET, Smith TW, Balschi JA, and Springer JS (1984) Aqueous shift reagents for high resolution cationic nuclear magnetic resonance. III. $Dy(TTHA)^{3-}$, $Tm(TTHA)^{3-}$, and $Tm(PPP)_2^{7-}$. J Magn Reson 46 : 33.

69. Nieuwenhuizen MS, Peters JA, Sinnema A, Kieboom APG, and van Bekkum H (1985) Multinuclear NMR study of the complexation of lanthanide (III) cations with sodium triphosphate: induced shifts and relaxation rate enhancements. J Am Chem Soc 107 : 12.

70. (a) Bryden CC, Reilley CN, and Desreux JF (1981) Multinuclear magnetic resonance study of three aqueous lanthnide shift reagents: complexes with EDTA and axially symmetric macrocylic polyamino polyacetate ligands. Anal Chem 53 : 1418. (b) Lauffer RB (1987) Paramagnetic metal complexes as water proton relaxation agents for NMR imaging: Theorey and design. Chem Rev 87 : 901.

71. Wenzel TJ (1987) In: "NMR Shift Reagents", CRC press, Boca Raton, Florida,p 5.

72. Horrocks WD and Hove EG (1978) Water soluble lanthanide porphyrins: shift reagents for aqueous solutions. J Am Chem Soc 100 : 4386.

73. Weissman SI (1971) On the action of europium shift reagents. J Am Chem Soc 93 : 4928.

74. Fischer RD (1973) Lanthanide and actinide complexes. In La Mar GN, Horrocks WD, and Holm RH (eds.), " NMR of Paramagnetic Molecules: Principles and Applications ", Academic Press, New York, p 521.

75. Cheng HN and Gutowsky HS (1972) The use of shift reagents in nuclear magnetic resonance studies of chemical exchange. J Am Chem Soc 94 : 5505.

76. Horrocks WD and Sipe JP (1972) Lanthanide complexes as nuclear magnetic

resonance structural probes: paramagnetic anisotropy of shift reagent adducts. Science 177 : 994.

77. Sanders JKM, Hanson SW, and Williams DH (1972) Paramagnetic shift reagents. The nature of the interactions. J Am Chem Soc 94 : 5325.

78. Lindoy LF and Moody WE (1977) Nuclear magnetic resonance studies of metal complexes using lanthanide shift reagents. Lanthanide-induced shifts in the H-1 (and C-13) spectra of diamagnetic metal complexes of quadridentate ligands incorporating oxygen-nitrogen donor atoms. J Am Chem Soc 99 : 5863.

79. Shapiro BL, Hlubucek JR, Sullivan GR and Johnson LF (1971) Lanthanide induced shifts in proton nuclear magnetic resonance spectra. I. Europium induced shifts to higher fields. J Am Chem Soc 93 : 3281.

80. McConnell HM and Robertson RE (1958) Isotropic nuclear resonance shifts. J Chem Phys 29 : 1361.

81. Bleaney B, Dobson CM, Levine BA, Martin RB, Williams RJP and Xavier AV (1972) Origin of lanthanide nuclear magnetic resonance shifts and their uses. J Chem Soc Chem Commun 791.

82. Bleaney B (1972) Nuclear magnetic resonance shifts in solution due to lanthanide ions. J Magn Reson 8 : 91.

83. Horrocks WD (1977) The temperature dependencies of lanthanide induced NMR shifts: evaluation of theoretical approaches and experimental evidence. J Magn Reson 26 : 333.

84. McGarvey BR (1979) Temperature dependence of the pseudocontact shift in lanthanide shift reagents. J Magn Reson 33 : 445.

85. Golding RM and Pyykko P (1973) On the theory of pseudocontact NMR shifts due to lanthanide complexes. Molec Phys 26 : 1389.

86. Stiles PJ (1975) Dipolar contributions to nuclear magnetic shielding anisotropic

molecules. Chem Phys Lett 30 : 259.

87. Horrocks WD (1970) Evaluation of dipolar nuclear magnetic resonance shifts. Inorg Chem 9 : 690.

88. Sanders JKM and Williams DH (1971) Evidence for contact and pseudocontact contributions in lanthanide induced P-31 NMR shifts. Tetrahedron Lett 2813.

89. Reuben J (1982) Structural information from chemical shifts in lanthanide complexes. J Magn Reson 50 : 233.

90. Reilley CN , Good BW, and Allendoerfer RD (1976) Separation of contact and dipolar lanthanide induced nuclear magnetic resonance shifts: evaluation and application of some structure independent models. Anal Chem 48 : 1446.

91. Desreux JF and Reilley CN (1976) Evaluation of contact and dipolar contributions to H-1 and C-13 paramagnetic NMR shifts in axially symmetric lanthanide chelates. J Am Chem Soc 98 : 2105.

92. Horrocks WD, Taylor RC and La Mar GN (1964) Isotropic proton magnetic resonance shifts in pi-bonding ligands coordinated to paramagnetic nickel (II) and cobalt (II) acetylacetones. J Am Chem Soc 86 : 3031.

93. (a) Dobson CM, Williams RJP, and Xavier AV (1973) J Chem Soc Dalton 2662.
(b) Walker IM, Rosenthal L, and Quereshi S (1971) Fermi contact and dipolar nuclear magnetic resonance shifts in paramagnetic ion-paired systems. Studies on some anionic lanthanide complexes. Inorg Chem 10 : 2463.

94. Gansow OA, Loeffler PA, Davis RE, Lekinski RE, and Willcott MR (1976) Contact vs. pseudocontact contributions to lanthanide induced shifts in the nuclear magnetic resonance spectra of isoquinoline and of endo-norbornenol. J Am Chem Soc 98 : 4250.

95. Hirayama M, Akutsu K, and Fukuzawa K (1982) The analysis of lanthanide induced C-13 shifts for naphthylamines. Contact shifts induced by Gd-chelates

and the spin-delocalization mechanism. Bull Chem Soc Jpn 55 : 704.

96. Hughes MS, Flavell KJ, and Birch NJ (1988) Transport of lithium into human erythrocytes as studied by ^{7}lithium nuclear magnetic resonance and atomic absorption spectroscopy. Biochem Soc Trans 16 : 827.

97. Degani H and Elgavish GA (1978) Ionic permeabilities of membranes: ^{23}Na and ^{7}Li NMR studies of ion transport across the membrane of phosphatidylcholine vesicles. FEBS Lett 10 : 357.

98. Ridell FG and Arumugam S (1988) Surface charge effects upon membrane transport processes: the effect of surface charge on the monensin-mediated transport of lithium ions through phospholipid bilayers studied by ^{7}Li NMR spectroscopy. Biochim Biophys Acta 945 : 65.

99. Shinar H and Navon G (1986) Novel organometallic ionophore with specificity toward Li^{+}. J Am Chem Soc 108 : 5005.

100. Fossel ET, Sarasua MM, and Koehler KA (1985) A lithium-7 NMR investigation of the lithium ion interaction with phosphatidylcholine-phosphatidylglycerol membranes. Observation of calcium and magnesium ion competition. J Magn Reson 64 : 536.

101. Seo Y, Murakami M, Suzuki E and Watari H (1987) A new method to discriminate intracellular and extracellular K by ^{39}K NMR without shift reagents. J Magn Reson 75 : 529.

102. Gadian DG (1982) In " NMR and its application to living systems". Clarendon Press, Oxford.

103. Cacei MS, Cacheris WP (1984) Fitting curves to data. The simplex algorithm is the answer. Byte 5 : 340.

104. Sherry AD, Malloy CR, Jeffrey FMH, Cacheris WP, Geraldes CFGC (1988) $Dy(DOTP)^{5-}$: A new, stable ^{23}Na shift reagent. J Magn Reson 76 : 528.

105. Zimmermann B and Soumpasis DM (1985) Effects of monovalent cations on red cell shape and size. Cell Biophysics 7 : 115.

106. Yingst DR and Hoffman, JF (1984) Passive Ca transport in human red blood cell ghosts measured with entrapped arsenazo III. J Gen Physiol 83 : 1.

107. Steck TL and Kant JA (1974) Preparation of impermeable ghosts and inside-out vesicles from human erythrocyte membranes. Methods in Enzymology 31 : 172.

108. Duhm J (1982) Lithium transport pathways in erythrocytes. Excerpta Medica 1 : 1.

109. Espanol MT (1989) Multinuclear magnetic resonance studies of lithium binding and transport in human erythrocytes. Ph.D Dissertation, p 54.

110. Taqui Khan MM, and Reddy PR (1974) Metal chelates of tripolyphosphate with rare earths. J Inorg Nucl Chem 36 : 607.

111. Anson SM, Homer RG, and Belton PS (1987) A ^{31}P and ^{23}Na NMR and Terbium(III) luminescence study of bistriphosphato-lanthanide(III) complexes including the cation shift reagent $[Dy(PPP)_2]^{7-}$. Inorg Chim Acta 138 : 241.

112. Martell AE and Schwarzenbach G (1956) Adenosinephosphate and triphosphate complexes of calcium and magnesium Helv Chim Acta 39 : 653.

113. Watters JL, Loughran ED, and Lambert SM (1956) The acidity of triphosphoric acid. J Am Chem Soc 78 : 4855 (1956).

114. Watters JL, Lambert SM, and Loughran ED (1957) The complexes of triphosphate ion with alkali metal ions. J Am Chem Soc 79 : 3651.

115. Gorenstein DG, In Gorenstein DG (ed.) "Phosphorus-31 NMR: Principles and Applications", Academic Press; London, 1984, Chap.1, p.7.

116. Elgavish GA (1986) Metal organophosphorous compounds for NMR analysis. Eur Pat Appl EP 173163.

117. Matwiyoff NA, Gasparovic C, Wenk R, Wicks JD,and Rath A (1986) ^{31}P and ^{23}Na

NMR studies of the structure and lability of the sodium shift reagent, bis(tripolyphosphate) dysprosium (III) $[Dy(P_3O_{10})_2]^{7-}$ ion, and its decomposition in the presence of rat muscle. Magn Reson Med 3 : 164.

118. Boulanger Y, Vinay P, and Desroches M (1985) Measurement of a wide range of intracellular sodium concentrations in erythrocytes by ^{23}Na nuclear magnetic resonance. Biophys J 47 : 553.

119. Yingst A and Martell AE (1969) New multidentate ligands. IX. Metal chelates of TTHA with trivalent metal ions. J Am Chem Soc 91 : 6927.

120. Szasz I, Sarkadi B, Schubert A, and Gardos G (1978) Effects of lanthanum on calcium dependent phenomenon in human red cells. Biochim Biophys Acta 512 : 331.

121. Burton KP, Hagler HK, Templeton GH, Willerson JT, and Buja ML (1977) Lanthanum probe studies of cellular pathophysiology induced by hypoxia in isolated cardiac muscle. J Clin Invest 60 : 1289.

122. Kirk K, Kuchel PW, and Labotka RJ (1988) Hypophosphite ion as a ^{31}P nuclear magnetic resonance probe of membrane potential in erythrocyte suspensions. Biophys J 54 : 241.

123. Gary-Bobo CM, and Solomon AK (1968) Properties of hemoglobin solutions in red cells. J Gen Physiol 52 : 825.

124. Glaser R (1979) The shape of red blood cells as a function of membrane potential and temperature. J Membr Biol 51 : 217.

125. Rink TJ, and Hladky SB (1982) Measurement of red cell membrane potential with fluorescent dyes. In " Red Cell Membranes: A Methodological Approach ", Ellory JC and Young JD, editors, Academic Press, London, p 321.

126. London RE and Gabel SA (1989) Determination of membrane potential and cell volume by ^{19}F NMR using trifluoroacetate and trifluoroacetamide probes.

Biochemistry 28 : 2378.

127. Martin RB and Mariam YH (1979) Interactions Between Metal Ions and Nucleic Bases, Nucleosides, and Nucleotides in Solution. In, " Metal Ions in biological Systems ", Sigel H editor, Marcel Dekker Inc., New York, vol. 8, p 58.

128. Gunther T and Vormann J (1989) Na^+-independent Mg^{2+} efflux from Mg^{2+}-loaded human erythrocytes. FEBS Lett 247 : 181.

129. Gupta RK, Benovic JL and Rose ZB (1978) The determination of the free magnesium level in the human red blood cell by ^{31}P NMR. J Biol Chem 253 : 6172.

130. Brock JL, Wenz B and Gupta RK (1985) Changes in intracellular Mg Adenosine Triphosphate and ionized Mg^{2+} during blood storage: Detection by ^{31}P nuclear magnetic resonance spectroscopy. Blood 65 : 1526.

131. Brock JL, Wenz B, and Gupta RK (1986) Studies on the mechanism of decreased NMR-measured free magnesium in stored erythrocytes. Biochim Biophysica Acta 928 : 8.

132. Davies DR and Corbridge DEC (1958) Crystal structure of triphosphate cheltes. Acta Crystallogr 11 : 315.

133. Gupta RK, (1987) In Gupta RK (ed.) 'NMR Spectroscopy of Cells and Organisms', Vol.2, CRC Press; Boca Raton, Chap.7, p 1.

134. Geisrecht E and Audrieth LF (1958) Phosphates and ploy phosphates of rare earth elements-II. J Inorg Nucl Chem 6 : 308

135. Gayhart RB and Moeller T (1977) Observations on the rare earths-LXXXIX. J Inorg Nucl Chem 39 : 49.

136. Inagaki F and Miyazawa T (1981) NMR analysis of molecular conformations and conformational equilibria with lanthanide probe method. Prog NMR Spectrosc 14 : 67.

137. Sheetz MP and Singer SJ (1974) Biological membranes as bilayer couples. A molecular mechanism of drug-erythrocyte interactions. Proc Natl Acad Sci USA 71:4457.

138. Johnson RM and Robinson J (1976) Morphological changes in assymetric erythrocyte membranes induced by electrolytes. Biochem Biophys Res Commun 70 : 926.

139. Puskin JS (1977) Divalent cation binding to phospholipids: An EPR study. J Membr Biol 35 : 39.

140. Marche P, Koutouzov S, Girard A, Elghozi JL, Meyer B, Ben-Ishay D (1985) Phosphoinositide turnover in erythrocyte membranes in human and experimental hypertension. J Hypertension 3 : 25.

141. Michell RH (1983) Ca^{2+} and protein kinase C: two synergistic cellular signals. Trends Biochim Sci 8 : 263.

142. Orlov SN and Postnov YuV (1982) Ca^{2+} binding and membrane fluidity in essential and renal hypertension. Clin Sci 63 : 281.

143. Allan D (1982) Inositol lipids and membrane function in erythrocytes. Cell Calcium 3 : 451.

144. Pettegrew JW, Short JW, Woessner RD, Strychor S, McKeag DW, Armstrong J, Minshew NJ, Rush AJ (1987) The effect of lithium on the membrane molecular dynamics of normal human erythrocytes. Biol Psychiatry 22 : 857.

APPROVAL SHEET

The dissertation submitted by **Ravichandran Ramasamy** has been read and approved by the following committee:

Dr. Duarte Mota de Freitas, Director
Assistant Professor of Chemistry, Loyola

Dr. Albert J. Rotermund
Associate Professor of Biology, Loyola

Dr. David S. Crumrine
Associate Professor of Chemistry, Loyola

Dr. Kenneth W. Olsen
Associate Professor of Chemistry, Loyola

Dr. K. S. Rajan
Scientific Advisor
IIT Research Institute, Chicago, Illinois

The final copies have been examined by the director of the dissertation and the signature which appears below verifies the fact that any necessary changes have been incorporated and that the dissertation is now given final approval by the committee with reference to content and form.

The dissertation is therefore accepted in partial fulfillment of the requirements for the degree of **Doctor of Philosophy**.

9/21/89
Date

Director's Signature